University of Southern Queensland
Faculty of Health, Engineering & Sciences

Structural Behaviour of Graphene-Epoxy Coated Timber Members

A dissertation submitted by

Thuong Phan

In fulfilment of the requirements of

ENG4111 and ENG4112 Research Project

Towards the degree of

Bachelor of Engineering (Honours) (Civil)

Submitted: October, 2018

Abstract

The use of innovative material such as graphene could potentially contribute to the strengthening of today's infrastructures, and further extending the service life of the infrastructures. Graphene material properties far exceed any other material and have been proven to be an advanced and durable material in structural applications. Since the discovery of graphene, the approach of utilising graphene combined with polymer matrices has been increasingly popular in today's civil industry. This has provided an opportunity for engineers to conduct analysis on the effectiveness of using graphene platelet (GPL)/polymer nanocomposites layer as a reinforcement method for timber materials.

The objective of this project was to analyse the structural behaviour of timber members reinforced with different ratios of graphene. Graphene was incorporated with polymer matrices to produce two ratio that would be used for testing. First ratio used for testing comprises of 0.25% graphene and 99.75% of epoxy, and the second comprises of 0.5% graphene and 99.5% epoxy. These ratios were applied to the timber members to conduct experimental testing, to obtain the materials modulus of elasticity (MOE) and modulus of rupture (MOR), which can describe the flexural modulus and strength of the timber material. It was assumed that the members reinforced with a higher graphene content should significantly increase the timber material resistance to bending, resulting in a reduction in deflection; furthermore, increasing the material yield strength, which also increases the stress level that the timber material can support without deforming.

Contradictory to the project assumptions, the experimental results concluded that the timber members reinforced with a low content of graphene (0.25% graphene) perform significantly better compared to members reinforced with a higher content of graphene (0.5% graphene). The members reinforced with 0.25% graphene can effectively resist deformation under the same loading condition, with a relatively low deflection compared to the members reinforced with a higher content of graphene.

To validate the experimental results, Strand7 finite element (FE) software was used. A parametric study was conducted to investigate the effective material properties of GPL/polymer nanocomposites layers based on 0.5 and 0.25 percentages of weight fraction using the Halpin-Tsai micromechanics model and rule of mixture. The numerical results show a logical agreement between the control samples and the Strand7 models. However, the reinforced models show large differences when compared to the Strand7 models. There are many possible reasons for this, which include modelling as an isotropic element and the indefinite material properties of the epoxy and graphene used for this research. Therefore, further work is needed to improve the accuracy of these results.

University of Southern Queensland

Faculty of Health, Engineering and Sciences

ENG4111/ENG4112 Research Project

Limitations of Use

Certification of Dissertation

I certify that the ideas, designs and experimental work, results, analyses and conclusions set out in this dissertation are entirely my own effort, except where otherwise indicated and acknowledged.

I further certify that the work is original and has not been previously submitted for assessment in any other course or institution, except where specifically stated.

Thuong Phan
[redacted]

Acknowledgments

I would like to acknowledge those who contributed to and assisted me throughout this research project. In particular, I would like to make special mention of;

- My family and colleague for their continued support in this research project and degree.
- Professor Karu Karunasena and Dr Weena Lokuge for the valuable guidance and academic support they have provided as my USQ project supervisor.
- David Pope and Dr Ashok Nanjundan from Graphene Manufacturing Group (GMG) for providing graphene for this research project, and assisting in mixing the graphene with epoxy resin.
- Mrs Piumika Ariyadasa for her assistance in testing

I am very grateful for the input and assistance provided by these people.

Thuong Phan

Table of Contents

List of Figures

List of Tables

Nomenclature

b	width
C_1	concentration of graphene
C_2	final concentration of the new solution
CFRP	carbon fibre reinforced polymer
CNT	carbon nanotube
CVD	chemical vapour deposition
δ	maximum central deflection
E_L	longitudinal modulus
E_T	transverse modulus
E_m	modulus of polymer
FEA	finite element analysis
FRP	fibre reinforced polymer
g_f	weight fraction of fibre
GPL	graphene platelets
GMG	Graphene Manufacturing Group
h	depth
h_f	thickness of fibre
I	moment of inertia
K	thermal expansion
L	length
l_f	length of fibre
MOE	modulus of elasticity
MOR	modulus of rupture
η_L	stress partitioning factors for matrix
η_T	stress partitioning factors for fibre
P	applied load
ρ	density
ρ_c	density of composite
ρ_f	mass density of fibre
ρ_{GPL}	effective mass density of GPL/polymer nanocomposites
ρ_M	mass density of polymer
SWNT	single-walled carbon nanotube
V_1	volume of the graphene required

V_2	final volume of the new solution
v	Poisson ratio
V_f	volume fraction of effective fibre
v_f	Poisson ratio of fibre
V_m	volume fraction of matrix
v_m	Poisson ratio of matrix
v_{GPL}	effective Poisson ratio of GPL/polymer nanocomposites
ω_f	width of fibre

Chapter 1 Introduction

1.1 Background information

Significant population growth has placed considerable strain and demand upon government infrastructures and services. Some of these infrastructures include residential buildings, sports complexes, commercial structures, bridges, etc. which serve to provide safe passages and networking across Australia, especially on local roads, as they connect towns to the main highway infrastructures. Most of these timber infrastructures are currently in a deteriorating condition, and with an estimation of 33,500 timber road bridges currently in service due to the increase of traffic loads, construction methods and environmental locations (Salonen 2015). Due to this, it is optimal for the continuous development of these timber infrastructures. Without this improvement to public transportation, most of the associated growth in transport demand will become more congested. The Fremantle Traffic Bridge located in Western Australia is an example of the primary infrastructure in Australia that is at risk of closure. This is a result of the continuous deterioration of the critical timber components of the bridge supports (Infrastructure Australia 2019).

The method used to monitor the deterioration process and failure mode within the timber structures base on the current maintenance system and routine inspection are inadequate due to the organic nature of the timber material. This has provided an opportunity for engineers to conduct in-depth analyses into different strength enhancement method that allow today's infrastructures to be more sustainable, and further extend the service life of the structure (Salonen 2015). An alternative method of strengthening and enhancing timber structures can be achieved through the reinforcement of GPL/polymer nanocomposites. Graphene nanocomposites have proven to be an advanced and durable material in a structural application based on its mechanical properties. Since its discovery, the approach of strengthening infrastructures component using graphene nanocomposites with epoxy polymer has been increasingly popular in the modern civil industry. This is due to graphene being the strongest material to be tested, with a modulus of elasticity of 1 TPa, thermal conductivity of $5000\ \mathrm{Wm^{-1}K^{-1}}$ and tensile strength of 130 GPa (Wang et. al. 2011).

Upon researching the use of fibre composites as reinforcement, André A & Kliger R (2009) identified that both the tension and compression side of the timber should be reinforced to fully optimise and increase the bearing strength and stiffness of the timber beam. This is supported through numerous studies and experiment, especially through Yusof, A & Saleh, A.L (2010) studies, which recognized the cause of failure for a timber beam during his experimental studies was due to the changes from tension failure to the compression failure. This has suggested that once the tension side fails, the compression side follows closely, therefore reinforcing both sides should effectively increase the strength capacity of the timber beam. The topic of this research project would focus on investigating the structural behaviour of the timber members reinforced with different ratio of graphene-platelet (GPL)/polymer nanocomposites on the tension and compression side of each member.

1.2 Challenges and Limitation

Numerous research has been conducted to analyse the structural behaviour of a timber beam reinforced with fibre composites, such as carbon fibre or glass fibre, generating successful results, proving that it is possible to enhance the strength characteristics of the timber members. Whereas, graphene is an emerging technology with limited research into the characteristics of the GPL/polymer nanocomposites. Hence, it was challenging to determine the realistic mechanical properties to compute precise mathematical models that can predict the structural behaviour of the timber members. Also, no previous studies have established a theoretical study that can identify the bending behaviour of timber beam reinforced with nanocomposites; therefore, Strand7 FE model was developed to validate the experimental data's.

Initially, 24 timber samples were intended for testing with high variation between the cross-sectional area and graphene-epoxy ratio, which was predicted to provide a more accurate data's. However, the problems lie with obtaining the required material for testing. The Graphene Manufacturing Group (GMG), which is founded by Craig Nicol is a global technology business that focuses on producing graphene for different applications to achieve the best applicable outcome. Different type of graphene is produced through GMG, which is known to be GMG X50, GMG X200 and GMG XE (Graphene Manufacturing Group 2019). For this study, GMG has generously provided GMG X50, which is most suitable for conductive applications, and furthermore help assisted in mixing 200 grams of graphene into the resin. One per cent of graphene (200 grams) could only be mixed into the resin because of the resin high viscosity that was observed during the mixing process. The material properties of graphene and epoxy used in this study is confidential and cannot be obtained from the manufacturers; therefore, the material properties for this research would be based on past literature. Additionally, the excessive costs of timber material made it hard to obtain the required 24 samples. Therefore, the test samples and ratio used for testing were limited to only 12 samples that consist of:

- 3 of 70 mm by 45 mm MGP10 Structural Pine
- 3 of 70 mm by 35 mm MGP10 Structural Pine

- 3 of 45 mm by 70 mm MGP10 Structural Pine
- 3 of 184 mm by 19 mm Radiata Pine

The graphene to epoxy ratio used was reduced to:

- 0.5% Graphene and 99.5% Epoxy
- 0.25% Graphene and 99.75% Epoxy

1.3 Project Aims and Objectives

This project aims to investigate the structural behaviour of the timber members reinforced with GPL/polymer nanocomposites, with the primary objective of identifying the effectiveness of the new method of design. This will include the analyses of each member's flexural strength and modulus through flexural testing, which in return would determine the effectiveness of the reinforced GPL/polymer nanocomposites. To achieve this, the following objectives are defined as:

1. Review the current standards of MGP10 timber in Australia and different type of reinforcement method involving the use of epoxy and graphene, in-order to gain an understanding of the current mechanical properties.
2. Collecting timber material properties data from Australian Standards with the intent of using a representative set of data to predict the behaviour of reinforced timber members.
3. Collecting structural performance data from testing of the timber members, and compare its effectiveness through analysing the ultimate loading and deflection, modulus of elasticity (MOE) and modulus of rupture (MOR).
4. Conduct parametric studies to identify the effective material properties of the GPL/polymer nanocomposite. Then create a mathematical computer model using Strand7 to validate and predict the results obtained from the experiment based on parametric studies.
5. Compare the ultimate deflection based on several loading conditions obtained from the model and experiment of the reinforced and non-reinforced timber members.
6. Submit an academic dissertation on the research conducted.

1.4 Overview of the dissertation

This dissertation consist of six chapters, which is organised as follows:

Chapter 1 introduces the research topic and project background, underlying reason for the commencement of this research, and followed by the challenges and the objectives of this dissertation.

Chapter 2 contains all the literature review on the past and current studies related to this research and the relevant Australian Standards. Additionally, conduct a literature review on the available research on graphene and epoxy nanocomposites material properties, and the relationship between graphene and timber materials.

Chapter 3 evaluates the effective material properties of the nanocomposites layers based on the material properties of graphene and epoxy, also identify the material properties of MGP10 timber obtained in Chapter 2. The material properties of the GPL/polymer nanocomposites layers, MGP10 and Radiata timber member would be used for FEA in Chapter 5.

Chapter 4 investigates the experimental behaviour of the MGP10 members reinforced with different ratio of graphene-epoxy subjected to loading of 1 mm per minute.

Chapter 5 discusses the development of convergence studies and bending analyses using Strand7 FE models that can stimulate the physical experiment. The models are subjected to several different loading conditions and are validated against the experimental data's. Further analysis can be conducted on epoxy-based reinforcement to predict the bending behaviour of the members.

Chapter 6 is the final chapter, which concludes the dissertation with a summary and conclusions of the major findings within this research project and suggesting further work/research opportunities available.

Chapter 2 Literature Review

2.1 Review of Graphene Nanocomposites in Civil Engineering Application

2.1.1 Graphene Nanocomposites

Graphene is a thin layer of sp^2 fused carbon atoms that are arranged in a hexagonal lattice structure, which are the building blocks to produce a variety of carbon-based nanostructures as shown in Figure 1. For example, the thin layer of graphene can be rolled up to produce a single-walled carbon nanotube (SWNT), whereas graphene platelets (GPL) comprised of one or more layers of graphene stacked together to form a two-dimensional sheets of carbon atoms. All nanostructures produce from graphene has exceptional mechanical properties due to the sp^2 carbon-bonding network within the carbon-based nanostructures. Its exceptional mechanical properties far exceed any other materials, with a modulus of elasticity (MOE) of 1 TPa and ultimate strength of 130 GPa, this has proven to be 200 times stronger than that of steel, and 30 times harder than diamond. This is due to its high specific surface area, low electrical resistivity, high thermal conductivity, high strength, modulus, and the ability to be dispersed in a variety of different polymer matrices. The use of graphene-based nanofillers combined with high-performance polymer has shown great potential for various engineering applications, such as electronics, green energy, aerospace and automotive industries (Anwar et. al. 2016).

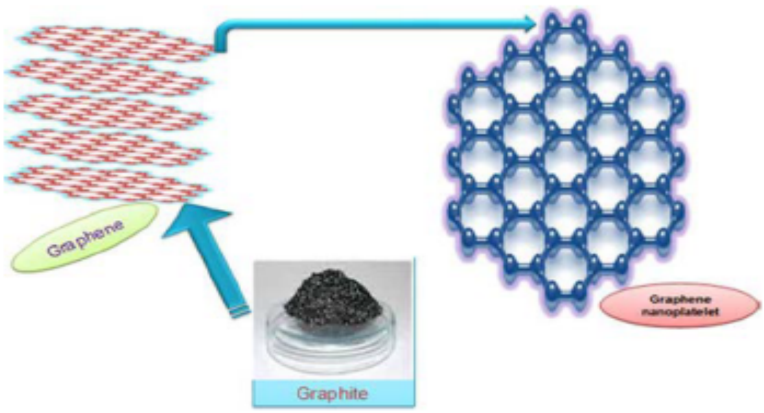

Figure 1: Structure of graphene (Gabriel 2018)

Polymer composites reinforced with GPL are known to display significant improvement in mechanical and physical properties. It could also be noted that graphene has recently become the most preferable nanofillers used for reinforcement due to the low fabrication cost, better dispersion and the bonding ability within the polymer matrix due to the increased surface area. The understanding of the full potential of using graphene in polymer composites remains a challenge in both laboratory and commercial scales. It was predicted that the main failure observed during an applied load is caused due to the poor dispersion of the fibre within the polymer matrix interface, resulting in a weakened adhesion and reduce stiffness in the graphene-polymer interfaces. Additionally, factors such as the structural defects and stability of timber materials can contribute to the behaviour of the graphene-polymer interface (Dhand et. al. 2013).

It was found in Yasmin and Daniel (2004) research that the significant increases in tensile strength and elastic modulus of composites are due to the addition concertation of GPL. Additionally, it has been identified that at high nanofiller concertation, GPL demonstrates significant improvement in mechanical properties compared to carbon nanotube (CNT) composites (Rafiee et. Al. 2009). These findings have suggested the addition of GPL in an epoxy matrix should result in extraordinary deflection reduction. Furthermore, have contributed to the understanding of GPL reinforcement effect, however, most studies involving GPL mechanical properties are limited, due to the studies involving the mechanical behaviour of GPL nanocomposites still gradually being improved on.

2.1.2 Mechanical Properties of Graphene Nanocomposites

The mechanical properties of graphene are much stiffer and durable when compared to CNT. Besides the size and geometric property, the temperature is a significant contributing factor towards the mechanical properties of graphene. Zhao et. al. (2007) suggested that the MOE of graphene does not change drastically until the temperature exceeds 1200 K, beyond this point graphene becomes softer. An increase in temperature also means a decrease in fracture strength and strain. Other important factors that can influence the mechanical properties of graphene are through the number of layers within the composites. Note that the results shown in Table 1 are based on the Atomic Force Microscopy measurements and Raman spectroscopy analysis. Table 1 shows the mechanical properties of a single, bilayer and trilayer of graphene (Wang et. al. 2011).

Table 1: Mechanical properties of graphene with single, bilayer and trilayer (Wang et. Al. 2011)

Material	Mechanical Properties	Method
Monolayer graphene	$E = 1 \pm 0.1TPa$	AFM
Graphene	$\sigma = 130 \pm 10GPa\ at\ \varepsilon = 0.25$	Raman
Monolayer	$E = 1.02TPa; \sigma = 130GPa$	AFM

Bilayer Trilayer	$E = 1.04TPa; \sigma = 126GPa$ $E = 0.98TPa; \sigma = 101GPa$	

2.1.3 Manufacturing Processes of Graphene

Over the past four decades, various attempt has been made to fabricate a large scale production of a pure and defect-free GPL. Numerous method such as epitaxial growth on metal carbide and chemical vapour deposition CVD method have shown promising results. These methods have been categorised into the 'top-down" and "bottom-up" approach (Dhand et. al. 2013).

2.1.3.1 Top Down

Top-down approach uses the existing form of the bulk material and improves it to produce the final product. This approach is cost-efficient due to the trivial lab-scale project, whilst also limiting its quality control. During this process, graphene or reformed graphene sheets are either separated, sliced or exfoliation of graphite or its by-products such as graphite oxide (GO), or graphite fluoride (GF). Researchers have successfully fabricated a few graphene sheets on a micro and nanoscales, however, due to the high cost in production and low yields; a proper approach is still required for mass-scale production. Many mechanical approaches have been used to produce high quality and defect-free graphene such as exfoliation method, sonication and functionalization. It has been suggested by Potts et. al. (2011) that the process of intercalation of alkali metal between the GPL layers, which aims to increase the interlayer arrangement and weaken the interlayer relation between the graphene layers, in-order to exfoliate the GPL through mechanical or thermal methods (Dhand et. al. 2013).

2.1.3.2 Bottom Up

The production of a high-quality graphene interface is achieved through the bottom-up approach. This approach is achieved through graphene growth via CVD on a metallic surface. This approach comes with a sequence of issues including costly production, possible damages in the carbon network and unfavourable effects on carrier flexibility. Though the bottom-up approach provides lesser defects compared to the top-down approach, the operation and procedure are much more complex, therefore making it hard to manage for mass production. However, this approach is the most widely used due to its potentials to modify the atomic size, composition, shape and stability in graphene (Dhand et. al. 2013).

2.2 Review of Epoxy in Civil Engineering Application

2.2.1 Polymer Matrix Resin

Polymer matrix resin plays a major role in holding the reinforcement in place; it adapts to a harsh environment and can transmit the loading to the surrounding fibres when a fracture is detected. The Polymer matrix can be classified into two fundamental categories known as thermoplastics and thermosets (Masuelli 2013). The thermoplastics become soft due to the increased temperature, while hardening during low temperature. The thermoplastic material can be cooled and heated several times without any changes in its mechanical properties. Some well-known thermoplastics include acrylic, nylon, polystyrene and polyethene. On the other hand, thermosets are set at room temperature or higher and are hardened by curing, which is prompted by heat, high pressure or mixing with a catalyst. This has made thermoset resin the preferable matrix material used for polymer-based composites, mainly because of their simple process and low cost (Martinez 2016). The most common type of thermosets are polyesters, vinyl esters and epoxies, further properties of these materials are provided in Table 2 (Huang 2004). For the purpose of this study, epoxy resin are chosen as the polymer adhesive combined with graphene nanocomposites for the experiment.

Table 2 Properties of Different Types of Polymer Matrix Resins (Huang 2004).

	Density $\left(\frac{Mg}{m^3}\right)$	**Tensile Modulus** (GPa)	**Tensile Strength** (MPa)	**Compression Strength** (MPa)	**Tensile Elongation** (%)	**Approximate Cost** $\left(\frac{AUD\$}{kg}\right)$
Polyester	1.2-1.5	2.8-3.4	40-90	100-120	1.4-3.3	2.50-4.00
Vinyl ester	1.0-1.2	3.3-3.6	70-80	105-125	5.0-6.0	4.00-6.00
Epoxy	1.1-1.4	2.6-6.0	35-100	90-115	2.6-6.0	7.00-50.00

2.3 Structural Behaviour of Timber and Australian Timber Grading System

2.3.1 Stress-Strain Behaviour

The stress to strain relationship for both wood and timber are similar with different compression and tension strength. The tensile strength of wood is significantly lower than timber due to the defects within the timber structure. When conducting a test to failure experiment for timber, the stress to strain relationship shows a linear result up until maximum loading, resulting in the failure of the specimen. In contrast, the axial compression testing for timber shows a more ductile relationship. Showing a linear relationship up to a relative limit, and anything beyond that limit would result in ductile yielding taking place (Gentile 2000).

2.3.2 Size Effects

Another behaviour that can contribute to the fracture of the timber is the size effect of the timber. To analyse this the brittle fracture theory proposed by Wiebull (1939) are used to analyse the effect of size with relation to the bending strength for the timber members. Assuming that at a region of low strength in the member, it would occur where the member has a large volume compared to a member with small volume. Therefore, the strength of a member could decrease where there is an increase in length and depth in the member. A statistical analysis of the data is described by Weibull distribution as shown in equation 1 (Barrett et. al. 1981).

$$F(x) = 1 - \exp\left[-\left(\frac{x - x_0}{m_1}\right)^k\right] \tag{1}$$

where;

x = Strength

$\mathrm{x_0}$ = Location paraeter or mimimum strength

$\mathrm{m_1}$ = Scale parameter

k = Dimensionless shape parameter

2.3.3 Natural Defects Mechanism and Durability Class

The durability of each timber can be classified into two types:

- Natural Effect - The decay, insect and marine borer attack on hardwood.
- Environmental Effect - The different type of environmental and the hazards the timber is exposed to.

Based on the second class (environmental effects), the main effect that contributes to the defect of the timber structure is due to the moisture condition. Moisture is an essential aspect in the growth, health and most importantly, the main source of deterioration and decay of the timber material. Controlling moisture condition is essential because it influences the bending elastic modulus of the timber, ultimate strength and bending stiffness. Moisture can be calculated by comparing the dry mass of a timber specimen to the wet mass of the same specimen (Salonen 2015). Based on this information, different types of hardwood have been classified into their durability classes shown in Table 3.

Table 3: Natural durability of hardwood is expressed as four durability classes (AS 5604-2005 and AS 1720.1-2010)

Class	Durability	Species
1	Highly Durable	Ironbark, Tallow-wood, Cypress, Turpentine, Forest red gum
2	Durable	Spotted gum, Blackbutt, River red gum, Western Cedar, Bark (yellow & white)
3	Moderately Durable	Brush box, Rose/flooded gum, Sydney blue gum, Silver topped stringy bark
4	Non-Durable	Douglas flr, Hoop pine, Radiata pine, Mountain ash/Tasmanian oak

2.3.4 Australian Timber Grading System

Strength Group

The timber's strength indicates its capability to maintain stress without failure, it can be classified into seven different strength groups for unseasoned and eight for seasoned.

- Unseasoned - S1 (strongest) to S7 (weakest)
- Seasoned - SD1 (strongest) to SD8 (weakest).

These strength groups are classified accordingly to the AS/NZS 2878:2000 Timber – classification into strength group. The different strength groups of seasoned and unseasoned timber are classified according to the mechanical properties of each timber conditions. Seasoned timbers are generally dry timber that has an enhanced stiffness property compared to unseasoned timbers (QTimber 2016).

Stress Grades

Structural Timber used in structural design is generally stress-graded, which is the classification of timber during structural applications. Stress graded timber can be identified through visual or machine grading methods. Both methods specify the stress limits applied to the timber that is used for structural applications. Timber that is used in a specific structural application must comply with the Australian Standards 2010 (QTimber 2016). Stress grades can be identified by:

- 'F' grades from F4 to F34

Table 4: Characteristic Values Design for F-Grades Timber as listed in AS1720.1:2010 Structural Timber - Design Methods Table H2.1.

Stress grade	Characteristic values, MPa						
	Bending	Tension parallel to grain		Shear in beam	Compression parallel to grain	Short duration average modulus of elasticity* parallel to the grain, MPa	Short duration average modulus of rigidity, MPa
		Hardwood	Softwood				
	(f'_b)	(f'_t)		(f'_s)	(f'_c)	(E)	(G)
F34	84	51	42	6.1	63	21 500	1 430
F27	67	42	34	5.1	51	18 500	1 230
F22	55	34	29	4.2	42	16 000	1 070
F17	42	25	22	3.6	34	14 000	930
F14	36	22	19	3.3	27	12 000	800
F11	31	18	15	2.8	22	10 500	700
F8	22	13	12	2.2	18	9 100	610
F7	18	11	8.9	1.9	13	7 900	530
F5	14	9	7.3	1.6	11	6 900	460
F4	12	7	5.8	1.3	8.6	6 100	410

- Machine graded pine from MGP, MGP10 to MGP15

Table 5: Characteristic Values for Design stress Grades Timber as listed in AS1720.1:2010 Structural Timber - Design Methods Table H3.1.

Stress grade	Section size		Characteristic values, MPa										Design density	Joint group
	Depth mm	Breadth mm	Bending (f'_b)	Tension parallel to grain (f'_t)	Compression parallel to grain (f'_c)	Shear in beams (f'_s)	Average modulus of elasticity (see Note1) parallel to grain (E)	Average modulus of rigidity (G)	Bearing: Perpendicular to grain (f'_p)	Bearing: Parallel to grain (f'_l)	Shear at joint details (f'_{sj})	Tension perpendicular to grain (f'_{tp})	(kg/m^3)	
MGP 10	70 to 140	35 and 45	17	7.7	18	2.6	10 000	670	10	30	4.2	0.5	500	JD5 (see Note 2)
	190		16	7.1	18	2.5								
	240		15	6.6	17	2.4								
	290		14	6.1	16	2.3								
MGP 12	70 to 140	35 and 45	28	12	24	3.5	12 700	850	10	30	4.2	0.5	540	JD4
	190		25	12	23	3.3								
	240		24	11	22	3.2								
	290		22	9.9	22	3.1								
MGP 15	70 to 140	35 and 45	39	18	30	4.3	15 200	1 010	10	30	4.2	0.5	570	JD4
	190		36	17	29	4.1								
	240		33	16	28	4.0								
	290		31	14	27	3.8								
A17	70 to 120	35	45	26	40	5.1	16 000	930	17	50	6.0	0.6	650	JD3
		45	40	24	35	4.5								
	140, 190	35	45	24	35	4.5								
		45	40	21	32	4.0								
	240, 290	35	40	18	27	3.6								
		45	40	17	25	3.3								

2.4 Analysis of Graphene Nanocomposites

2.4.1 Graphene with Timber

In a research conducted by Sheshmani et. al. (2013) which has successfully improved the mechanical and physical properties of wood polymer composites filled with graphene nanocomposites. This study focus on investigating the reinforcement effect of graphene nanoplatelets in wood polymer composites, in this case, wood flour has been used as the research species rather than raw timber. By adding 0.8 w.t.% of graphene nanoplatelets into the wood polymer, the composites have increased the tensile and flexural strength compared to the unreinforced composites. With the further addition of 0.8 w.t.%, it has yielded further improvement in the reinforcing effect, which was believed to be the result of nanoparticle agglomeration (Sheshmani et. al. 2013).

A study conducted by Macias et. al. (2018) identified that agglomeration of graphene sheets can cause unfavourable effects on the overall stiffness of the nanocomposites. Another depended variable that can contribute to the mechanical and physical properties of composites are the particle content, shape, size, surface interfaces and the degree of dispersion. Therefore the importance of incorporating an efficient and reliable dispersion technique is required to obtain the optimal results for reinforcing composites (Macias et. al. 2018).

2.5 Other Methods Used in Strengthening Timber Member Structures

2.5.1 Reinforced Planks Connected by Dowels to Main Beam

Various strengthening methods are available in reinforcing timber designs using either innovative or traditional methods. Traditional methods involved placing reinforced planks above the existing timber beam and fixing them with wooden dowels shown in Figure 2. The flexural strength of a timber bream has proven to be improved using this method. Furthermore, this method has been applied in numerous case studies, for example, the University of Padova has successfully adopted this method, and therefore has signified the reliability of this method (Valluzzi et. al. 2007).

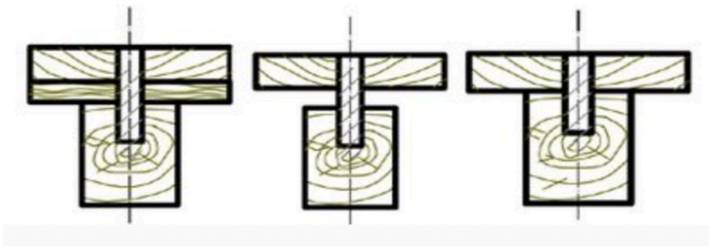

Figure 2: Method of using planks as reinforcement and dowels as the bonding material (Valluzzi et. al. 2007)

2.5.2 Strength Enhancement using Steel Plates Bonded to Beam

One of the oldest technique used in reinforcing timber structure is the use of adhesive to bond the steel plates, aluminium sheet or rods, placed inside the beam, as shown in Figure 3. Borgin et. al. (1968) conducted research in the early 1960s, using epoxy to bond steel plates inside the beam in the compression zone. The experiment shows that the beam was only reinforced in the compression zone, while the tension zone of the beam suffered extraordinarily. Overal, the experiment still shows a satisfactory increase in stiffness and loading capacity on the reinforced beam (Nowak et. al. 2016).

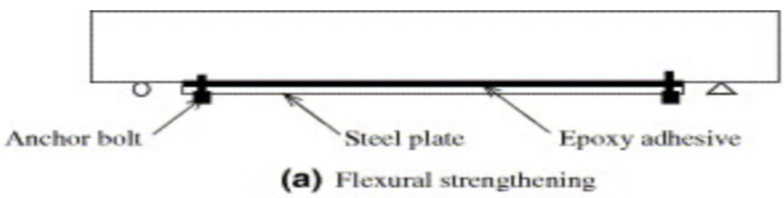

Figure 3: Steel plate bonded towards the tension side of the beam (Nowak et. al. 2016)

2.5.3 Fibre reinforcement polymer enhancement

The approach of strengthening infrastructures component using fibre reinforced polymer composites (FRP) as an enhancement or substitute has also become increasingly popular in today's civil industry. Mainly glass or carbon fibres are the preferable commercial material for thermosetting polymers, such as epoxy or polyester resins. These FRP composites continuously expand at an extraordinary rate, as this material can be located in almost all type of civil infrastructures such as bridges and buildings. This is due to the light weighted, non-corrosive, easily constructed, high specific strength and stiffness, and most importantly the new advance forms of FRP materials (Masuelli 2013). The aim of this is to improve the structural integrity of degraded materials with a simple and cost-efficient approach, such as using the FRP composites.

Recently the FRP composites have proven success in bonding with reinforced concrete, pre-stressed concrete, cast iron, and steel and timber structures to repair and strengthen those structures. Numerous research has shown that FRP composites bonded with a different structural member can increase the structural stiffness and load capacity beyond the achievement of conventional methods. A research project 'Bridging the Gap' was conducted through the collaboration of CEEFC, CarbonLOC, Wagners CFT and QDTMR focusing on replacing degraded girders in existing timber bridges in Queensland. This has increased the Australian market of commercially feasible fibre composite bridge beams and satisfying the requirement of the load and performance criteria of stiffness and strength provided by QDTMR (Aravinthan & Manalo 2012).

Plevris, N and Triantafillou T.C. (1992) have conducted research on the use of fibre composites from the department of a civil engineer at Massachusetts Institute of Technology, Cambridge MA. This research shows the analytical and experimental research on the FRP applied to the tension zone of the timber beam. Three-point bending test is conducted on the reinforced timber beam to yield the flexural strength and modulus of the members. A sudden rupture of the FRP was observed, immediately the wood shows a fracture in the tension zone, causing the specimen to collapse. This result shows that the FRP has successfully carried the loading of the specimen until rupture occurs causing the specimen to fail. This experiment had successfully enhanced the member's strength, stiffness and ductility, by means of epoxy resin as the bonding adhesive (Plevris & Triantafillou 1992).

2.6 Summary

Based on prior research, it can be seen that increasing the percentage of GPL would ultimately increase the tensile strength and elastic modulus of the composites. Additionally, prior research has investigated the bending behaviour of timber structures reinforced with materials, such as fibre-polymer, plank reinforcement and steel plate's reinforcement, which has generated successful results. These past researches will enable the gathering of data to make reliable predictions on the behaviour of timbers reinforced with nanocomposites. This research will focus on determining the flexural strength and modulus of timber material reinforced with GPL/polymer nanocomposites. Further to this, the FEA is conducted to validate the experimental data's. To achieve this, it was necessary to identify the material properties of the nanocomposites and timber materials used in this study. In-depth analyses are conducted throughout the next Chapter on the material properties of MGP10 and GPL/polymer nanocomposites, based on Australian Standards, Halpin-Tsai micromechanics model and rule of mixture.

Chapter 3 Materials Properties

3.1 Introduction

The objective of this research project is to investigate the ultimate flexural strength and stiffness of each MGP10 members reinforced with GPL/polymer nanocomposites layers through experimental procedures. Strand7 FE software was used to validate the results obtained from the experiment to guarantee a reliable analysis. To provide high accuracy of results, the material properties for timber and GPL/polymer nanocomposites layer has been determined.

This chapter will focus on identifying the material properties for MGP10 structural pine of cross-section; 70 mm by 45 mm, 70 mm by 35 mm and 45 mm by 70 mm. In addition to this, the effective material properties for GPL/polymer nanocomposites layer will also be determined. This was achieved by implementing micromechanics analyses based on the Halpin-Tsai model, which assisted in predicting the effective modulus of elasticity of the GPL/polymer nanocomposites. Rule of mixture was also used to obtain the Poisson ratio and effective mass density at a different percentage of weight fraction. These important findings will then be inputted into Strand7 FE software in Chapter 5.

3.2 Timber Material Properties

The evaluation of MGP10 timber elastic strength and elastic properties are required to model the timber member with precise accuracy. All members are modelled as an isotropic element; therefore, Strand7 software requires the input of the thermal expansion K, Poisson ratio v, density ρ and modulus of elasticity MOE. The elastic properties of MGP10 can be found in AS1720.1:2010 Structural Timber - Design Methods Table H3.1. As there is no explicit information on the Poisson ratio for MGP10 timber, another similar Australian grown pine specimen is known as the slash pine with a Poisson ratio of 0.444 was used in this study instead (Green et. al. 1999). The timber properties that were selected for the purpose of this studies are presented in Table 6. Note that additional information on rolling shear modulus G was also provided.

Table 6: Timber material properties for Strand7 FE model.

Material Property	MGP10
E	10 000 MPa
G	670 MPa
v	0.444
ρ	500 $(\mathrm{kg/m^3})$
K	5 K^{-1}

3.3 Material Properties of GPL/polymer Nanocomposites

Numerous research has suggested the use of graphene to increase the strength of the thermoplastic matrix, which can then be applied onto infrastructures as reinforcement. In most cases, combining graphene with epoxy composites has shown favourable results, leading to higher strength improvement compared to pure epoxy. In the least favourable resulting cases, it only showed minor decreases in strength, this might be due to the poor dispersion of graphene in the epoxy resin, and consequently, the results from the experiment will primarily be influenced by the dispersion of the GPL/polymer nanocomposites (Pal 2008).

The material properties of GPL/polymer nanocomposites depend largely on the fillers properties, area of interface and the strength of the intermolecular interface. In-depth research has suggested the effectiveness of using the modified Halpin-Tsai micromechanics model to predict the elastic properties of nanocomposites materials, specifically for short fibre composites. Lewis and Nielsen considered an additional parameter, which is the aspect ratio of the fillers. As a result, this has further improved the prediction ability of the original Halpin-Tsai model (Young et. al. 2018).

The effective modulus of elasticity of the GPL/polymer nanocomposites layer can be calculated using the Voigt-Reuss model below (Villoria & Miravete 2007):

$$E_c = \frac{3}{8}E_L + \frac{5}{8}E_T \tag{2}$$

Reuss model have adopted $E_L$and E_T which are the longitudinal and transverse modulus, respectively, that fail to take into account any geometry of the reinforcement, therefore using Halpin-Tsai model, which has considered five independent parameters, proves more reliable results (Villoria & Miravete 2007).

$$E_L = \frac{1 + \xi_L \eta_L V_f}{1 - \eta_L V_f} E_m \tag{3}$$

$$E_T = \frac{1 + \xi_W \eta_T V_f}{1 - \eta_T V_f} E_m \tag{4}$$

The volume fraction (V_f) of the effective fibre is given by:

$$V_f = \frac{g_f}{g_f + (\rho_f/\rho_M)(1 - g_f)} \tag{5}$$

where g_f is the weight fraction of fibre (graphene nanocomposites) and ρ_f and ρ_M is the mass density of fibre and polymer (epoxy resin) (Villoria & Miravete 2007).

The characteristics of geometry and size of the graphene nanocomposites fibres are given as: (Villoria & Miravete 2007).

$$\xi_L = 2\left(\frac{l_f}{h_f}\right) \tag{6}$$

$$\xi_W = 2\left(\frac{\omega_f}{h_f}\right) \tag{7}$$

$$\eta_L = \frac{\left(\frac{E_f}{E_m}\right) - 1}{\left(\frac{E_f}{E_m}\right) + \xi_L} \tag{8}$$

$$\eta_T = \frac{\left(\frac{E_f}{E_m}\right) - 1}{\left(\frac{E_f}{E_m}\right) + \xi_W} \tag{9}$$

where E_m are Young's modulus of the epoxy matrix, η_T and η_L are the stress partitioning factors for the fibre and matrix respectively, l_f is the average length, h_f is the average thickness and ω_f is the average width of the fibre (Villoria & Miravete 2007).

Substituting equations 3 and 4 into equations 2 yields the modified Halpin-Tsai model shown below:

$$E_c = \frac{3}{8}\frac{1 + \xi_L \eta_L V_f}{1 - \eta_L V_f} E_m + \frac{5}{8}\frac{1 + \xi_W \eta_T V_f}{1 - \eta_T V_f} E_m \tag{10}$$

3.4 Rule of Mixture

Rule of mixture is a method used to predict the composite material properties as a weighted means. Through the practices of rule of mixture, the effective mass density (ρ_c) and effective Poisson's ratio (v_c) of the GPL/polymer nanocomposites can be calculated as (Liu 1997):

Density:

$$\rho_c = \rho_m * V_m + \rho_f * V_f \tag{11}$$

where;

ρ_c, ρ_m, ρ_f – Densities of the Composite, matrix and dispersed phase

V_m, V_f – volume fraction of the matrix and dispersed phase

Poisson's Ratio:

$$v_c = V_f v_f + V_m v_m \tag{12}$$

where;

v_f, v_m – Poisson's ratio of fibre material and matrix material, respectively.

The GPL dimensions that would be adopted into the study are $l_f = 2.5\ \mu m$, $\omega_f = 1.5\ \mu m$ and $h_f = 1.5\ nm$ (Rafiee et. al. 2009). The material properties of epoxy resin and graphene nanocomposites, as shown in Table 7, and GPL dimensions are based on previous literature from Yasmin & Daniel (2004) and Rafiee et. al. (2009), which will assist in determining a good approximation of the effective material properties of GPL/polymer nanocomposites. The materials properties that are used to calculate the effective material properties of GPL/polymer nanocomposites layers based on several percentages of weight fraction are tabulated in Appendix C.

Table 7: Material Properties of Epoxy and Graphene Nano-platelets

Material	Material Property		
Epoxy	$E\ (GPa)$	3.0	Yasmin & Daniel 2004
	ν	0.34	Yasmin & Daniel 2004
	$\rho\ \left(\frac{kg}{m^3}\right)$	1200	Rafiee et. Al. 2009
GPL	$E\ (TPa)$	1.01	Rafiee et. Al. 2009
	ν	0.186	Rafiee et. Al. 2009
	$\rho\ \left(\frac{kg}{m^3}\right)$	1060	Rafiee et. Al. 2009

3.5 Summary

This chapter has successfully determined the methods to achieve the effective modulus of elasticity, effective mass density and effective Poisson's ratio for GPL/polymer nanocomposites based on the Halpin-Tsai micromechanics model and rule of mixture, respectively. The effective material properties of GPL/polymer nanocomposites are calculated based on 0.25 and 0.5 per cent of weight fraction. The material properties for MGP10 structural pine member were obtained from the Australian Standards. These material properties are then used for FEA in chapter 5. The aim of obtaining the material properties of MGP10 and GPL/polymer nanocomposites is to accurately simulate the experiment results. The following chapter will focus on the preparation procedure of GPL/polymer nanocomposites, and conducting flexural testing to determine the bending behaviour for each member reinforced with the GPL/polymer nanocomposites.

Chapter 4 Member Deflection Testing

4.1 Introduction

This chapter investigates the preparation procedure for the different graphene-epoxy ratio used in this experiment and determining the flexural strength, modulus, ultimate deflection, and loading of each member subjected to loading of 1 mm per minute, using the Sans Machine. This analysis contributes to the knowledge and framework of GPL/polymer nanocomposites as the new reinforcement material. For this study, The Graphene Manufacturing Group (GMG), located in Brisbane, provided graphene in a powder form. The epoxy resin (Jotacote 605) was obtained from Jotun, which is a worldwide company specialises in supplying paints and coatings (Jotun 2019). The safety data sheets for Jotacote 605 and graphene is shown in Appendix A. All MGP10 structural pine members were obtained from Bunnings. Note that a visual observation was undertaken, which identifies several defects within the timber members to be a contributing factor towards the experiment. These defects would be further discussed in this chapter. GMG assisted in mixing 1 per cent of graphene (200 grams of graphene) into the Resin (Part A) consisting of 2 Litres. Figure 4 show the hardener (Part B) and graphene/resin (Part A) that are used for this experiment.

The objective of this experiment is to test all individual member with a cross-sectional area of; 70 mm by 45 mm, 35 mm by 70 mm and 45 mm by 70 mm reinforced with different graphene-epoxy ratio. The first ratio for testing is 0.5% graphene and 99.5% epoxy, and the second ratio for testing is 0.25% graphene and 99.75% epoxy. Based on previous literature on graphene, this experiment is predicted to yield effective results at a higher percentage level of graphene in the graphene/epoxy mix. In other words, using 0.5% graphene and 99.5% epoxy is expected to yield more effective results compared to the control samples and the members reinforced with 0.25% graphene.

Figure 4 Jotacote 605 Fast Cure Comp B (Hardener) on the left and the Comp A (Resin) is shown on the right.

This experiment aims to determine the effectiveness through the structural behaviour of the MGP10 and radiata members reinforced with GPL/polymer nanocomposites, the test samples are shown in Figure 5. To understand the structural behaviour of the reinforced members, three-point bending test is carried out to determine the deflection of the member at mid-span of the beam, subjected to a loading condition of 1 mm per minute. In return, the deflection that is obtained would provide an understanding of the effectiveness of using reinforced GPL/polymer nanocomposites as an alternative beam enhancement method.

Figure 5: MGP10 structural and radiata pine test samples

4.2 Methodology

4.2.1 Mixing and Diluting Graphene and Epoxy into Desired Ratio

In order to obtain the correct ratio of graphene and epoxy needed for the experiment, equation 13 was used to dilute Ratio 1 (0.5% Graphene/ 99.5 Epoxy) and Ratio 2 (0.25 Graphene and 99.75 Epoxy)

$$C_1V_1 = C_2V_2 \tag{13}$$

C_1 is a concentration of graphene, V_1 is the volume of graphene needed to create the new solution, C_2 is the final concentration of the new solution and V_2 is the final volume of the new solution. Using this equation, the new concentration was calculated for the new ratio, as shown below (Bintzler 2018);

Ratio 1: (0.5%Graphene/99.5%Epoxy)

$$C_1V_1 = C_2V_2$$
$$0.01 \times 0.5 = C_2 \times 1$$
$$C_2 = 0.005 = 0.5\%$$

Mixing 0.5 litres of 1% graphene/resin and 0.5 litres of hardener would dilute the graphene down to 0.5%, producing a total of 1 litre of 0.5% graphene and 99.5% epoxy.

Ratio 2: (0.25%Graphene/99.75%Epoxy)

$$C_1V_1 = C_2V_2$$
$$0.01 \times 0.25 = C_2 \times 1$$
$$C_2 = 0.0025 = 0.25\%$$

Mixing 0.25 litres of 1% graphene/resin and 0.75 litres of hardener would dilute the graphene down to 0.25%, producing a total of one litre of 0.25% graphene and 99.75% epoxy. Electric mixing paddles were used to mix ratio one and two proficiently at high speed to obtain the required solution, as shown in Figure 6. Note that the accurate method is to mix the product by volume at the same ratio; however, one percentage of graphene has been mix with the resin beforehand, through the assistance of GMG. This error is irreversible and has consequently resulted in an incorrect mix of 3:1 ratio between the graphene/resin and the hardener. Due to this reason, it was predicted that the experimental results would be affected due to the low amount of hardener within the 0.25% graphene solution.

Figure 6: 0.25% Graphene and 99.75% Epoxy (on the left) and 0.5% Graphene and 99.5% Epoxy (on the right)

The required quality of surface preparation for this experiment can vary depending on the area used, in this case when preparing the surfaces for painting; it is required to ensure that the surface is free from residual corrosion and is suitable for painting. The drying and curing time for Jotacote 605 Fast Cure is recommended to be four days at a substrate temperature of $23°C$, which means four days is the minimum time before the coating can be permanently exposed to the intended environment. The coating of ratio one and two were applied to the width of the members using a paintbrush; extreme care was taken into consideration to avoid excessive film thickness, as shown in Figure 7. Both sides of all individual members used for testing was applied so the tension and compression side can be tested, using the Sans machine shown in Figure 8.

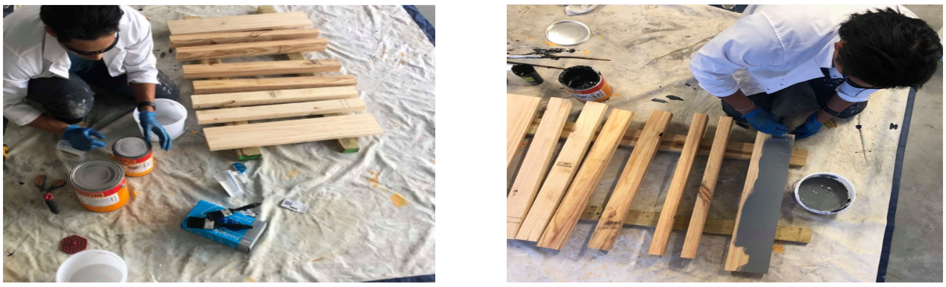

Figure 7: Preparing and applying the nanocomposites coating to the timber materials.

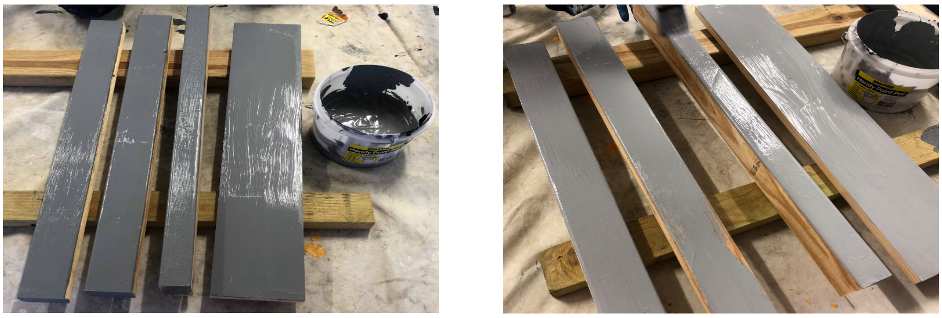

Figure 8: Ratio one and two fully coated on both side of the timber material

4.2.2 Machine Testing

After 4 days of sufficient curing time, all timber members shown in Table 8 with a span of 700 mm was subjected to three-point loading. This experiment was conducted to determine the flexural strength and modulus for the reinforced MGP10 structural pine, which is then used for Strand7 FE modelling.

Table 8: All test samples with its cross section and graphene-epoxy ratio

Sample 1	Solution 1 (0.5% Graphene) – 70 mm x 45 mm
Sample 2	Solution 1 (0.5% Graphene) – 70 mm x 35 mm
Sample 3	Solution 1 (0.5% Graphene) – 45 mm x 70 mm
Sample 4	Solution 1 (0.5% Graphene) – 184 mm x 19 mm
Sample 5	Solution 2 (0.25% Graphene) – 70 mm x 45 mm
Sample 6	Solution 2 (0.25% Graphene) – 70 mm x 35 mm
Sample 7	Solution 2 (0.25% Graphene) – 45 mm x 70 mm
Sample 8	Solution 2 (0.25% Graphene) – 184 mm x 19 mm
Sample 9	Control Sample – 70 mm x 45 mm
Sample 10	Control Sample – 70 mm x 35 mm
Sample 11	Control Sample – 45 mm x 70 mm
Sample 12	Control Sample – 184 mm x 19 mm

The supports were placed 250 mm relative to the centre line of the loading, which leaves an overhang of 100 mm on both sides of the members. This would result in a simply supported beam with a distance of 500 mm between supports as shown in Figure 9 and 10. A 40 mm by 40 mm steel tube was placed in the centre line of the loading rig to distribute a bending load of 1 mm per minute constantly across the width of the member as shown in Figure 10.

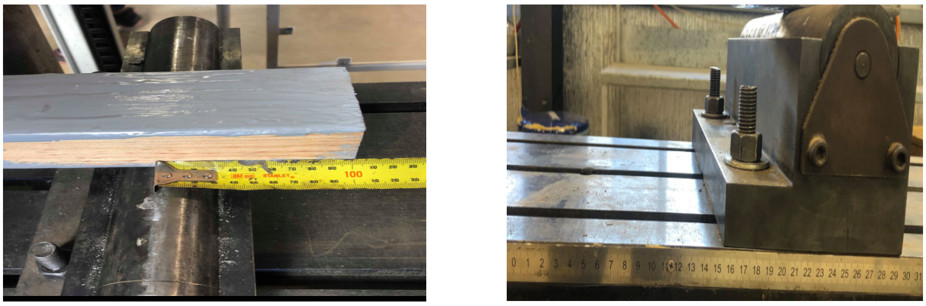

Figure 9: 100 mm overhang of the member

Figure 10: 40 mm x 40 mm steel tube used in the experiment (on the left) and 500 mm from loading to support (on the right)

The movement of the support was fixed using bolts shown in Figure 11 to ensure that the alignment of each sample does not vary relative to the central axis. The maximum deflection results were obtained electronically at the centre location of each member, which are then used to plot a load-displacement graph. All testing of members was undertaken until multiple failures were observed to obtain an accurate description of the pattern of loading and failure.

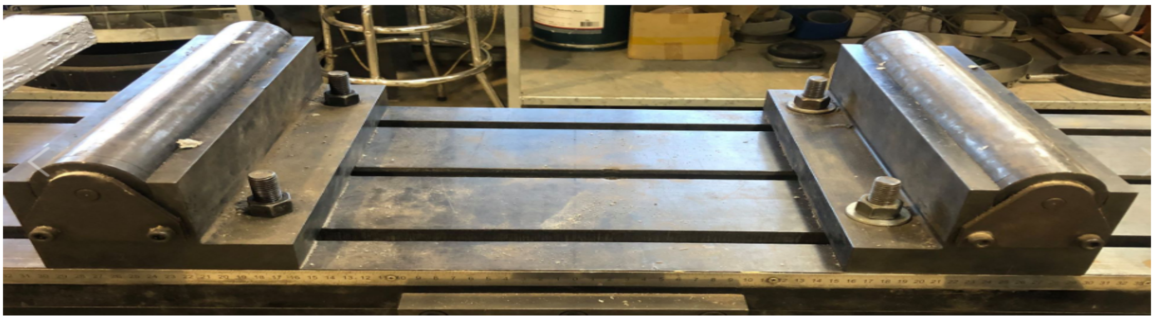

Figure 11: Supports was placed 250 mm away from the centre line. Note that the support was bolted on the table to allow no movement.

Equation 14 describes the deflection behaviour of a rectangular beam subjected to three-point loading, as shown in Figure 12, behaving as an isotropic linear material (Hibbeler 2006). The theory to determine the flexural modulus (MOE) and flexural strength (MOR) are shown below, which would provide information on the effectiveness of the reinforcement for the timber materials.

$$\delta = \frac{PL^3}{48EI} \tag{14}$$

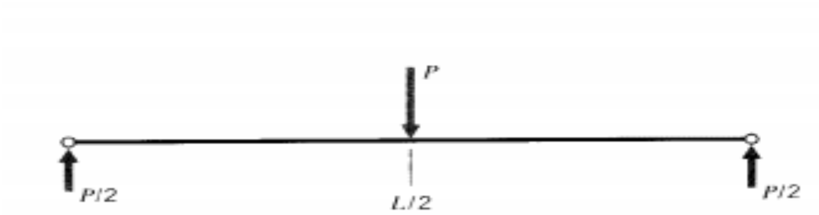

Figure 12: Three-point bending diagram (Beer, et. al. 2015)

Modulus of Elasticity:

Modulus of elasticity can be identified as the material resistance to bending, which can be determined through the load-deflection curve produce from the flexural testing (Engineers Edge 2019). The results from the testing were analysed through an excel spreadsheet, which was able to produce a load-deflection curve. The load-deflection curve is then used to determine the slope for each sample, that can represent the linear portion of the graph, combined with equation 15, it was then possible to determine the MOE of a timber member subjected to three-point loading.

$$E = \frac{L^3 m}{4bd^3}; \quad m = \frac{P_2 - P_1}{\delta_2 - \delta_1} \tag{15}$$

where; L = The length between the span

b = The width of the beam

h = The depth of the beam.

P_2 = Maximum load applied in the linear portion of the load-deflection graph

P_1 = Minimum load applied in the linear portion of the load-deflection graph

δ_2 = Deflection corresponding to P_2

δ_1 = Deflection corresponding to P_1

Modulus of Rupture:

Modulus of rupture, also known as flexural strength is defined as the maximum stress the material can support at its yielding point. It is measured in term of stress, which is given in equation 16 (Beer et. al. 2015).

For a rectangular member under three-point loading:

$$\sigma = \frac{3PL}{2bh^2} \tag{16}$$

where P is the load (force) at the fracture point.

It was observed that there was an inconsistency in thickness when applying the nanocomposite layer onto the samples, which varies from 0.5 mm to 1 mm. In this study, the coating of GPL/polymer nanocomposites layer is assumed to be 1 mm on the top and bottom of each members, as shown in Figure 15a, b, c and d. Note that E1 is the GPL/polymer nanocomposites layer and E2 is the timber members used in the experiment. In order to consider the realistic MOE, it is necessary to identify the realistic depth of the reinforced member; therefore, the new depth that is to be used for analysis includes the nanocomposites layer are; 70 mm by 47 mm, 70 mm by 37 mm, 45 mm by 72 mm and 184 mm by 21 mm. Furthermore, the applied load (P) is distributed evenly along the width of each members as shown in the Figure.

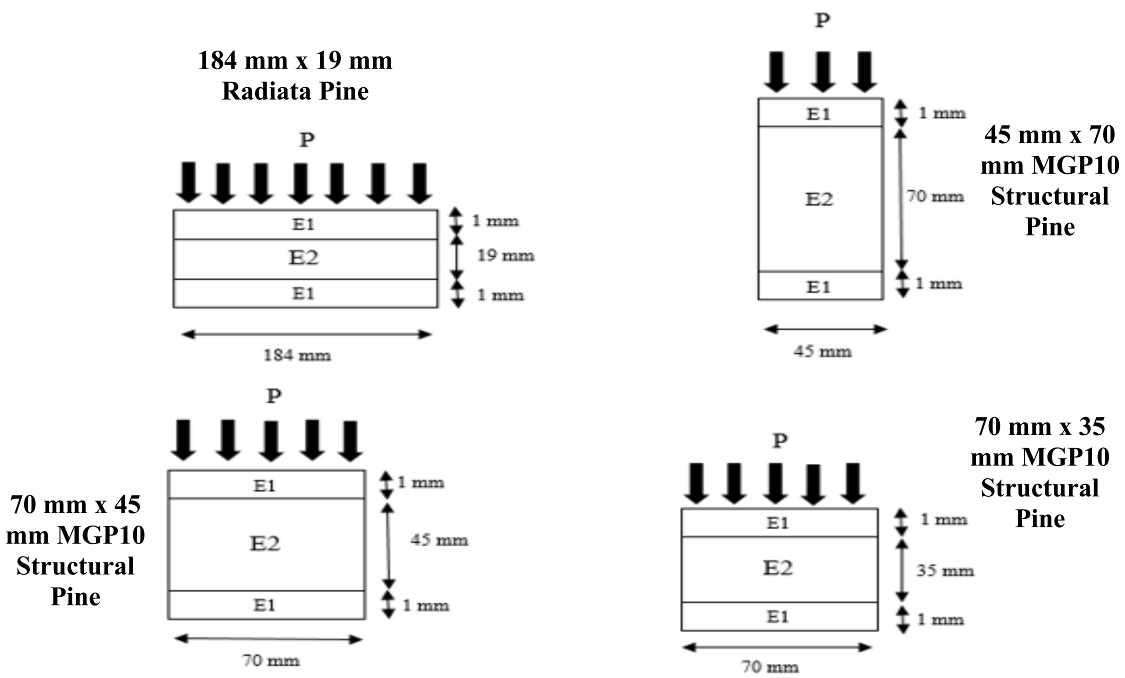

Figure 13: The dimension of each timber used for testing and the location of the applied loads.

4.3 Results and Discussion

4.3.1 Defects within Timber

It is well known that timber is a naturally grown material, and every natural material has some limitations. Most of the problems that lie within the timber members are due to the natural defects that can impact the strength of the timber member, which constitutes a major unpredictability during the experiment. As previously mentioned in the literature review, the most common type of defect presented in wood is known to be knots, twist and shakes. During the experiment, several knots were observed, as shown in Figure 15, especially, the presence of a dead knot, has affected the strength of timber members drastically. Crack propagation along the grain direction of each sample was greatly affected by the close vicinity of the knot, which resulted in a reduction of the member's fracture strength.

Figure 14: Defects observed before the coating of the nanocomposites.

Cracking on the members due to the weak section around the knots is visible in all of the samples, resulting in a reduction of MOE compared to the recommended value from the Australian Standards, which are discussed later on.

4.3.2 Failure Mode

The typical failure modes are shown in Figure 15, which is subjected to a loading of 1 mm per minute. The samples used in the experiment show the grain running parallel to the timber members. The loading applied to the central location of the members continues until the fibre stresses in the tensile zone reach the failure strength of the members and brittle fracture occurs. It was shown that there was a bearing deformation accumulated at the loading head, however, the stresses continued to increase at the central part of the members, quickly after, the maximum tensile strength of the members in the bottom fibres is reached and fast-growing cracks occurred. Comparatively, members with the cross-sections of 45 mm by 70 mm exhibited a diagonal shear failure from the base support of the member, which could be restored to its original form again, after the load are released, as shown in Figure 15a, 15e and 15i. The other cross-sections cannot be restored to their original form after the first crack was observed.

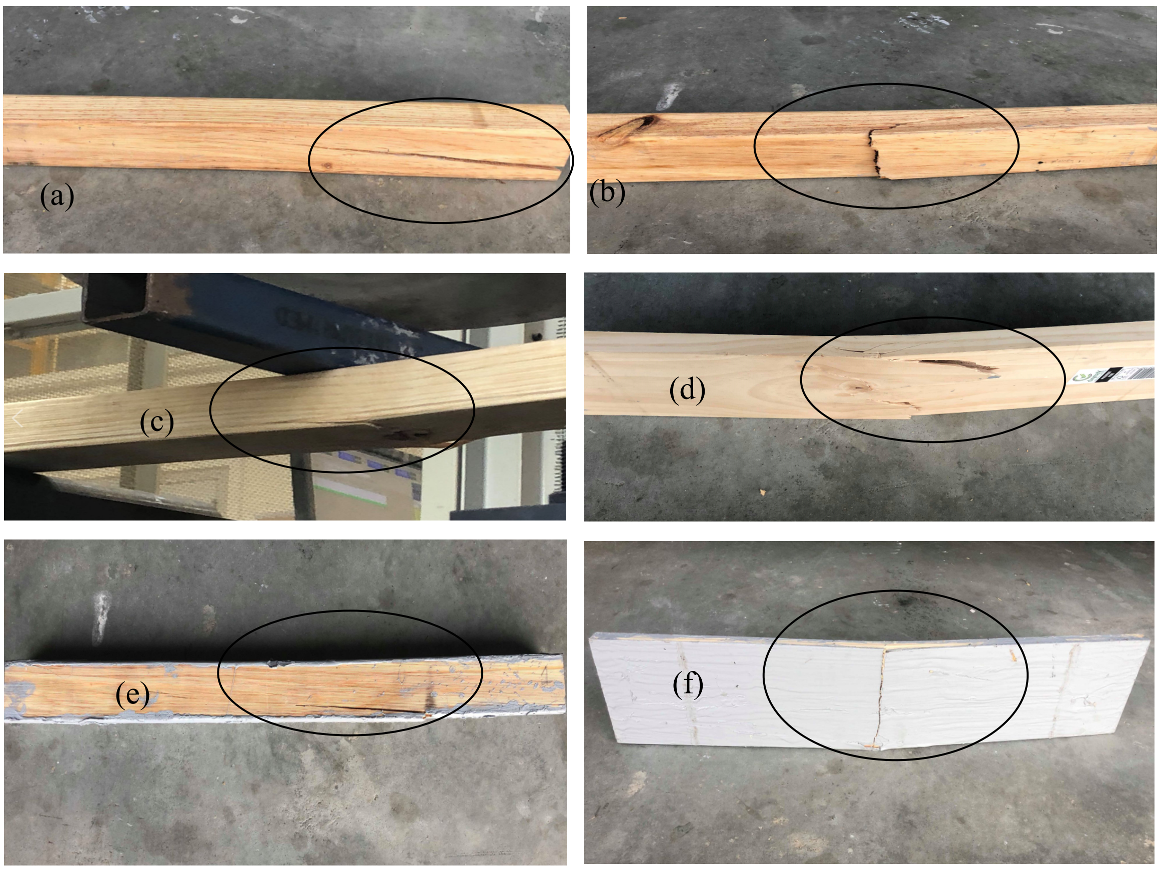

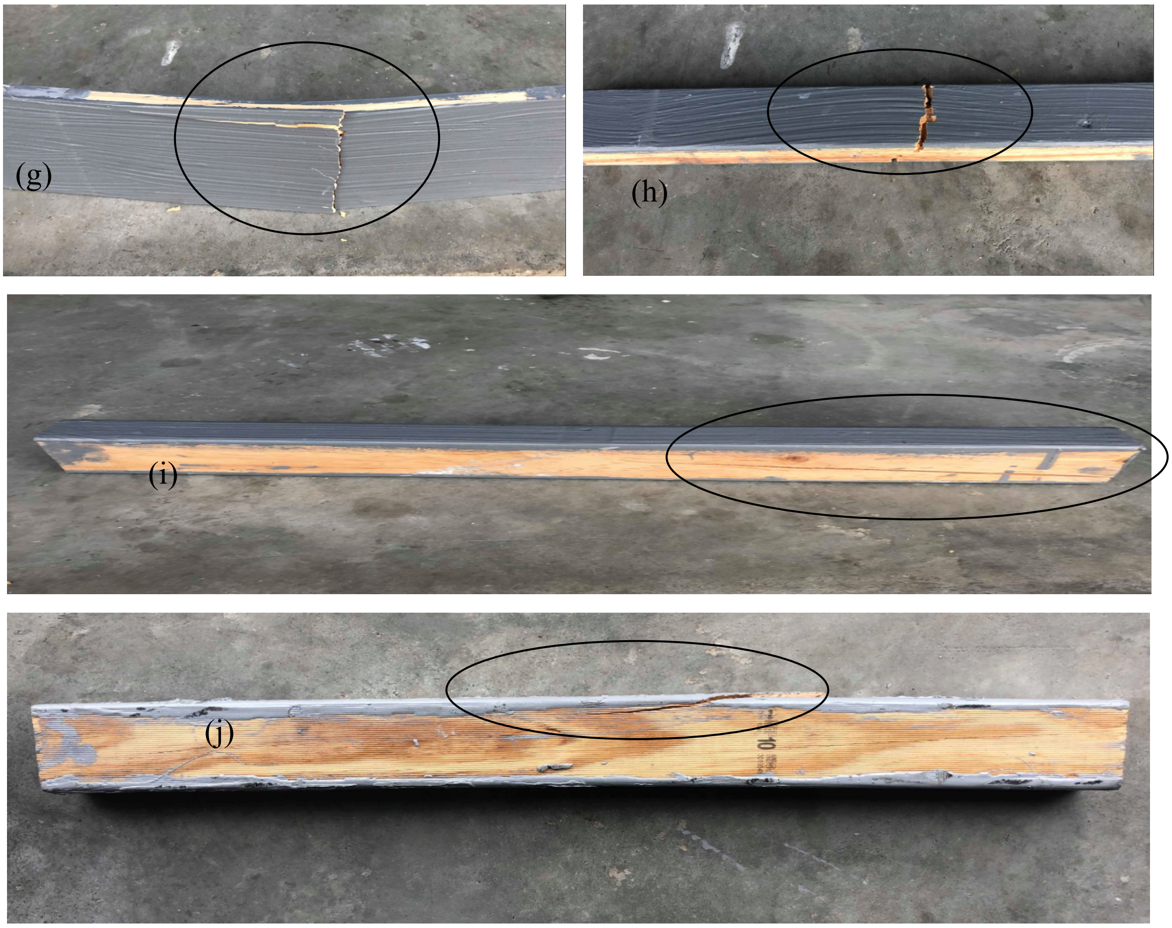

Figure 15: Cracks and failure mode observed after testing

The failure mode for the members reinforced with 0.25% and 0.5% graphene experience a ductile behaviour, which shows numerous cracks until the point of rupture was reached, this can be supported by the load-deflection graph in Figure 16, 17, 18 and 19 below. In contrast to this, the member with cross-section 45 mm by 70 mm shows a brittle bending failure, which observed a very abrupt and rapid cracking with little evidence of ductility or plastic deformation before the fracture occurs. Additional image of the crack and fracture are presented in Appendix B.

4.3.3 Un-reinforced (Control Samples) MGP10 Members

An Excel spreadsheet was developed to determine the MOE and MOR for the control samples (Sample 9, 10, 11 & 12) based on equation 15 and 16 that was discussed previously. The average MOE for MGP10 structural pine (samples 9, 10 & 11) and the radiata pine (sample 12) was determined to be 6342 MPa and 4675.45 MPa, respectively, as shown in Table 9 and 10. In addition to this, the MOR for MGP10 structural pine and the radiata pine was calculated to be 56.9 MPa and 40.6 MPa respectively. These values would be used to compare against the members reinforced with 0.25% and 0.5% graphene to demonstrate the effectiveness of the reinforcement.

Table 9: Ultimate load and deflection, MOE and MOR for Control Samples.

Samples	Ultimate Load (kN)	Ultimate Deflection (mm)	MOE (MPa)	MOR (MPa)
Sample 9 (70 mm x 45 mm)	14.626	11.676	7898.555	77.3
Sample 10 (70 mm x 35 mm)	6.906	11.286	7057.83	60.4
Sample 11 (45 mm x 70 mm)	9.707	9.214	4069.587	33
Sample 12 (184 mm x 19 mm)	3.599	27.949	4675.45	40.6

Table 10 Average MOE and MOR for Control Samples.

<table>
<tr><th>Samples</th><th>Average MOE (MPa)</th><th>Average MOR (MPa)</th></tr>
<tr><td>Sample 9 (70 mm x 45 mm)</td><td rowspan="3">6342</td><td rowspan="3">56.9</td></tr>
<tr><td>Sample 10 (70 mm x 35 mm)</td></tr>
<tr><td>Sample 11 (45 mm x 70 mm)</td></tr>
</table>

4.3.4 Reinforced MGP10 Members

The ultimate load and MOR for the member reinforced with 0.25% and 0.5% graphene are presented in Table 11 and 12 respectively. Compared to the control samples in Table 9 and 10, all the reinforced members were significantly enhanced in flexural strength. The average flexural strength for the MGP10 members reinforced with 0.5% and 0.25% graphene was calculated to be 61.2 MPa and 70 MPa, this shows that there is an average increase of 8% and 23% respectively, compared to the control samples. Similarly, the radiata member of cross-section 184 mm by 21 mm also displayed an increase of 20% and 26% respectively. In both cases, the members reinforced with 0.25% graphene can undergo a higher stress level before yielding, compared to the control samples and the 0.5% graphene members.

The members that exhibit a higher flexural strength should result in a lower deflection to satisfy the initial assumption. However, Table 16 shows that the deflection for the MGP10 members reinforced with 0.5% graphene has an average increase of 36%, while the 0.25% graphene members only increased by 13.4%. Similarly, the radiata pine reinforced with 0.5% and 0.25% graphene displayed an average increase of 62% and 30% respectively, as shown in Table 15. These values indicate that, although the reinforced members exhibit an increase in flexural strength, it has failed to reduce its deflection, compared to the control samples. Furthermore, the results also imply that by applying a ratio of 0.25% graphene and 99.75% epoxy, as a reinforcement coating, it can effectively resist deformation under the same loading condition, with a relatively low deflection compared to the members reinforced with a higher content of graphene. Note that there is a 13% decrease in deflection for members with a cross-section of 45 mm by 70 mm reinforced with 0.25% graphene, compared to the control samples. This has proven to be the most effective results, due to its high flexural strength and low deflection, compared to the control samples.

Table 13 and 14 present the MOE results for the reinforced radiata and MGP10 members, respectively, compared against the control samples. The MGP10 members reinforced with 0.5% graphene shows an average MOE reduction of 6%; this proves that the member can easily deform but does not fail under the same load, compared to the control samples. In contrast, members reinforced with 0.25% graphene shows an improvement in MOE, which increased by 14%, meaning that it can withstand a higher loading with little deformation, compared to the control samples and the 0.5% graphene members. The material stiffness is dependent on the MOE, while the material strength is dependent on the material MOR. In-order to obtained favourable results, its necessary to increase the span to depth ratio of the member, since the moment of inertia is a major influencing factor on the members MOE and MOR.

Ultimate Load and Modulus of Rupture for Radiata Pine and MGP10 Structural Pine Compared to the Control Samples

Table 11: Comparing the MOR values between the Radiata Pine and Control Samples reinforced with 0.5% and 0.25 Graphene.

Reinforcement	Samples	Ultimate Load (kN)	MOR (MPa)	Enhancing Ratio (%)
0.5% Graphene	**Sample 4 (184 mm x 21 mm)**	5.273	48.737	20
0.25% Graphene	**Sample 8 (184 mm x 21 mm)**	5.546	51.260	26

Table 12: Comparing the MOR values between the MGP10 Structural Pine and Control Samples reinforced with 0.5% and 0.25 Graphene.

Reinforcement	Samples	Ultimate Load (kN)	MOR (MPa)	Average MOR (MPa)	Enhancing Ratio (%)	Average Enhancing Ratios (%)
0.5% Graphene	**Sample 1 (70 mm x 47 mm)**	15.606	75.694	61.2	-2	8
	Sample 2 (70 mm x 37 mm)	9.352	73.192		21	
	Sample 3 (45 mm x 72 mm)	10.82	34.787		5	
0.25% Graphene	**Sample 5 (70 mm x 47 mm)**	17.113	83	70	7	23
	Sample 6 (70 mm x 37 mm)	11.3	88.438		46	
	Sample 7 (45 mm x 72 mm)	11.772	37.847		15	

Modulus of Elasticity for Radiata Pine and MGP10 Structural Pine Compared to the Control Samples

Table 13: Comparing the MOE values between the Radiata Pine and Control Samples reinforced with 0.5% and 0.25 Graphene.

Reinforcement	Samples	MOE (MPa)	Enhancing Ratio (%)
0.5% Graphene	**Sample 4 (184 mm x 21 mm)**	3715.59	-21
0.25% Graphene	**Sample 8 (184 mm x 21 mm)**	5172.462	11

Table 14: Comparing the MOE values between the MGP10 Structural Pine and Control Samples reinforced with 0.5% and 0.25 Graphene.

Reinforcement	Samples	MOE (MPa)	Average MOE (MPa)	Enhancing Ratio (%)	Average Enhancing Ratios (%)
0.5% Graphene	**Sample 1 (70 mm x 47 mm)**	6268.077	5956.85	-21	-6
	Sample 2 (70 mm x 37 mm)	8043.32		14	
	Sample 3 (45 mm x 72 mm)	3559.147		-13	
0.25% Graphene	**Sample 5 (70 mm x 47 mm)**	8170.832	7205.04	3	14
	Sample 6 (70 mm x 37 mm)	9423.65		34	
	Sample 7 (45 mm x 72 mm)	4020.625		-1	

Ultimate Deflection for Radiata Pine and MGP10 Structural Pine Compared to the Control Samples

Table 15: Comparing the Ultimate Deflection values between the Radiata Pine and Control Samples reinforced with 0.5% and 0.25 Graphene.

Reinforcement	Samples	Ultimate Deflection (mm)	Enhancing Ratio (%)
0.5% Graphene	**Sample 4 (184 mm x 21 mm)**	45.327	62
0.25% Graphene	**Sample 8 (184 mm x 21 mm)**	36.326	30

Table 16: Comparing the Ultimate Deflection values between the MGP10 Structural Pine and Control Samples reinforced with 0.5% and 0.25 Graphene.

Reinforcement	Samples	Ultimate Deflection (mm)	Enhancing Ratio (%)	Average Enhancing Ratios (%)
0.5% Graphene	**Sample 1 (70 mm x 47 mm)**	15.013	29	36
	Sample 2 (70 mm x 37 mm)	13.024	15	
	Sample 3 (45 mm x 72 mm)	15.137	64	
0.25% Graphene	**Sample 5 (70 mm x 47 mm)**	11.689	0.1	13.4
	Sample 6 (70 mm x 37 mm)	17.269	53	
	Sample 7 (45 mm x 72 mm)	8.059	-13	

The load-deflection behaviour of the control samples and members reinforced with 0.25% graphene and 0.5% graphene are shown in Figure 16, 17, 18 and 19. Further inspection shows a non-linear and high deflection variation during the 0 kN to 1 kN region for all the reinforced members, excluding the 0.5% graphene radiata member. Above the 1 kN region, all members experience a linear elastic fashion until ductile deformation occurs, resulting in the failure of the samples. However, the member with cross-section 45 mm by 70 mm shows very little plastic deformation resulting in a brittle behaviour. Note that the control samples for cross-section 70 mm by 35 mm also shows a brittle behaviour at the 6.2 kN load shown in Figure 18. This sudden behaviour is due to the defect that is located at the centre of the loading point, which has caused a sudden fracture for the member, as shown previously in Figure 14e.

Note that the data's collected from the experiment is included in Appendix D.

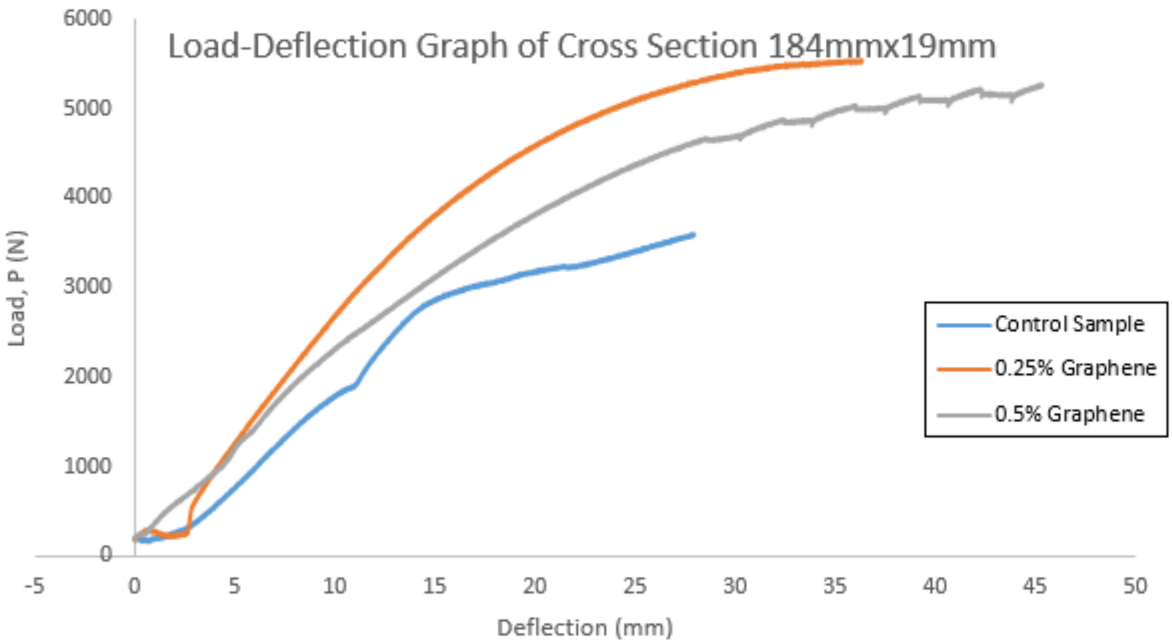

Figure 16: Load deflection graph for reinforced members with cross-section 184 mm x 19 mm

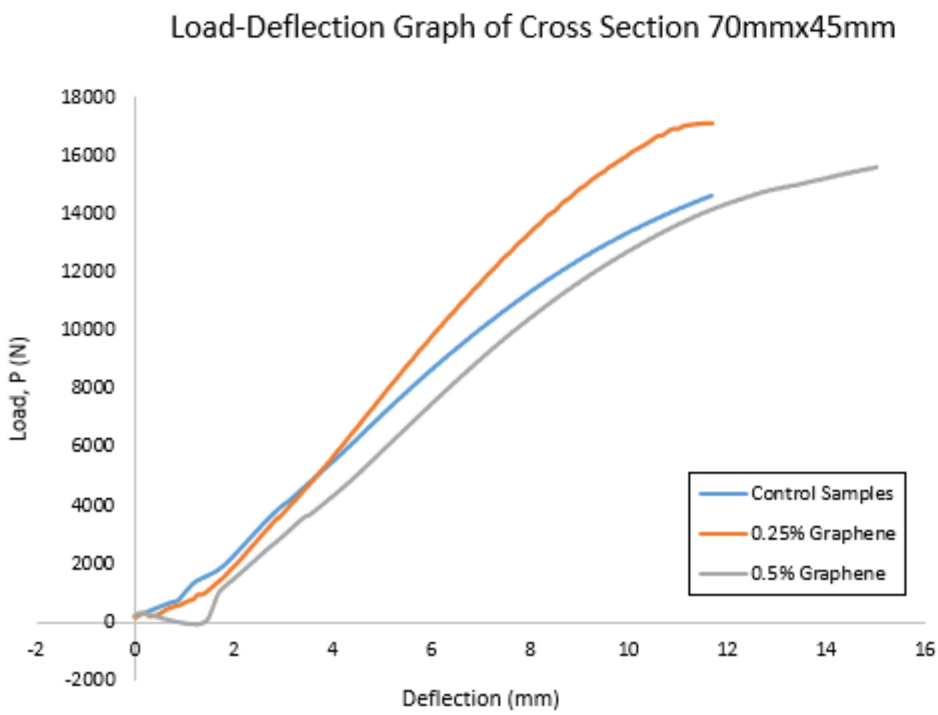

Figure 17: Load deflection graph for reinforced members with cross-section 70 mm x 45 mm

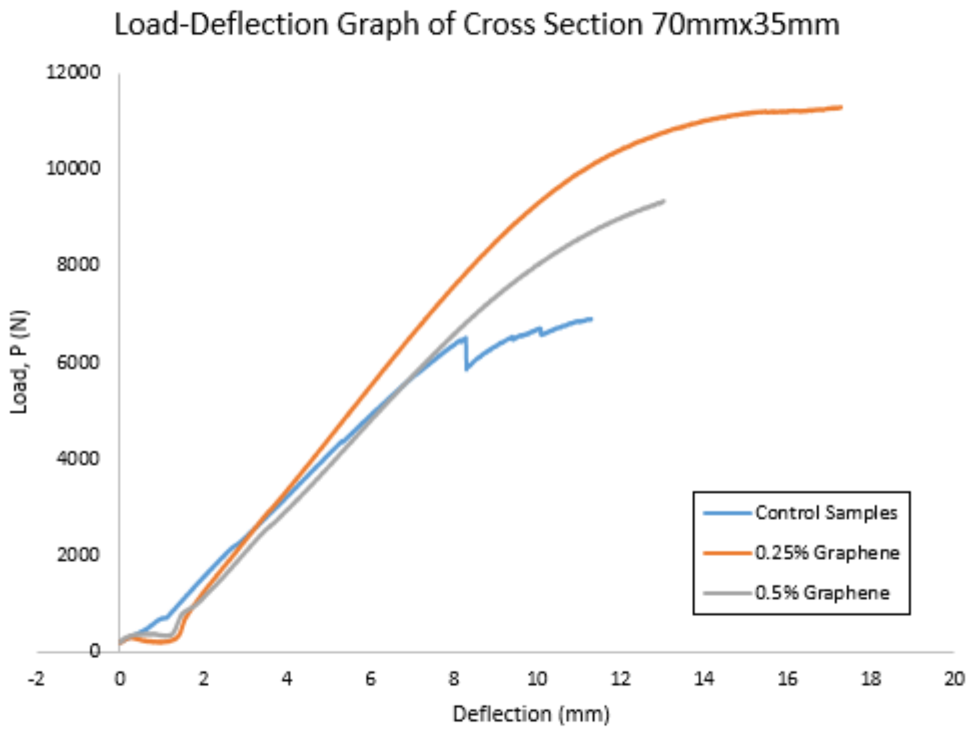

Figure 18: Load deflection graph for reinforced members with cross-section 70 mm x 35 mm

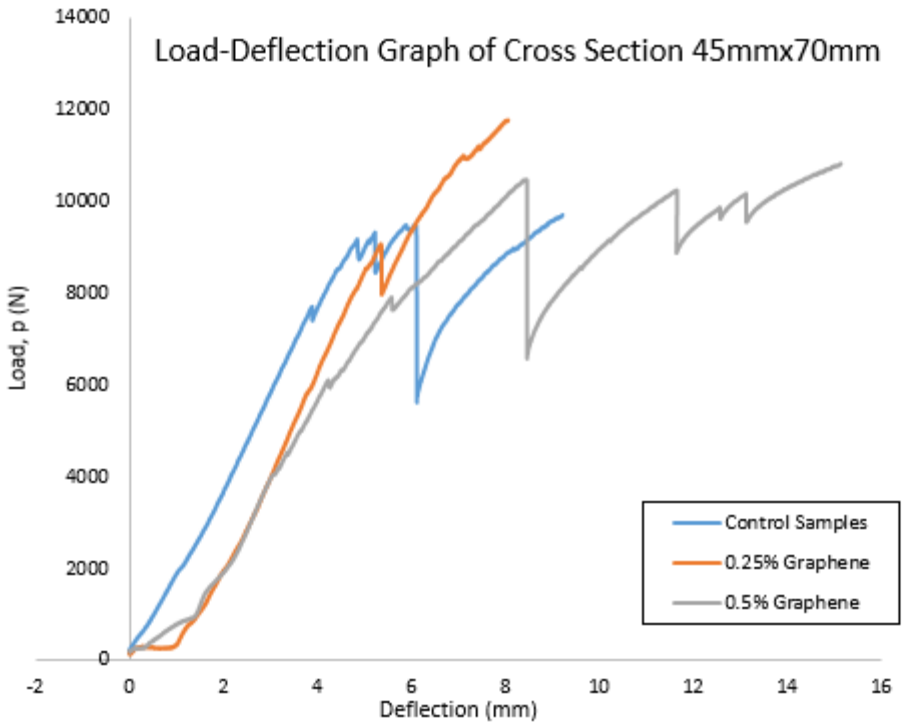

Figure 19: Load deflection graph for reinforced members with cross-section 45 mm x 70 mm

4.3.5 Comparison of the Modulus of Elasticity obtained from Experiment and Australian Standards

The average MOE obtained previously for the control samples in Table 10 is compared to the MOE from the AS1720.1:2010 Structural Timber, which is identified to be 10000 MPa, as shown in Table 17. The values demonstrate a very poor consistency of individual control samples subjected to loading. The main contributing factor is due to the presence of defects within the timber, which is responsible for the high differences in characteristics, averaging to 44.8% differences between the MOE from the experiment and the MOE calculated based on the Australian standards. This has resulted in a difference of 4.5 mm, 4.1 mm and 7.2 mm for Sample 9, 10 and 11, respectively, as presented in Table 18.

Table 17: Comparison between the average modulus of elasticity from the experiment and the modulus of elasticity from Australian standards.

Samples	Average MOE from Experiment (MPa)	MOE (MPa) from Australian Standards	Differences (%)
Sample 9 (70 mm x 45 mm)	6342	10000	44.8
Sample 10 (70 mm x 35 mm)			
Sample 11 (45 mm x 70 mm)			

Table 18: Comparison between the deflection from the experiment and the deflection based on Australian standards.

Samples	Deflection (mm) from Experiment	Deflection (mm) based on Australian Standards MOE	Differences (mm)
Sample 9 (70 mm x 45 mm)	11.676	7.165	4.5
Sample 10 (70 mm x 35 mm)	11.286	7.191	4.1
Sample 11 (45 mm x 70 mm)	9.214	1.965	7.2

4.3.6 Maximum Deflection Limitation

The Maximum allowable deflection using Australian Stadards AS1684 is:

$$\delta_{MAX} = \frac{L}{250}$$

The limit must be considered to determine the allowable deflections that can occur within a member when it is subjected to a load. This study will identify the allowable deflection limit and stress limit for the MGP10 members. Using a deflection limit of span/250 would yield a deflection limit of 2 mm; 17 MPa was taken as the bending stress limit from Australia Standard AS1720.1 – 2002 for MGP10 timber grade. The deflection limit (Table 19, column 2) and stress limit (Table 19, column 4) were adopted into equation 15 (MOE) and equation 16 (MOR), to generate a new load limit that can satisfy the deflection and stress limit, as shown in Table 19, column 3 and 4, respectively. The load limit for deflection and stress would serve as the limiting criteria, based on limits observed in the Australia Standards.

The comparison between the deflection and bending stress obtained previously for the reinforced and non-reinforced samples, compared to the deflection limit and stress limit obtained from the Australian Standards in Table 19 below, demonstrated that all samples have reached its limiting design criteria. Further testing of a variety of samples may yield more consistent results. Due to the limited samples tested, the ultimate load defined in the experiment may not be the most accurate load that can cause the member to fracture, hence further testing of the members should be carried out to verify this assumption, and a factor of safety should be used in all calculations.

Table 19: Load limit based on deflection and stress limits obtained from Australian Standards.

Samples (1)	Deflection limit (mm) (2)	Deflection based load limit (kN) (3)	Stress limit (MPa) (4)	Stress based load limit (kN) (5)
Sample 1 (70 mm x 47 mm)	2	1.458	17	3.505
Sample 2 (70 mm x 37 mm)	2	0.913	17	2.172
Sample 3 (45 mm x 72 mm)	2	1.913	17	5.288
Sample 5 (70 mm x 47 mm)	2	1.900	17	3.505
Sample 6 (70 mm x 37 mm)	2	1.069	17	2.172
Sample 7 (45 mm x 72 mm)	2	2.161	17	5.288
Sample 9 (70 mm x 45 mm)	2	1.612	17	3.213
Sample 10 (70 mm x 35 mm)	2	0.678	17	1.944
Sample 11 (45 mm x 70 mm)	2	2.010	17	4.998

4.4 Conclusions

It was predicted that applying a reinforcement of 0.5% graphene should effectively reduce the deflection and increase the loading capacity of each members. This prediction aims to increase the strength and stiffness of the members compared to the control samples. However, the results obtained from the experiment are contradictory to the initial predictions. It was found that, compared to the control samples, the radiata members reinforced with 0.5% and 0.2%% graphene has displayed an increase in deflection of 62% and 30%, respectively. Similarly, the MGP10 members also increase by 36% and 13.4%, respectively. Although there is an increase in deflection, all the reinforced members still achieved a higher flexural strength, compared to the control samples.

The MGP10 members reinforced with 0.25% graphene displayed a higher flexural strength (MOR), averaging to 70 MPa, which is an average increase of 23%, compared to the control samples. Similarly, for the radiata members, which also shows that the reinforced 0.25% graphene members exhibited a higher flexural strength of 51.3 MPa, hence an increase of 26% was displayed, compared to the control samples. A high MOR would also result in a high MOE. This gives rise to the MGP10 and radiata members reinforced with 0.25% graphene becoming stiffer, with an average MOE of 7205.04 MPa and 5172.462 MPa, which is enhanced by 14% and 11%, respectively, compared to the control samples.

Both radiata and MGP10 members have displayed an increased in flexural strength when reinforced with GPL/polymer nanocomposites, especially the 0.25% graphene layer, which shows more promising results for flexural strength and modulus. Three main contributing factors were predicted to cause this contradictory outcome. Firstly, during the mixing of the 0.25% graphene ratio, more resin was added, compared to the hardener, which could potentially be a contributing factor towards the effectiveness of using 0.25% graphene as a reinforcement solution. Defects is another contributing factor to the inconsistent results obtained from the experiment. During the experiment, several defects was observed to be on the tension side of the members reinforced with 0.5% graphene, this could significantly reduce the bending strength of the members. Therefore, the uncertainty about the defects within timber material has caused a high unpredictability while experimenting. Additionally, the inconsistent thickness of the GPL/polymer nanocomposites layers applied onto the timber has caused a variation in the results during the experiment.

Wooden structure is widely used throughout the civil infrastructure industries. Aiming to achieve high flexural strength and high elastic modulus with low deflection characteristic within the timber members. By conducting a test on 12 samples, the flexural capacity test was performed and the experimental yields uncertainty in the results. The members used in this study, reinforced with the nanocomposites displayed an improvement in flexural rigidity and flexural capacity compared to the control samples. However, as there are many errors and limitation in the testing and analysis of the timber members, further work is necessary to successfully adopt GPL/polymer nanocomposites layer as an effective reinforcement method.

Chapter 5 Finite Element Modelling

5.1 Introduction

The experimental results must be validated to give confidence in further assumptions on the use of GPL/polymer nanocomposites. To verify the experimental results, FEA modelling was conducted to measure the deflection of a reinforced and non-reinforced (control samples) MGP10 and radiata member. The analysis was performed on Strand7 software, which can analyse beam, plate and brick elements using a variety of solvers. In this project, the main solver and elements used is the linear static analysis and brick element, respectively.

The following procedure is adopted in conducting the FEA models:

1. Create the geometric model using three-dimensional brick elements;
2. Input the material properties;
3. Apply restrains conditions (fixed and roller ends restraints);
4. Apply a distributed load at the centreline of the model;
5. Solve for linear static analysis;
6. Conduct convergence studies on different mesh size until results start to converge on a specific mesh size;
7. Check the model results and validate against the experimental results
8. Repeat the procedure on the same cross-section used in the experiment, to replicate the experimental test data (70 mm x 45 mm, 70 mm x 35 mm, 45 mm x 70 mm and 184 mm x 19 mm);

The effective material properties of the GPL/polymer nanocomposites layer were calculated previously using the Halpin-Tsai model and rule of mixture based on the material properties of epoxy and graphene, as shown previously in chapter 3, Table 7. These values would be entered into the model with the reinforcement placed at the top (compression) and bottom (tension) of the members as shown in Figure 20 to stimulate the real-life experiment and obtain precise results.

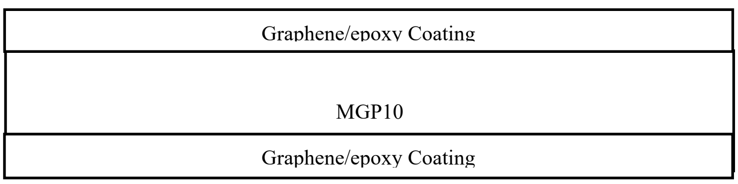

Figure 20: Reinforcement setup for Strand7 FE

The material properties of the MGP10 members that would be used in the FEA were discussed earlier in Chapter 3, which included the density, Poisson ratio and thermal expansion obtained from the Australian Standards, as shown in Table 21, column 3, 4 and 5 below. The FEA was conducted on a loading condition of 2, 4, 6 and 8 kN, which was all in the elastic portion of the load-deflection curve. Using equation 15, the MOE for each member can then be determined based on the loading condition and the corresponding deflection values, which can be obtained from the experimental data's. The calculated MOE is shown in Table 20, column 2. All samples were modelled with consistency in material properties from the control sample and is coated with reinforcement, to simulate the experimental test data. Note that the MOE for the member with cross-section 70 mm by 35 mm was neglected at the 8 kN region in this FEA because its ultimate load only reaches 6.9 kN. The table represents the mechanical properties of the GPL/polymer nanocomposites layer used in this FEA for the 0.5 and 0.25 w.t. % GPL, using the Halpin-Tsai micromechanics model. The data's for different w.t.% of GPL are calculated and shown in Appendix C.

Table 20: Material properties of each individual control specimen based on different loading conditions

Load, P (kN)	**Cross section (mm) (1)**	**Modulus of Elasticity for Control Samples (MPa) (2)**	**Poisson's Ratio (3)**	**Density $(\mathrm{kg/m^3})$ (4)**	**Thermal Expansion (/K) (5)**
2	**70 x 45**	5327.981	0.444	500	3.5×10^{-6}
	70 x 35	8306.604	0.444	500	3.5×10^{-6}
	45 x 70	3697.934	0.444	500	3.5×10^{-6}
4	**70 x 45**	6540.826	0.444	500	3.5×10^{-6}
	70 x 35	8522.470	0.444	500	3.5×10^{-6}
	45 x 70	3759.738	0.444	500	3.5×10^{-6}
6	**70 x 45**	6788.562	0.444	500	3.5×10^{-6}
	70 x 35	8392.526	0.444	500	3.5×10^{-6}
	45 x 70	3937.671	0.444	500	3.5×10^{-6}
8	**70 x 45**	7031.329	0.444	500	3.5×10^{-6}
	70 x 35	N/A	0.444	500	3.5×10^{-6}
	45 x 70	3890.693	0.444	500	3.5×10^{-6}

Table 21 Graphene/Epoxy material properties for different ratios used

		Modulus of Elasticity (MPa)	**Poisson's Ratio**	**Density (kg/m^3)**	**Thermal Expansion (/K)**
Graphene/Epoxy	**0.5%**	7992.9	0.33913	1199.2	0
	0.25%	5496.4	0.33956	1199.6	0

5.2 Methodology and Results

5.2.1 The Use of Isotropic Element

Wood can be classified as an orthotropic material, the modulus of elasticity E_1 in the grain direction will generally be larger than the transverse direction (E_2 and E_3), which means the wood is strongest in its direction. When $E_1 \neq E_2 \neq E_3$, the material is then considered to be orthotropic. Orthotropic materials have three distinctive directions with different properties along with each principal directions, as shown in Figure 21. On the other hand, an isotropic material will have the same mechanical properties in all directions (Gillia 1972). To obtain the highest degree of accuracy, the timber members are required to be modelled as three-dimensional orthotropic elements. However, the three required modulus is not available due to no prior studies being carried out in this specific field. Based on the assumption that E_1 is the dominant MOE that contributes to bending, this assumption is reasonable for the MGP10 members to be modelled as a three-dimensional isotropic element to undertake a good approximation of the deflection.

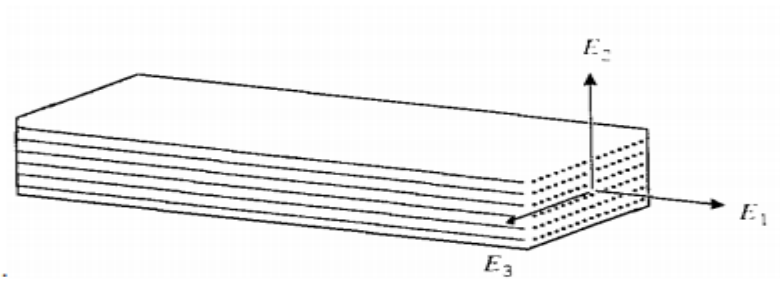

Figure 21: Diagram of an orthotropic material (Gillia 1972)

5.2.2 Convergence Study

The accuracy of the results depends on the element size and the total number of elements that is considered during the modelling procedure, which forms the basis of convergence studies. Convergence studies focus on identifying the number of elements needed, to ensure the results from the FEA are not affected by the changes in mesh sizes (Gu & Conte 2003). In the study conducted, an initial mesh size of 40 mm by 10 mm by 5 mm was examined on members with a cross-section of 70 mm by 45 mm, 70 mm by 35 mm and 45 mm by 70 mm. Loading of 200 kN was subjected to each model, which is distributed evenly across the centre line with restraints on both sides of the member. Based on Chapter 3, the mechanical properties of the MGP10 timber member, such as modulus of elasticity 10 000 MPa, Poisson's ratio 0.444 and density 500 kg/m^3 were used for this convergence study. It was acknowledged that the results start to converge at a mesh size of 80 mm by 20 mm by 15 mm for all control samples, reinforced and non-reinforced members, as shown in Table 22, 23 and 24.

Convergence Studies Conducted on Difference Size Meshes for Control Samples and Reinforced Members

Table 22: Convergence studies for non-reinforced Strand7 model with different mesh sizes conducted on a simply supported MGP10 member with cross-section of 70 mm x 45 mm, 70 mm x 35 mm and 45 mm x 70 mm.

MGP10 Cross Section (mm)	Maximum Deflection (mm) (for P = 200 kN, E = 10000 MPa)			
	Mesh Size (mm) $(\boldsymbol{x} \times \boldsymbol{y} \times \boldsymbol{z}) - (\boldsymbol{B} \times \boldsymbol{A} \times \boldsymbol{C})$			
	40x10x5	**60x15x10**	**80x20x15**	**100x25x20**
70 x 45	101.6	102	102.1	102.2
70 x 35	212.9	213.3	213.5	213.6
45 x 70	44.3	44.8	45.1	45.3

Table 23: Convergence studies for 0.5% graphene reinforced Strand7 model with different mesh sizes conducted on a simply supported MGP10 member with cross-section of 70 mm x 45 mm, 70 mm x 35 mm and 45 mm x 70 mm.

MGP10 Cross Section (mm)	Maximum Deflection (mm) (for P = 200 kN, E = 10000 MPa)			
	Mesh Size (mm) $(\boldsymbol{x} \times \boldsymbol{y} \times \boldsymbol{z}) - (\boldsymbol{B} \times \boldsymbol{A} \times \boldsymbol{C})$			
	40x10x5	**60x15x10**	**80x20x15**	**100x25x20**
70 x 45	91.3	92	92.2	92.3
70 x 35	184.9	186.5	186.7	186.8
45 x 70	41.8	42.3	42.6	42.8

Table 24: Convergence studies for 0.25% graphene reinforced Strand7 model with different mesh sizes conducted on a simply supported MGP10 member with cross-section of 70 mm x 45 mm, 70 mm x 35 mm and 45 mm x 70 mm.

MGP10 Cross Section (mm)	Maximum Deflection (mm) (for P = 200 kN, E = 10000 MPa)			
	Mesh Size (mm) $(\boldsymbol{x} \times \boldsymbol{y} \times \boldsymbol{z}) - (\boldsymbol{B} \times \boldsymbol{A} \times \boldsymbol{C})$			
	40x10x5	**60x15x10**	**80x20x15**	**100x25x20**
70 x 45	94.4	95	95.3	95.6
70 x 35	192.8	194.3	194.5	194.7
45 x 70	42.7	43.3	43.7	43.9

5.2.3 Developing the non-reinforced (control samples) models for the MGP10 timber member

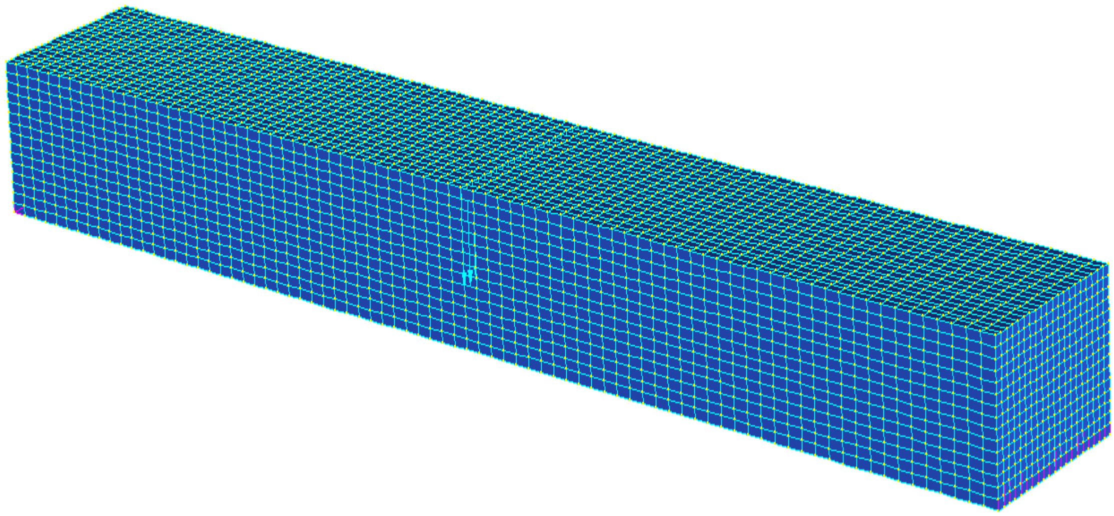

Figure 22: Three-dimensional brick element model of a non-reinforced (control samples) MGP10 member

Three-dimensional brick elements modelling are predicted to yield more accurate results compared to one and two-dimensional plate element models. The member geometric model was assembled into four nodes, spaced length (L) and width (W), using quard4 and extruded in the z-direction by depth (D). It was found that a higher number of brick elements would generate a more accurate stress distribution results. Furthermore, different mesh sizes can be used for convergence studies and were shown that the convergence starts at a mesh size of 80 mm by 20 mm by 15 mm. The model was then subdivided according to the converge mesh size, 80 times in the x-direction, 20 times in the y-direction and 15 times in the z-direction, which resulted in 24000 brick elements.

Translational restraints in the x, y and z (fixed end) was applied on one side of the beam while the other side was restrained in the z-direction only (roller end), this restrains at the nodes stimulate a simply supported beam. Material properties were then assigned in the model according to the timber material properties in Table 20. A resultant force of 2 kN, 4 kN, 6 kN and 8 kN was applied at the centre line of the model. Figure 23, 24 and 25 show an example of an MGP10 member at a cross-section of 70 mm by 45mm, 70 mm by 35mm and 45 mm by 70 mm subjected to loading of 8 kN. The maximum deflection is represented in the blue region while minimum deflection is displayed in the pink region.

Strand7 Models of the Control Samples for the MGP10 members

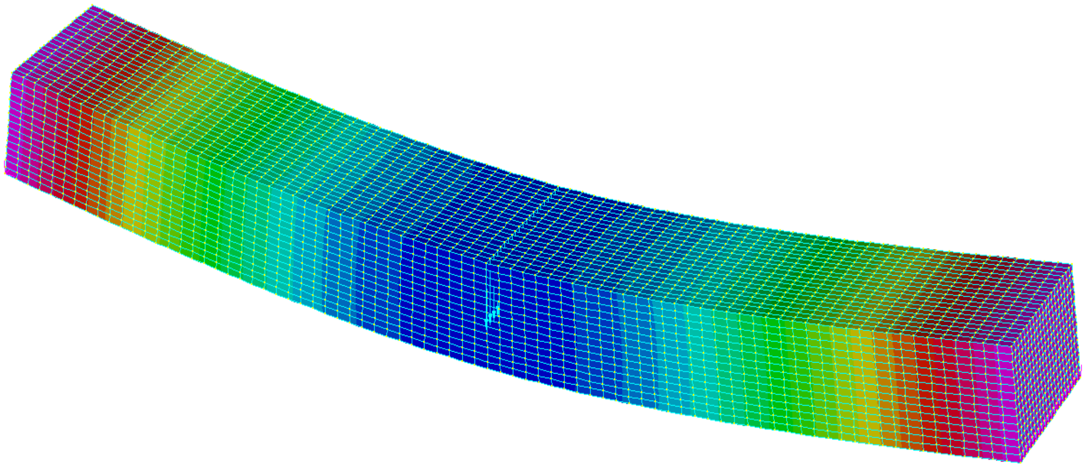

Figure 23: Non-reinfroced (control sample) MGP10 with 70 mm x 45 mm subjected to 8 kN

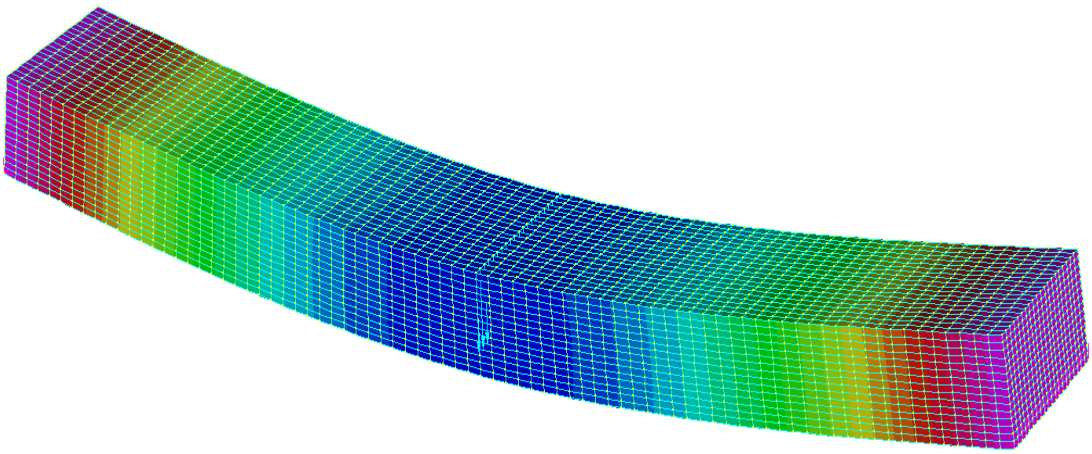

Figure 24: Non-reinfroced (control sample) MGP10 with 70 mm x 35 mm subjected to 8 kN

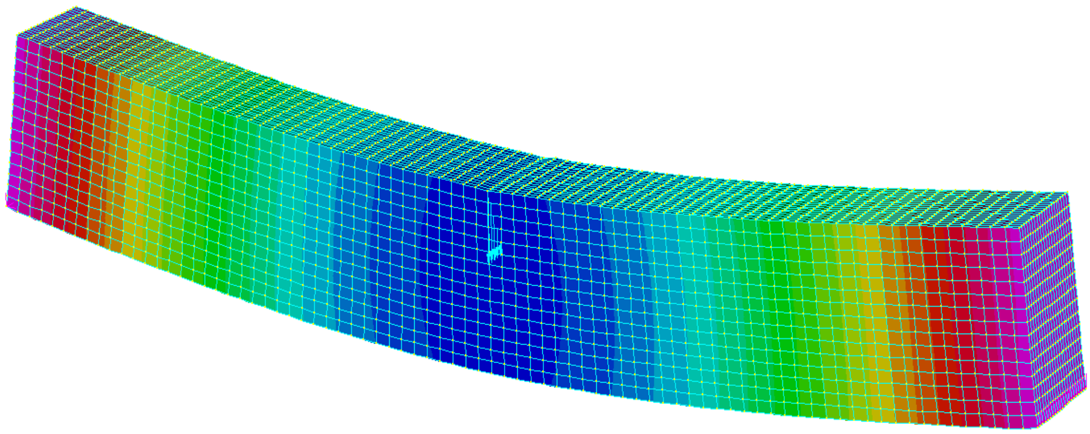

Figure 25: Non-reinforced (control sample) MGP10 with 45mmx70mm subjected to 8 kN

5.2.3.1 Results and Discussion

Three-dimensional elements modelling has provided an advantage in predicting the accuracy of the relationship between the load and deflection, due to its in-depth description of stress distribution within the element. The members are modelled as a three-dimensional isotropic element due to the high degree of accuracy compared to the experimental data's. Table 25 compares the maximum central deflection for the control samples obtained from Strand7 model with those obtained from the experiment for the specified cross-section and loading. Logical results were achieved between the methodologies, with the highest variation between the model and experiment to be 0.5 mm at the 8 kN region. Note that the MGP10 timber members of cross-section 70 mm by 35 mm are excluded from this FEA because its ultimate load was observed to be lower than the 8 kN limit required for analysis.

Logically the MOE that is used for this FEA should be calculated using the linear proportion of the load-deflection curve because the load does not affect the MOE of the material, and thus should be constant throughout the FEA for each cross-section. This study has considered different MOE for each loading condition based on the loading and corresponding deflection, which is obtained using equation 14 in chapter 4. This method is considered reasonable due to the load-deflection graph shown in Figure 26, which exhibits a relatively linear relationship and the intersection point are close to zero (preliminary load), which has proven to be sufficient for this FEA. Note that the loading condition (2, 4, 6 and 8 kN) selected for this study was all located in the elastic portion of the load-deflection graph.

The non-reinforced MGP10 members were modelled as an isotropic element due to the assumption that E_1 is the dominant MOE during bending. This is the reason for the slight difference observed between the model and the experimental data's, which fails to consider the MOE in all three directions of the material. This could be seen in Figure 26, which shows the load-deflection graph for the non-reinforced MGP10 members. The graph identified a difference of 0.1 millimetres between the experiment and modelled data at the 2 kN region for all members. However, as the load increases, the load-deflection relationship starts to be non-linear for all members. The highest difference was observed for the members with a cross-section of 45 mm by 70 mm.

Table 25: Maximum deflection results obtained from experiment and Strand7 at different loading of 2 kN, 4 kN, 6kN and 8 kN for cross-section of 70 mm x 45 mm, 70 mm x 35 mm and 45 mm x 70 mm.

Load, P (kN)	Members Cross Section (mm)	Deflection from Experiment (mm)	Deflection from Strand7 (mm)	Differences (mm)
2	**70 x 45**	1.839	1.917	0.1
	70 x 35	2.507	2.570	0.1
	45 x 70	1.095	1.219	0.1
4	**70 x 45**	2.996	3.123	0.1
	70 x 35	4.887	5.010	0.1
	45 x 70	2.154	2.398	0.2
6	**70 x 45**	4.33	4.513	0.2
	70 x 35	7.444	7.632	0.2
	45 x 70	3.085	3.435	0.4
8	**70 x 45**	5.574	5.81	0.2
	70 x 35	N/A	N/A	N/A
	45 x 70	4.163	4.635	0.5

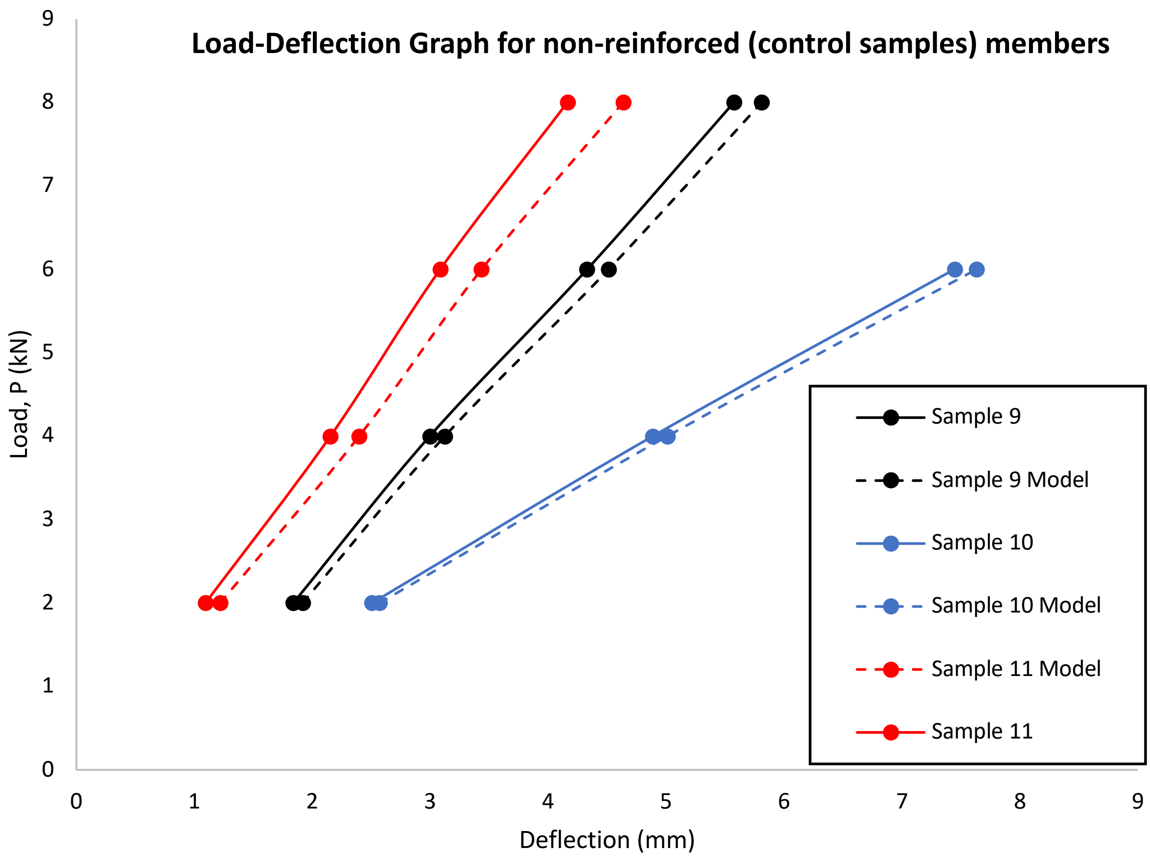

Figure 26: Comparison between the experimental results and Strand7 models for cross-section of 70 mm x 45 mm, 70 mm x 35 mm and 45 mm x 70 mm for control samples.

5.2.4 Developing the reinforced model for the MGP10 timber member

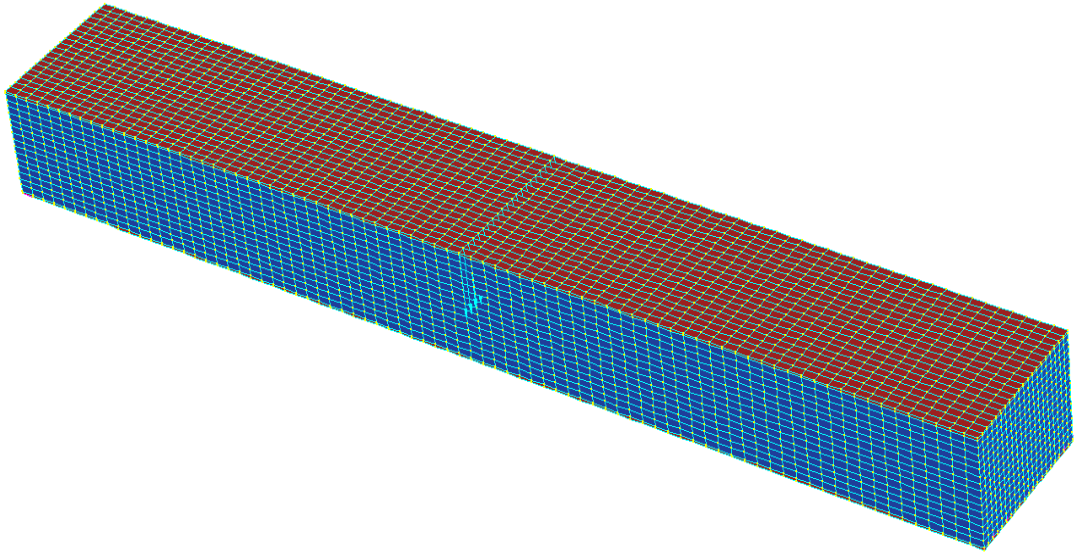

Figure 27: Three-dimensional brick element model of a reinforced MGP10 member

Three-dimensional modelling elements were also used to model the reinforced MGP10 members with 0.25% graphene and 99.75% epoxy, and 0.5% graphene and 99.5% epoxy, as shown in Figure 27. The same quantity of brick element was used and combined with one layer of one millimetre of nanocomposite coating on the top and bottom of the members, which resulted in 27 200 brick elements. Mechanical properties for the MGP10 members and different w.t. percentage GPL was inputted into the model as shown in Table 20 and Table 21, respectively. The restraints conditions and force applied are identical to the non-reinforced model, however, the force and restraint were placed on top of the coated reinforcements. Figure 28, 29 and 30 show an example of three members of cross-section 70 mm by 45 mm, 70 mm by 35 mm and 45 mm by 70 mm reinforced with a coating of 0.5% graphene and 99.5% of epoxy on the tension and compression side, subject to a force of 8 kN.

Strand7 Models for MGP10 members Reinforced with 0.5% Graphene

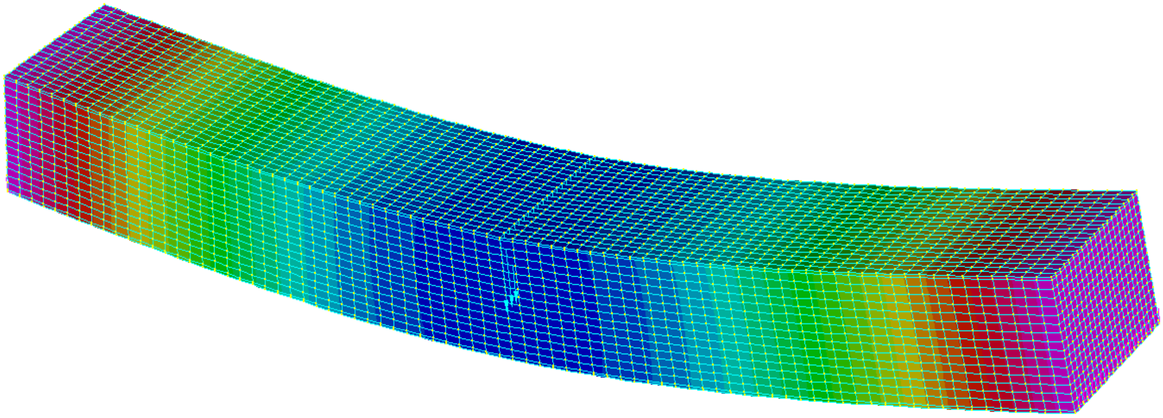

Figure 28: MGP10 70 mm x 45 mm – 0.5% Graphene-99.5%Epoxy

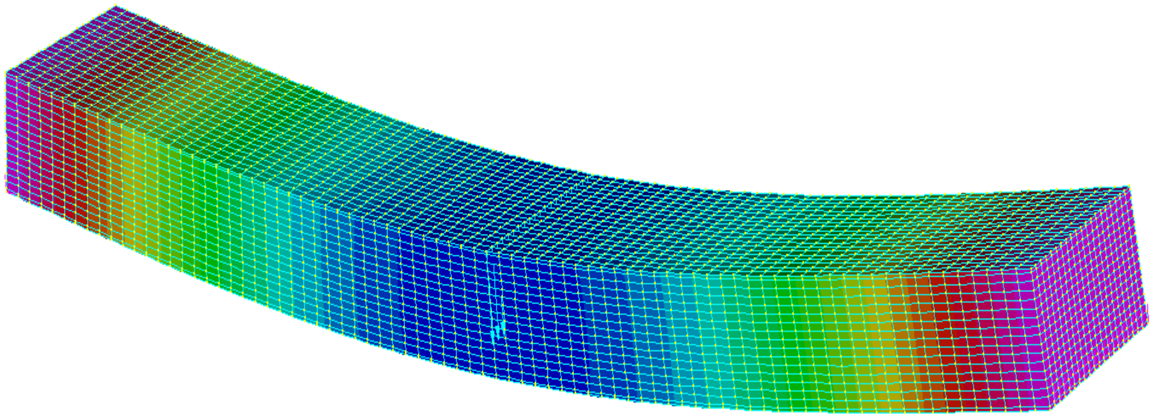

Figure 29: MGP10 70 mm x 35 mm – 0.5% Graphene-99.5%Epoxy

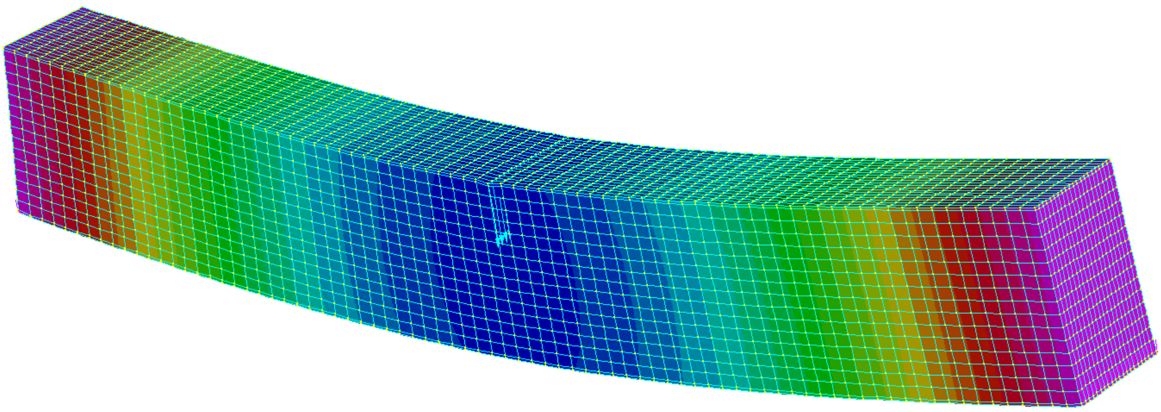

Figure 30: MGP10 45 mm x 70 mm – 0.5% Graphene-99.5%Epoxy

5.2.4.1 Results and Discussion

To verify the model, the deflection results from Strand7 models were to be compared against the corresponding values obtained from the experiment for the same loading condition as presented in Table 26 and 27. The comparison of the deflections values obtained from Strand7 models and the experimental results, ranges from 0.1 mm to 0.9 mm for the 0.25% graphene members and 0.7 mm to 2 mm for the 0.5% graphene members. Although there is a slight variation in deflection observed for the members reinforced with 0.25% graphene, it was still considered reasonable to validate the model. However, the members reinforced with 0.5% graphene shows a slightly higher variation in deflection. This relationship can be seen in the load-deflection graph in Figure 31 and 32, which shows a relatively linear relationship and close vicinity of the preliminary load (0 kN). The variations observed between the two methodologies for 0.25% and 0.5% are affected by several factors, mainly because of the use of the isotropic elements and the material properties of the nanocomposites.

Previously, the control samples have been assumed to be sufficient for validation between the two methodologies due to the low variation observed, despite the use of isotropic element; which only consider the MOE in the direction parallel to the grain, the results still achieve a reasonable linear-deflection relationship. For this reason, it can be assumed that the differences in deflection observed from the reinforced models, is not mainly because of the use of isotropic element but the inaccurate material properties of the GPL/polymer nanocomposites used in this study. The material properties of the graphene and epoxy resin that was supplied by GMG and Jotum are confidential and cannot be provided for this study, therefore the material properties for graphene and epoxy were based on a study conducted by Yasmin and Daniel (2004) and Rafiee et. al. (2009). Note that the timber model with a cross-section of 45 mm by 70 mm shows also shows the highest difference between the two methods.

Table 26: Central deflections in simply supported MGP10 members reinforced with 0.25% Graphene and 99.75% Epoxy, subjected to loading of 2, 4, 6 and 8 kN as determined using Strand7 and compared to the experiment data's.

Load, P (kN)	Members Cross Section (mm)	Deflection from experiment (mm)	Deflection from Strand7 (mm)	Differences (mm)
2	**70 x 45**	2.064	1.681	0.4
	70 x 35	2.718	2.3	0.4
	45 x 70	2.041	1.565	0.5
4	**70 x 45**	3.149	2.805	0.3
	70 x 35	4.622	4.493	0.1
	45 x 70	3.023	2.142	0.9
6	**70 x 45**	4.169	4.07	0.1
	70 x 35	6.462	6.833	0.4
	45 x 70	3.903	3.084	0.8
8	**70 x 45**	5.127	5.258	0.1
	70 x 35	N/A	N/A	N/A
	45 x 70	4.774	4.157	0.6

Table 27: Central deflections in simply supported MGP10 members reinforced with 0.5% Graphene and 99.5% Epoxy, subjected to loading of 2, 4, 6 and 8 kN as determined using Strand7 and compared to the experiment data's.

Load, P (kN)	Members Cross Section (mm)	Deflection from experiment (mm)	Deflection from Strand7 (mm)	Differences (mm)
2	**70 x 45**	2.343	1.591	0.8
	70 x 35	2.934	2.191	0.7
	45 x 70	2.078	1.033	1
4	**70 x 45**	3.779	2.677	1.1
	70 x 35	5.177	4.075	1.1
	45 x 70	3.036	2.038	1
6	**70 x 45**	5.087	3.894	1.2
	70 x 35	7.318	6.517	0.8
	45 x 70	4.182	2.94	1.2
8	**70 x 45**	6.333	5.032	1.3
	70 x 35	N/A	N/A	N/A
	45 x 70	5.917	3.959	2

Load-deflection characteristics between the Strand7 model and experimental data's are shown in the Figure 31 and 32.

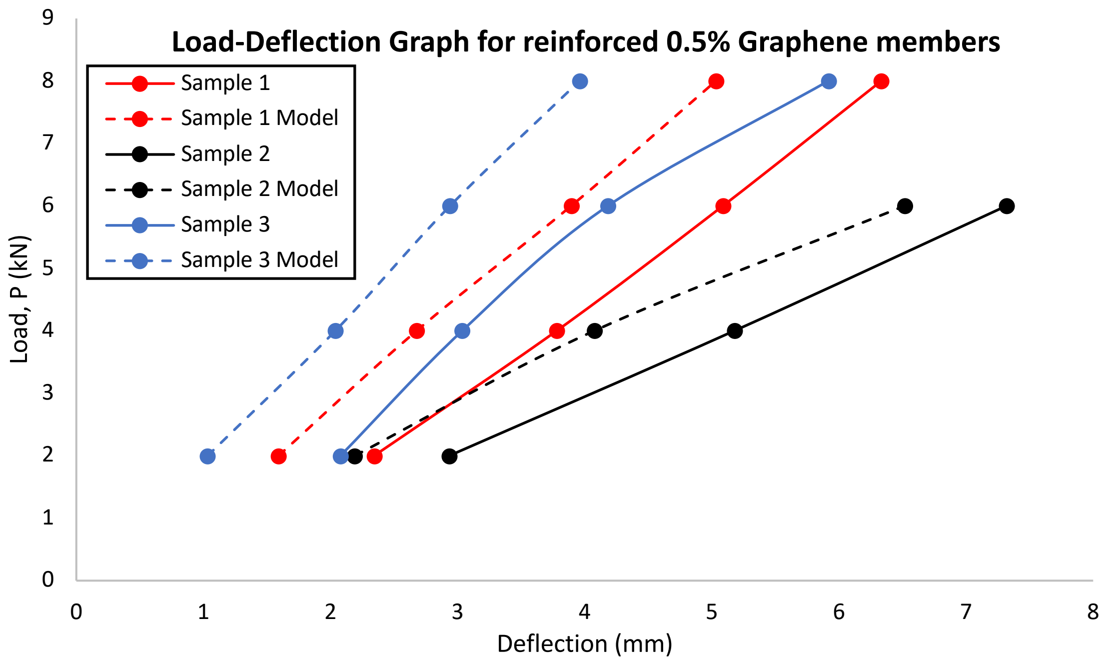

Figure 31: Comparison between the experimental results and Strand7 models for cross section of 70 mm x 45 mm, 70 mm x 35 mm and 45 mm x 70 mm for members reinforced with 0.5% graphene.

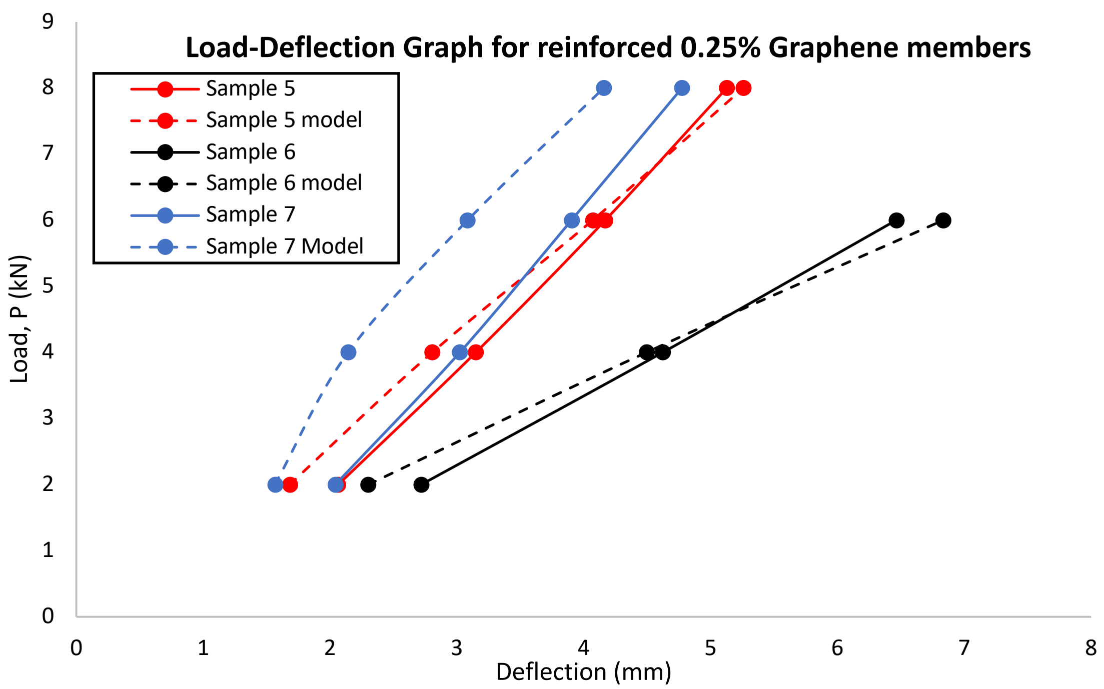

Figure 32: Comparison between the experimental results and Strand7 models for cross section of 70 mm x 45 mm, 70 mm x 35 mm and 45 mm x 70 mm for members reinforced with 0.25% graphene.

5.2.5 Developing the reinforced and non-reinforced (control samples) models for the MGP10 and radiata members.

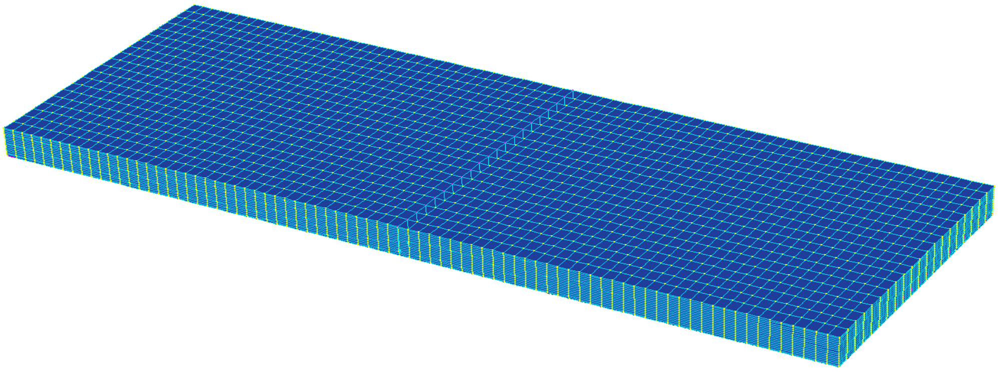

Figure 33: Three-dimensional brick element model of a Non-reinforced (control samples).

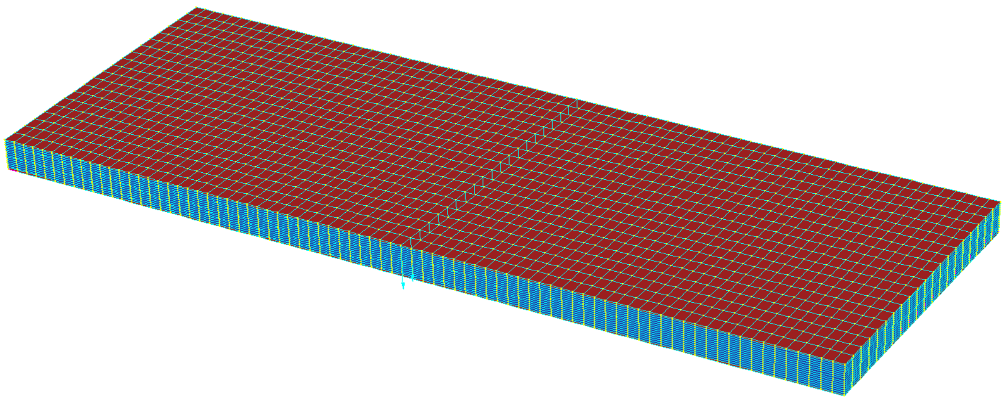

Figure 34: Three-dimensional brick element model of a reinforced (control samples).

The same methodology was applied to the analysis for the reinforced and non-reinforced radiata model. The geometric model was constructed with the same mesh size of 80 mm by 20 mm by 15 mm, and dimensions of 184 mm by 19 mm and a length of 500 mm. The MOE values shown in Table 28 was used in this analysis, which was calculated using equation 15. This equation parameter is based on the loading and corresponding deflection obtained from the control samples of the radiata members in the experiment. The radiata pine has a density of 500 kg/m^3 in 30 to 40 years period and about 405 kg/m^3 during the 10 to 20 years period (KiwiLumber 2014). Due to not knowing the exact age of the radiata used in this experiment, it was assumed that the radiata members have a maximum density of 500 kg/m3 and Poisson ratio of 0.444. Note that the radiata member's maximum loading for the control samples is 3.599 kN, 5.546 kN and 5.273 kN respectively. For this reason, the analysis of the radiata model would be conducted on loading of 1, 2 and 3 kN, which is within its loading region.

Table 28: Material properties of radiata members that would be used in the FEA

Load, P (kN)	MOE of Control Samples from Experiment (MPa)	Poisson ratio	Density (kg/m^3)
1	4057.215	0.444	500
2	4368.593	0.444	500
3	4369.621	0.444	500

5.2.5.1 Results and Discussion

Table 29 compares the maximum central deflection of a simply supported 184 mm by 500 mm with a depth of 19 mm radiata member subjected to loading of 1, 2 and 3 kN obtained from Strand7 with those determined from the experimental data's. The differences between the Strand7 model and the experiment for the control samples are slightly higher compared to the previous studies on the MGP10 member, however, the comparison still achieved a reasonable agreement between the methodologies. In contrast, the reinforced members displayed very high differences, which was due to the uncertainty of the material properties for the radiata member and the GPL/polymer nanocomposites. Further understanding of the precise material properties used for testing will enable a more accurate modelling result.

Table 29: Comparison between Strand7 models and experimental data's for the control samples, and the reinforced 0.25% and 0.5% graphene, based on the loading condition of 1, 2 and 3 kN.

Maximum Loading	Samples	Deflection from experiment (mm)	Deflection from Strand7 (mm)	Differences (mm)
1	**Control Sample**	6.103	6.286	0.1
	0.25% Graphene	4.22	3.269	0.9
	0.5% Graphene	4.431	3.038	1.4
2	**Control Sample**	11.336	11.675	0.3
	0.25% Graphene	7.595	6.034	1.5
	0.5% Graphene	8.451	5.885	2.6
3	**Control Sample**	17	17.508	0.5
	0.25% Graphene	11.324	9	2.3
	0.5% Graphene	14.353	9.587	5

5.2.6 Developing the reinforced epoxy based radiata and MGP10 members

As there was limited resources available to experiment with pure epoxy base reinforcement, FEA was carried out instead to undertake a prediction of the possible outcome of using pure epoxy as a reinforcement method compared to GPL/polymer reinforcement method. A three-dimensional brick element model was used to predict the flexural strength and modulus of the reinforced epoxy based members. The material properties for epoxy based reinforcement used in this modelling were shown previously in chapter 3, Table 7, which includes MOE of 3000 MPa, Poisson ratio of 0.34 and density of 1200 kg/m^3. The MOE used for the members would be based on the control samples obtained during the experiment for the MGP10 and radiata members. These control samples would be reinforced with one layer of one millimetre coated epoxy on the compression and tension side of each member of cross-section 70 mm by 45 mm, 70 mm by 35 mm, 45 mm by 70 mm and 184 mm by 19 mm.

5.2.6.1 Results and Discussion

Comparison for the Radiata members

Table 31 present the calculated MOE based on the deflection and loading acquired from the model as shown in Table 30. Compared to the control samples, the radiata members displayed an average decrease in deflection of 17%, which resulted in a MOE increase of 21%. This result has concluded that the 184 mm by 19 mm radiata member can resist deflection or bending under the same applied load compared to the control samples.

Table 30: Deflection results comparison between the epoxy base reinforcement and the control samples of cross-section 184 mm x 19 mm Radiata.

Maximum Loading (kN)	Samples	Deflection (mm)	Enhancing Ratio (%)	Average Enhancing Ratios (%)
1	184 mm x 19 mm	4.988	-18.270	-17
2		9.404	-17.043	
3		14.103	-17.041	

Table 31: MOE results comparison between the epoxy base reinforcement and the control samples of cross-section 184 mm x 19 mm plank.

Maximum Loading (kN)	Samples	MOE (MPa)	Average MOE (MPa)	Enhancing Ratio (%)	Average Enhancing Ratios (%)
1	184 mm x 19 mm	4964.151	5165.821	22.354	21
2		5266.096		20.544	
3		5267.216		20.542	

Comparison for the MGP10 members

Table 32 compares the maximum central deflection of a simply supported MGP10 member of cross-section 70 mm by 45 mm, 70 mm by 35 mm and 45 mm by 70 mm subjected to loading of 2, 4, 6 and 8 kN to those of the control samples with the same cross-section observed during the experiment. It was observed that model with cross-section 70 mm by 45 mm and 70 mm by 35 mm also displayed a decrease in deflection, compared to the control samples. Note that the model with a cross-section of 45 mm by 70 mm showed a deflection increase when compared to the control samples.

Table 33 presents the MOE values calculated using equation 15 based on the loading and corresponding deflection obtained in Table 32 at each loading condition. This value was then compared against the MOE of the control samples obtained from the experiment to identify the enhancing ratio of each member. It is worth noting that the cross-section 45 mm by 70 mm had failed to show its effectiveness due to its high deflection and low MOE when compared to the control samples. Based on these results, it was assumed that the main contributing factor towards this undesirable results for the member of cross-section 45 mm by 70 mm is due to the low content of GPL/polymer nanocomposites applied on the width of the member, compared to the members that has a larger width. Since the member of cross-section 45 mm by 70 mm has a much larger depth compared to the other samples, it's required to have a thicker layer of GPL/polymer nanocomposites to reduce its deflection, which would significantly improve its flexural strength. Overall, members of cross-section 70 mm by 45mm and 70mm by 35 mm reinforced with epoxy-based coating displayed logical prediction for the effectiveness of using epoxy based coating as a reinforcement method.

Table 32: Deflection results comparison between the epoxy base reinforcement and the control samples of cross-section 70 mm x 45 mm, 70 mm x 35 mm and 45 mm x 70 mm.

Members Cross-Section (mm)	Maximum Loading (kN)	Deflection (mm)	Enhancing Ratio (%)	Average Enhancing Ratios (%)
70 x 45	**2**	1.785	-2.936	-2
70 x 35		2.419	-3.510	
45 x 70		0.819	-25.205	
70 x 45	**4**	2.951	-1.502	0.1
70 x 35		4.724	-3.335	
45 x 70		2.266	5.200	
70 x 45	**6**	4.275	-1.270	0.2
70 x 35		7.188	-3.439	
45 x 70		3.257	5.575	
70 x 45	8	5.515	-1.058	2.2
70 x 35		N/A	N/A	
45 x 70		4.391	5.477	

Table 33: MOE results comparison between the epoxy base reinforcement and the control samples of cross-section 70 mm x 45 mm, 70 mm x 35 mm and 45 mm x 70 mm.

Members Cross-Section (mm)	Maximum Loading (kN)	MOE (MPa)	Average MOE (MPa)	Enhancing Ratio (%)	Average Enhancing Ratios (%)
70 x 45	**2**	5489.164	6347.359	3.025	13
70 x 35		8608.787		3.638	
45 x 70		4944.125		33.700	
70 x 45	**4**	6640.567	6343.670	1.525	0.01
70 x 35		8816.535		3.450	
45 x 70		3573.908		-4.943	
70 x 45	**6**	6875.900	6432.350	1.287	-0.14
70 x 35		8691.425		3.561	
45 x 70		3729.725		-5.281	
70 x 45	8	7106.551	5397.611	1.070	-2
70 x 35		N/A		N/A	
45 x 70		3688.671		-5.192	

Comparison for the MGP10 and Radiata members reinforced with 0.25% and 0.5% graphene and epoxy based.

The comparison between the epoxy-based coating against the GPL/polymer reinforcements for the MGP10 and radiata members is shown in Table 34 and 35, respectively. This comparison shows that using GPL/polymer nanocomposites as a reinforcement resulted in a more effective solution for the MGP10 members, bringing about an increase in MOE of 6.8% and 22% for the 0.25% and 0.5% graphene, respectively. On the other hand, the radiata model shows a decrease in MOE of 18.2% and 6.8% for the 0.25% and 0.5% graphene, resulting in an unfavourable outcome, when compared to the control samples. In general, the study that was conducted shows just a prediction of the possible outcome that could occur when assuming a reinforcement of pure epoxy-base. This result has no concrete data from experiments that can validate this prediction, therefore further work can be done on multiple cross-section and duplicates in-order to further improve these results, and recommend epoxy-based reinforcement as a reliable design method.

Table 34: Comparing the MGP10 members reinforced with Epoxy-Based to the MGP10 members reinforced with 0.25% and 0.5% Graphene.

	Epoxy Based	0.25% Graphene	Enhanced Ration (%)	0.5% Graphene	Enhanced Ration (%)
Deflection (mm)	3.712	3.823	-2.9	4.380	-15.25
MOE (MPa)	6130.248	5743.1	6.7	5024.771	22

Table 35: Comparing the Radiata members reinforced with Epoxy-Based to the Radiata members reinforced with 0.25% and 0.5% Graphene.

	Epoxy Based	0.25% Graphene	Enhanced Ration (%)	0.5% Graphene	Enhanced Ration (%)
Deflection (mm)	9.498	7.713	23.1	9.078	4.6
MOE (MPa)	5165.821	6315.934	-18.2	5541.195	-6.8

5.4 Conclusion

This chapter aimed to undertake an FEA to predict and validate the behaviour of the control samples and reinforced timber members, which is subjected to different loading conditions. The parametric study investigated in Chapter 3 was used to undertake a good approximation of the deflection that would produce an accurate result. The main findings of this chapter are presented below:

- All Strand7 models for MGP10 and radiata members (control samples) compared to the experimental results for the identical member's shows a logical agreement. This has also validated the method of using the isotropic brick elements to model the MGP10 and radiata member, despite the consideration of a single direction MOE.
- All Strand7 models for the MGP10 and radiata members reinforced with 0.25% and 0.5% graphene show a higher variation compared to the control samples. The slight differences that were observed are mainly due to the unknown material properties of the graphene and epoxy used in this study. For this reason, the material property of graphene and epoxy was based on successful results obtained from the previous literature conducted by Yasmin & Daniel (2004) and Rafiee et. al. (2009).
- Further analysis was conducted on an epoxy-based reinforced member to predict the possible behaviour of the member under different loading condition (2, 4, 6 and 8 kN). The result concluded that the radiata members has displayed effective results compared to the control samples. Similarly, the MGP10 members displayed an increase in strength and lower deflection values; however, for members with cross-section 45 mm by 70 mm, the member starts to fail above the 2 kN region. This is thought to be the effect of a lower GPL applied onto the width of the beam compared to other members that has a width of 70 mm.

The findings of this chapter highlight the needs for further research to be done on this topic for both experimental and theoretical studies. This new reinforcement method using GPL/polymer nanocomposites has proven to be reasonably adequate, despite the errors and limitation. To achieve higher accuracy in results, a more precise material property should be identified. Additional samples need to be tested and a cost-benefit analysis should be conducted before adopting GPL/polymer nanocomposites for the use of strengthening timber infrastructures.

Chapter 6 Conclusions

6.1 Summary

This project has investigated the structural behaviour of MGP10 and radiata members reinforced with different ratio of GPL/polymer nanocomposites layers and comparing its effectiveness against the non-reinforced members. Different cross-section of 70 mm by 45 mm, 70 mm by 35 mm and 45 mm by 70 mm for the MGP10 members were investigated to identify whether the cross-section would affect the bending behaviour of the reinforced members. An in-depth analysis was conducted on the results obtained from the experiment for individual members through the three-point bending flexural test to acquire the flexural strength and modulus of the members. A detailed parametric study was also conducted to obtain the effective modulus of elasticity, Poisson's ratio and effective mass density at a different percentage of weight fraction for the GPL/polymer nanocomposites. Additionally, the parameter of the MGP10 material properties was obtained from the Australian Standards. Based on the obtained parametric values, finite element analyses was used to solve for the static deflections of the reinforced members, these values are then used to compare and validate against the experimental data's.

6.2 Conclusion

From this research, it can be concluded that;

- GPL/polymer nanocomposites layer reinforcement can increase the strength capacity of the MGP10 and radiata members under loading. Compared to the control samples, a reinforcement of a 0.5% graphene shows an average increase of 61.2%, while a reinforcement of 0.25% graphene displays an average of 70% increase for the MGP10 members. On the other hand, the radiata member shows an increase of 20% and 26% for the members reinforced with 0.5% and 0.25% graphene, respectively.
- Compared to the control samples, the MGP10 and radiata members reinforced with 0.25% graphene displayed an average increase in MOE of 14% and 11%, respectively; however, the 0.5% graphene shows a decrease of 6% and 21% for the MGP10 and radiata members, respectively. This has proven the ability of the members reinforced with 0.25% graphene to be able to resist bending better, compared to the 0.5% graphene members.
- GPL/polymer reinforcement also shows an increase in deflection for both 0.25% and 0.5% graphene, which displayed an average increase of 36% and 13.4%, respectively, compared to the control samples.

- Stnad7 FE models have successfully validated the control samples models observed from Strand7 and the experiment. However, the reinforced members show a slight difference, mainly due to the unknown material properties of graphene and epoxy used in the experiment.
- Further analysis was conducted on a pure epoxy based reinforcement. The results show that above the 2 kN loading the epoxy starts to lose its effect compared to the control samples for the MGP10 members with cross-section 45 mm by 70 mm. On the other hand, the radiata and MGP10 models of cross-section 70 mm by 35 mm and 70 mm by 45 mm, reinforced with pure epoxy are more effective in resisting bending under the applied load, compared to the control samples. Overall, these values are just a prediction of the possible outcome that pure epoxy can have on a timber material. Due to the numerous errors and limitation, which involves the material properties, epoxy-based reinforcement was not considered a major finding in this study.

Initially, it was predicted that a higher ratio of graphene would yield more effective results, however the reinforced 0.25% graphene displayed more effective results due to its high strength capacity and relatively low deflection observed compared to the 0.5% graphene and control samples. The undesirable result could be due to the dispersion process of the nanocomposites onto the members as the thickness observed is not consistent. A major contributing factor could also be due to the defects observed in the members, which has caused unpredictable results. Despite the errors and limitation, the experiment shows favourable results for the flexural strength of members reinforced with the nanocomposites, further research and experiment needs to be done before the possibility of recommending GPL/polymer nanocomposites as a new type of reinforcement method.

6.3 Achievement of Project Objectives

This project aims to investigate the potential relationship between timber materials reinforced with graphene nanocomposites. The specific objective described was conducted to assess the outcome of this project.

Objective 1: Review the current standards of MGP10 timber in Australia and different type of reinforcement method involving the use of epoxy and graphene to gain an understanding of the current mechanical properties.

An in-depth literature review has been undertaken to examine previous work done on different strengthening methods that are used on MGP10 timber and its mechanical properties. Due to this paper being the first to examine the strengthening method of a timber material based on GPL/polymer nanocomposites, no literature review has been found which can be used as a comparison to my results. However, a sufficient amount of successful studies has been conducted on the different type of method to strengthen timber material using varies methods such as fibre reinforcement polymer or using steel plate as a reinforcement technique, which can be found in Chapter 2.

Objective 2: Collecting timber material properties data from Australian Standards to use a representative set of data to predict the behaviour of reinforced timber member.

The timber material for MGP10 structural pine is obtained from the Australia Standards AS1720.1:2010 Structural Timber. As there is no explicit information on the Poisson ratio for MGP10 timber, another similar Australian grown pine specimen is known as the slash pine with a Poisson ratio of 0.444 was used in this study, which is discussed previously in Chapter 3. These values are also used in the Strand7 FE software modelling shown in Chapter 5.

Objective 3: Collecting structural performance data from testing of the timber member and compare its effectiveness through analysing the ultimate loading and deflection, modulus of elasticity (MOE), modulus of rupture and

The experiment is separated into two parts. First parts consisted of collecting the required material and dispersing the correct ratio of graphene-epoxy onto the tension and compression side of the timber. The second part deals with the testing of each sample, which were subjected to loading of 1 mm per minute until failure to obtain the load-deflection graph. A total of 12 samples were tested, 3 samples were reinforced with 0.25% graphene, 3 samples reinforced with 0.5% graphene and the last 3 were used as control samples. Numerical studies were then conducted to determine the MOE and MOR, these values represent the strength and stiffness of the samples tested. The experiment was determined to be a success due to the members reinforced with graphene showing an increase in strength capacity compared to the control samples; however, the 0.25% reinforced graphene-displayed results that are more favourable.

Objective 4: Conduct parametric studies to identify the effective material properties of GPL/polymer nanocomposite. Create a mathematical computer model using Strand7 to validate and predict the results obtained from the experiment based on parametric studies.

As there are limited literature review that can identify the bending behaviour of timber reinforced with GPL/polymer nanocomposites. Strand7 FE model was used to validate the test results obtained in Objective 3. The literature review identified numerous research on the material properties of graphene and epoxy nanocomposites, which was then incorporated to determine the effective material properties of GPL/polymer nanocomposites. It was then identified that the effective material properties of the reinforced nanocomposites material can be obtained through the uses of the modified Halpin-Tsai micromechanics model and the rule of mixture. This objective remains an uncertainty, due to the slight differences observed in the FE model, which was the results of inaccurate material properties that was adopted.

Objective 5: Compare the ultimate deflection based on several loading conditions obtained from the model and experiment of the reinforced and non-reinforced timber member

A comparison was made between the reinforced and non-reinforced member, as shown in chapter 3, showing that all reinforced members displayed a great increase in flexural strength compared to the control samples. However, members reinforced with 0.25% graphene displayed an increase in MOE with a relatively lower deflection, compared to members reinforced with 0.5% graphene. This result concluded that the effectiveness of 0.25% graphene is the superior ratio. This could be due to various factors, such as the inconsistent dispersion of the nanocomposites onto the timber, defects within the timber samples, moisture content or the limited testing samples that was conducted, which has all contributed to the inconsistency in the results. Overall, this experiment yields logical results, however, due to numerous errors and limitation surrounding this research project; further work has to be done before recommending using GPL/polymer nanocomposite layers as a widely reinforcement method.

6.4 Recommendations and Future Work

This research has underlined the potential of using GPL/polymer nanocomposites as a new reinforcement method for a structural MGP10 pine. As a result of the experiments, several recommendations can be made.

- Experiment with a variety of duplicate samples to accurately validate the results presented in this study.
- Conduct experimental and numerical studies on the buckling behaviour of MGP10 pine reinforced with GPL/polymer nanocomposites layers.
- Conducting an experiment on several cross-section with larger differences could potentially display more effective results
- Conduct an experiment on the bending and buckling of MGP10 pine member reinforced with pure epoxy based coating.
- Different epoxy and graphene ratio can be used with a higher volume of graphene to analyses its effectiveness.

- Numerical studies on the vibration analysis of MGP10 pine members reinforced with GPL/polymer nanocomposites layer.
- Testing the bond strength between the graphene and epoxy nanocomposites and the timber.
- Assess the cost-benefit of GPL/polymer nanocomposites to demonstrate the overall benefit of this new method compared to the conventional method.
- Investigate the effect of moisture content in the timber material to further increase the accuracy of the results.

List of References

André, A, & Kliger, R 2009, 'Strengthening of timber beams using FRP, with emphasis on compression strength: A state of the art review', The second official International Conference of International Institute for FRP in Construction for Asia-Pacific Region, Seoul, Korea, pp. 193-197.

Anwar, Z, Kausar, A, Rafique, I & Muhammad, B 2016, 'Advances in Epoxy/Graphene Nanoplatelet Composite with Enhanced Physical Properties: A Review', *Polymer-Plastics Technology and Engineering*, vol. 55, no. 6, pp. 643-662.

Aravinthan, T & Manalo, A 2012, Field applications and case studies of FRP in civil infrastructure: the Australian experience. In: 6th International Conference on FRP Composites in Civil Engineering (CICE 2012), 13-15 Jun 2012, Rome, Italy.

Engineers Edge 2019, Engineers Edge, Monroe, Georgia, viewed 16 October 2019, <https://www.engineersedge.com/strength_of_materials.htm>.

Beer, FP, Johnston, ER, Dewolf JT, Mazurek, DF 2015, Mechanics of Materials, McGraw-Hill Education, New York.

Barrett, J, Haigh, I & Lovegrove, J 1981, 'Philosophical Transactions of the Royal Society of London. Series a Mathematical and Physical Sciences', *Fracture Mechanics in Design and Service: Living with Defects,* vol. 299, pp. 217-226.

Bintzler, D 2018, Sciencing, Santa Monica, California, viewed 14 May 2019, <https://sciencing.com/calculate-mix-chemical-solutions-8706412.html>.

Borgin, K, Loedolff, G & Saunders, G 1968, 'Laminated wood beams reinforced with steel strips', *Journal of Structural Division*, vol. 7, pp. 1681-1705.

Dhand, V, Rhee, KY, Kim, HJ & Jung, DH 2013, 'A Comprehensive Review of Graphene Nanocomposites: Rsearch Status and Trends', *Journal of Nanomaterials*, vol. 2013, pp. 1-14.

Gentile, C 2000, 'Flexural Strengthening of Timber Bridge Beam Using FRP', Dissertation, University of Manitoba, Winnipeg, Manitoba, Canada.

Gillia, PP 1972, ‘Orthotropic Elastic Constants of Wood’, *Wood Science and Technology,* vol. 6, pp. 138-156.

Graphene Manufacturing Group 2019, Graphene Manufacturing Group, Darra, Queensland, viewed 14 October 2019, <https://www.graphenemg.com/>.

Green, D, Winandy, J & Kretschmann, D 1999, `Mechanical properties of wood in Forest Products Laboratory', in Forest Products Laboratory, Wood Handbook - Wood as an Engineering Material, General Technical Report FPL-GTR-113, Madison, WI, viewed 22 May 2019, <https://www.fpl.fs.fed.us/documnts/fplgtr/fplgtr113/ch04.pdf>.

Gu, Q & Conte, JP 2003, ‘Convergence Studies in Nonlinear Finite Element Response Sensitivity Analysis’, Proceedings of the Ninth International Conference on Applications of Statics and Probability in Civil Engineering (ICASP9), San Francisco, USA, July 6-9, 2003.

Hibbeler, R 2006, Structural Analysis, 6th edn, Prentice Hall, Pearson Education South Asia Pte Ltd, Singapore.

Huang, D 2004, ‘Structural Behaviour of Two-Way Fibre Reinforced Composite Slabs’, Dissertation, University of Southern Queensland, Toowoomba.

Infrastructure Australia 2019, Infrastructure Priority List: Australian Infrastructure Plan, Project and Initiative Summaries, Infrastructure Australia, Australia, viewed 10 October 2019, <https://www.infrastructureaustralia.gov.au/sites/default/files/2019-07/ia18-4005_priority_list_2019_acc_1_0.pdf>.

Jotun 2019, Jotun, Brisbane, Queensland, viewed 14 October 2019, <https://www.jotun.com/au/en/corporate/contact/>.

KiwiLumber 2014, KiwiLumber, New Zealand, viewed 17 October, <https://www.kiwilumber.com/radiata-pine/radiata-pine-characteristics/>

Gabriel, K 2018, ‘Potential of Softwood Engineered Timber with Graphene’, Dissertation, University of Southern Queensland, Toowoomba.

Liu, G 1997, ‘A step-by-step method of rule-of-mixture of fiber-and particle-reinforced composite materials’, *Composite Structures*, vol. 40, pp. 313-322.

Macias, E, Tembleque, L & Saez, A 2018, ‘Bending and free vibration analysis of functionally graaded graphene vs. carbon nanotube reinforced composite plates’, *Composite Structures,* vol. 186, pp. 123-138.

Martinez, L 2016, Instron, Norwood, Massachusetts, viewed 16 October 2019, <https://www.instron.us/our-company/press-room/blog/2014/april/thermoset-and-thermoplastic-composites-what-is-the-difference>.

Masuelli, M 2013, ‘Introduction of Fibre-Reinforced Polymers – Polymers and Composites: Concepts, Properties and Processes’, *Fibre Reinforced Polymer – The Technology Applied for Concrete Repair*, vol. 1, pp. 3-40.

Nowak, T, Jasienko, J, Kotwica, E & Krzosek, S 2016, ‘Strength Enhancement of Timber Beams Using Steel Plates – Review and Experimental Tests’, Drewno, vol. 59, pp. 196.

Pal, R 2008, ‘On the Lewis-Nielsen model for thermal/electrical conductivity of composites’, *Composites Part A: Applied Science and Manufacturing*, vol. 39, pp. 718-726.

Villoria, G & Miravete, A 2007, ‘Mechanical model to evaluate the effect of the dispersion in nanocomposites’, *Acta Materialia*, vol. 55, pp. 3025-3031.

Plevris, N & Triantafillou, T.C 1992, ‘FRP-Reinforced Wood as Structural Material’, *Journal of Materials in Civil Engineering*, vol. 4, pp. 300-317.

Potts, J, Dreyer, D, Bielawski, C & Ruoff, R 2011, ‘Graphene-based polymer nanocomposites’, *Polymer*, vol. 52, pp. 5-25.

QTimber 2016, Queensland Government, Queensland, viewed 27 May 2019, < https://qtimber.daf.qld.gov.au/guides/strength-groups-and-stress-grades>.

Rafiee, M, Rafiee, J,Wang, Z, Song, H, Yu, Z & Koratkar, N 2009a, `Enhanced mechanical properties of nanocomposites at low graphene content’, *Nano*, vol. 3, no. 12, pp. 3884-3890.

Salonen, M 2015, ‘Prediction of Timber Bridge Girder Strength and Stiffness using Stress Wave Analysis’, Dissertation, University of Southern Queensland, Toowoomba.

Sheshmani, S, Ashori, A & Fashapoyeh, M 2013, `Wood plastic composite using graphene nanoplatelets', *International Journal of Biological Macromolecules*, vol. 58, pp. 1-6.

Standards Australia 2010, Timber – Natural durability ratings, AS 5604-2005, Standards Australia, Sydney, viewed 1 October 2019, <https://www-saiglobal-com.ezproxy.usq.edu.au/online/autologin.asp>.

Standards Australia 2010, Timber Structures - Design Methods, AS 1720.1-2010, Standards Australia, Sydney, viewed 1 October 2019, <https://www-saiglobal-com.ezproxy.usq. edu.au/online/autologin.asp>.

Valluzzi, M, Garbin, E & Modena, C 2007, ‘Flexural strengthening of timber beam by traditional and innovative techniques’, *Journal of Building Appraisal*, vol. 3, pp. 125-143.

Wang, M, Yan, C, & Ma, L 2011, ‘Composites and Their Properties’, IntechOpen, Graphene Nanocomposites, IntechOpen, London, viewed 14 October 2019, <https://www.intechopen.com/books/composites-and-their-properties/graphene-nanocomposites>.

Yasmin, A, Daniel, IM 2004, ‘Mechanical and thermal properties of graphite platelet/epoxy composites’, *Polymer*, vol. 45, pp. 8211-8219.

Young, R, Liu, M, Kinloch, I, Li, S, Zhao, X, Valles, C & Papageorgiou, D 2018, ‘The mechanics of reinforcement of polymers by graphene nanoplatelets’, *Composites Science and Technology,* vol. 154, pp. 110-116.

Yusof, A & Saleh, A. L 2010, ‘Flexural Strengthening of Timber Beam Using Glass Fibre Reinforced Polymer’, *Electronic Journal of Structural Engineering*, vol. 10, pp. 45-56.

Zhao, Z, Feng, C, Wang, Y & Yang, J 2017, `Bending and vibration analysis of functionally graded trapezoidal nanocomposite plates reinforced with graphene nanoplatelets’, *Composite Structures*, vol. 180, pp. 799-808.

Appendix A

Project Specification

Project Specification

For:	Thuong Phan
Title:	Structural behaviour of graphene-epoxy coated timber members
Major:	Civil Engineering
Supervisors:	Prof Karu Karunasena
	Dr. Weena Lokuge
Enrolment:	ENG4111 – ONC S1, 2019
	ENG4112 – ONC S2, 2019
Project Aim:	To investigate the effect of graphene-epoxy coatings on timber structura members
Programme:	**Version 1, 11th March 2019**

1. Conduct a literature review on the possible use of graphene on timber structural members (strength and fire aspects).

2. Review existing standards for testing of timber structures.

3. Designing and planning the experiments. Test variables include:
    - Member cross section
    - Thickness epoxy coating
    - Length
    - Graphene percentage

4. Evaluate the Strength and deflection using strand7 Programme and comparing it to the experimental results

5. Prepare an academic dissertation.

If time and resource permit:

6. Conduct test on column buckling of the timber reinforced with Epoxy + Graphene

7. Expand research to CLT (cross laminated timber) reinforced with graphene + epoxy

Project Timeline

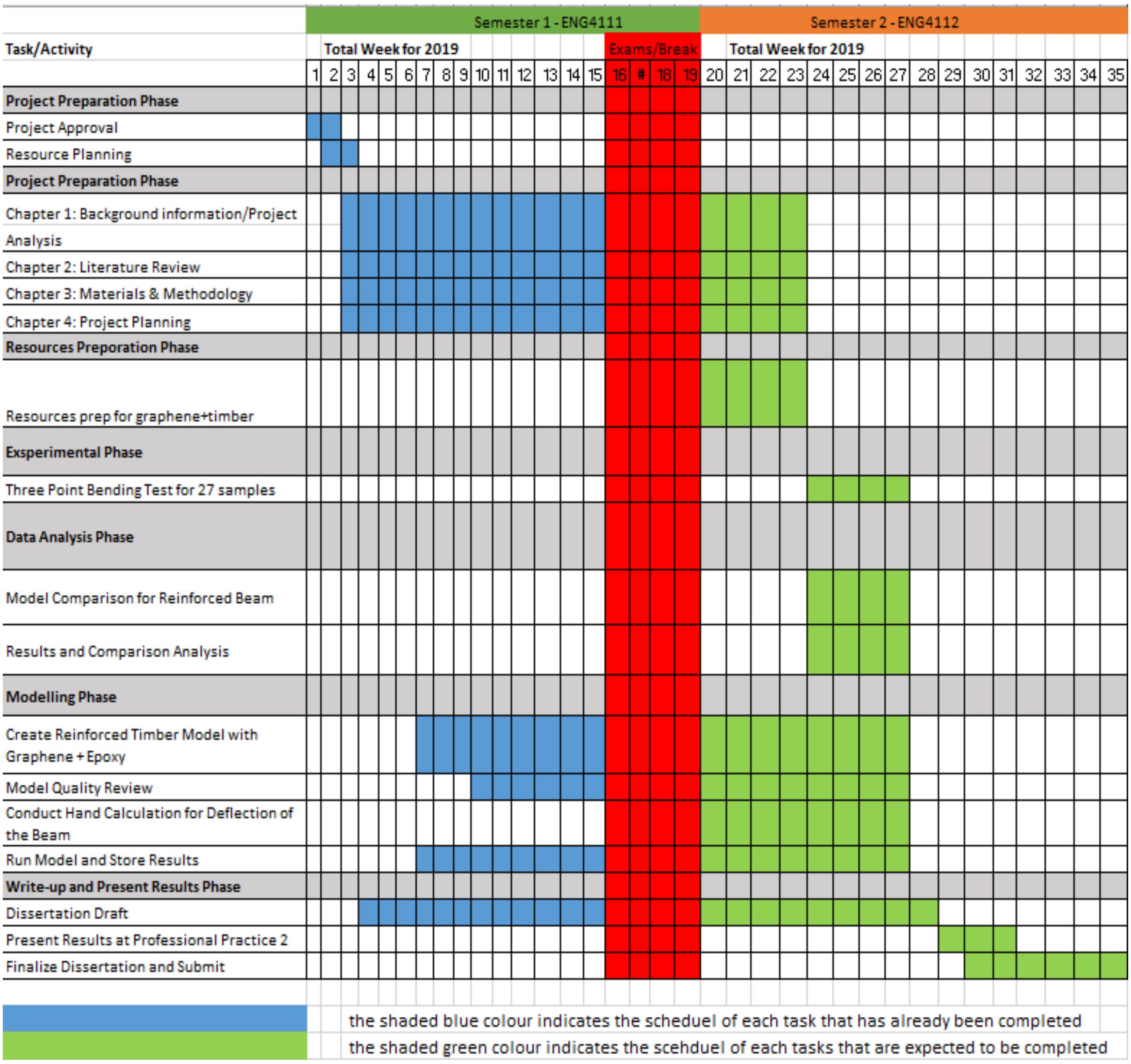

Project Risks Assessment:

UNIVERSITY OF SOUTHERN QUEENSLAND

University of Southern Queensland — Print View

USQ Safety Risk Management System

Version 2.0

Safety Risk Management Plan

Risk Management Plan ID:	Status:	Current User:	Author:	Supervisor:	Approver:
RMP_2019_3685	Approve	i:0#.w|usq\u1082257	i:0#.w|usq\u1082257	i:0#.w|usq\lokuge	i:0#.w|usq\lokuge

Assessment Title:	Flexural testing of graphene-reinforced timber beam	Assessment Date:	13/08/2019
Workplace (Division/Faculty/Section):	204060 - School of Civil Engineering and Surveying	Review Date:	13/08/2019 (5 years maximum)

Approver: *Weena Lokuge*	*Supervisor: (for notification of Risk Assessment only)* *Weena Lokuge*

Context

DESCRIPTION:

What is the task/event/purchase/project/procedure?	Flexural testing of graphene-reinforced timber beam		
Why is it being conducted?	BENG(Civil) Research project work		
Where is it being conducted?	USQ laboratory P11 Toowoomba		
Course code (if applicable)	ENG4111/ENG4112	Chemical Name (if applicable)	Graphene

WHAT ARE THE NOMINAL CONDITIONS?

Personnel involved	Thuong Phan, Piumika Ariyadasa
Equipment	Flexural Test Machine
Environment	laboratory (room temperature with dry condition)
Other	
Briefly explain the procedure/process	The procedure of this experiment is to prepare a normal MGP10 Pine and a MGP10 Pine reinforced with Graphene in a standard process for flexural strength testing.

Assessment Team - who is conducting the assessment?

Assessor(s):	Dr Weena Lokuge, Professor Karu Karunasena, Piumika Ariyadasa
Others consulted: (eg elected health and safety representative, other personnel exposed to risks)	

Risk Matrix

Probability	Consequence: Insignificant No Injury 0-$5K	Minor First Aid $5K-$50K	Moderate Med Treatment $50K-$100K	Major Serious Injury $100K-$250K	Catastrophic Death More than $250K
Almost Certain 1 in 2	M	H	E	E	E
Likely 1 in 100	M	H	H	E	E
Possible 1 in 1,000	L	M	H	H	H
Unlikely 1 in 10,000	L	L	M	M	M
Rare 1 in 1,000,000	L	L	L	L	L

Recommended Action Guide

Extreme:	E– Extreme Risk – Task ***MUST NOT*** proceed
High:	H – High Risk – Special Procedures Required (Contact USQSafe) Approval by VC only
Medium:	M– Medium Risk - A Risk Management Plan/Safe Work Method Statement is required
Low:	L– Low Risk - Manage by routine procedures.

Risk Register and Analysis

	Step 1	Step 2	Step 2a	Step 2b	Step 3			Step 4				
	Hazards: **From step 1 or more if identified**	*The Risk:* **What can happen if exposed to the hazard without existing controls in place?**	*Consequence:* **What is the harm that can be caused by the hazard without existing controls in place?**	*Existing Controls:* **What are the existing controls that are already in place?**	*Risk Assessment:* **Consequence x Probability = Risk Level**			*Additional Controls:* **Enter additional controls if required to reduce the risk level**	*Risk assessment with additional controls:* **Has the consequence or probability changed?**			
					Probability	*Risk Level*	*ALARP*		*Consequence*	*Probability*	*Risk Level*	*ALARP*
	Example											
	Working in temperatures over 35^{0} C	*Heat stress/heat stroke/exhaustion leading to serious personal injury/death*	*catastrophic*	*Regular breaks, chilled water available, loose clothing, fatigue management policy.*	*possible*	*high*	*No*	*temporary shade shelters, essential tasks only, close supervision, buddy system*	*catastrophic*	*unlikely*	*mod*	*Yes*
1	Manual liftin...	Back or spinal injury	Minor	Lab safety induction provided, Wear personal protective equipment (steel cap safety shoes, heavy duty gloves). and using proper manual handling procedure according to USQ safety manual. The action is taking place under the supervision of technical staff.	Unlikel	Low	☑					☐
2	Setting up of ...	Crushing of fingers, physical injury due to falling parts	Minor	Lab safety induction provided, Wear personal protective equipment, The action is taking place under supervision of trained person, make sure fixtures are undamaged, Seek second person help for heavy items	Unlikel	Low	☑					☐
3	Fixing jaws of...	Hand and head injuries	Minor	Wear personal protective equipment (Safety helmet, Steel caps safety shoes, Safety gloves, safety goggles) Lab safety induction provided, The action is taking place under the supervision of well trained person.	Unlikel	Low	☑					☐
4	Projectile fra...	Material can fly from Sans machine causing Body injuries	Minor	Lab safety induction provided, Wear personal protective equipment (steel cap safety shoes, heavy duty gloves,safety goggles and safety helmet). The action is taking place under the supervision. maintain clear distance while the machine is running. Refer to SOP for the emergency stops attached to the sans machine.	Unlikel	Low	☑					☐
5	Testing of ma...	Physical injury from flying broken specimen, crushing fingers from moving parts	Minor	Lab safety induction provided, Wear personal protective equipment. Use safety screen and eye protection, keep clear during testing from moving parts, The action takes place under trained person. use gloves when handling broken specimen, adopt to safety work procedure attached to the machine.	Unlikel	Low	☑					☐
6	Switching on ...	Electrical shock	Minor	Lab safety induction provided. Wear PPE. Use of leather gloves, Trained personnel operates machine,emergency procedures are in place.	Unlikel	Low	☑					☐

Safety Data Sheet

Version 1.0 Rev date 25.10.2017

1. IDENTIFICATION OF THE MATERIAL AND SUPPLIER

Product Name: Multilayer Graphene nanoplates

Recommended Use: Manufacture of substances

Supplier: Graphene Manufacturing Australia Pty Ltd (GMA)

ABN: 83 614 164 877

Street Address: 90 Staghorn Street, Enoggera, 4051, Queensland, Australia

Telephone Number: +61 434 432 002

Emergency Telephone: +61 0434 432 002

2. HAZARDS IDENTIFICATION

GHS Classification – Not a hazardous substance or mixture

GHS Label elements, including precautionary statements

Pictogram:	none
Signal word:	none
Hazard statement(s):	none
Precautionary statement(s):	none

Not a hazardous substance or mixture

Other hazards – none

3. COMPOSITION/INFORMATION ON INGREDIENTS

Components / CAS Number Proportion Risk Phrases

Substances

Formula	:	C
Molecular weight	:	12.01 g/mol
CAS-No.	:	7782-42-5
EC-No.	:	231-955-3

4. FIRST AID MEASURES

If inhaled

If breathed in, move person into fresh air. If not breathing, give artificial respiration.

In case of skin contact

Wash off with soap and plenty of water.

In case of eye contact

Flush eyes with water as a precaution.

If swallowed

Never give anything by mouth to an unconscious person. Rinse mouth with water.

Most important symptoms and effects, both acute and delayed

The most important known symptoms and effects are described in section 11.

Indication of any immediate medical attention and special treatment needed

No data available

5. FIRE FIGHTING MEASURES

Extinguishing media

Use water spray, alcohol-resistant foam, dry chemical or carbon dioxide.

Special hazards arising from the substance or mixture

No data available

Advice for fire-fighters

Wear self-contained breathing apparatus for fire fighting if necessary

Further Information

No data available

6. ACCIDENTAL RELEASE MEASURES

Personal precautions, protective equipment and emergency procedures

Avoid dust formation. Avoid breathing vapours, mist or gas. For personal protection see section 8.

Environmental precautions

No special environmental precautions required.

Methods and materials for containment and cleaning up

Sweep up and shovel. Keep in suitable, closed containers for disposal.

Reference for other sections

For disposal see section 13

7. HANDLING AND STORAGE

Precautions for safe handling

Provide appropriate exhaust ventilation at places where dust us formed. For precautions see section 2.

Conditions for safe storage, including any incompatibilities

Store in a cool place. Keep container tightly closed in a dry and well-ventilated place.

Specific end use(s)

Apart from the uses mentioned in section 1, no other specific.

8. EXPOSURE CONTROLS/PERSONAL PROTECTION

Control parameters

Occupational Exposure Limits

Component	CAS-No.	Value	Control parameter	Basis
Graphite	7782-42-5	TWA	3 mg/m3	Australia. Workplace Exposure Standards for Airborne Contaminants.
	Remarks	See Chapter 14 National Commission documentation available for these values containing no asbestos and <1% crystalline silica, all forms except fibres		
		TWA	3 mg/m3	Australia. Workplace Exposure Standards for Airborne Contaminants
		Containing no asbestos and <1% crystalline silica		

Exposure controls

Appropriate engineering controls

General industrial hygiene practice

Personal protective equipment

Respiratory protection: Protect against inhalation by using type N95 (US) or type P1 (EN 143) dust masks. A respiratory protection program that meets applicable OHSA requirements should be maintained in the workplace.

Eye protection: Protect against contact with eyes by wearing suitable safety eyeglasses or chemical protective goggles or other face protection.

Skin protection: Protect against skin contact by wearing protective gloves. Protect against skin contact by wearing suitable clothing.

9. PHYSICAL AND CHEMICAL PROPERTIES

Physical state and appearance:	Solid.
Odor:	Odorless.
Taste:	Tasteless.
Molecular Weight:	12.01 g/mole
Color:	Black
pH (1% soln/water):	Not applicable.
Boiling Point:	Not available.
Melting Point:	3650°C (6602°F)
Critical Temperature:	681°C (1257.8°F)
Specific Gravity:	Not available.
Vapor Pressure:	Not applicable.
Vapor Density:	Not available.
Volatility:	Not available.
Odor Threshold:	Not available.
Water/Oil Dist. Coeff.:	Not available.
Ionicity (in Water):	Not available.
Dispersion Properties:	Not available.
Solubility:	Insoluble in cold water.

Other safety information

No data available

10. STABILITY AND REACTIVITY

Stability: The product is stable.

Instability Temperature: Not available.

Conditions of Instability: Excess heat, incompatible materials.

Incompatibility with various substances: Highly reactive with oxidizing agents.

Corrosivity: Non-corrosive in presence of glass.

Special Remarks on Reactivity:

Reacts vigorously with liquid potassium, and potassium peroxide. If graphene contacts liquid potassium, rubidium or caesium at 300 C, intercalation compounds may be formed.

Special Remarks on Corrosivity: Not available. Polymerization: Will not occur.

Chemical stability: Stable under normal conditions of use.

Conditions to avoid: Avoid contact with foodstuffs. Avoid exposure to heat, sources of ignition, and open

flame.

Incompatible materials: Incompatible with oxidising agents.

Hazardous decomposition products:

Hazardous decomposition products formed under fire conditions – Carbon oxides

Other decompositions products – No data available

11. TOXICOLOGICAL INFORMATION

Routes of Entry: Inhalation. Ingestion.

Toxicity to Animals:

LD50 (oral, rat): >2000mg/kg (OECD Test Guideline 423)

LC50 (inhalation, rat): 4h – 2,000mg/m3 (OECD Test Guideline 403)

Serious eye damage/eye irritation

Eyes – Rabbit

Result: No eye irritation (OECD Test Guideline 405)

Skin corrosion/irritation

Skin – Rabbit

Result: No skin irritation (OECD Test Guideline 404)

Respiratory or skin sensitisation

- Mouse; Did not cause sensitisation on laboratory animals (OECD Test 429)

Germ cell mutagenicity

In vitro assay

S. typhimurium

Results: negative

Carcinogenicity

IARC: No component of this product present at levels greater than or equal to 0.1% is identified as probable, possible or confirmed human carcinogen by IARC

Reproductive toxicity

No data available

Specific target organ toxicity – single exposure

No data available

Specific target organ toxicity – repeated exposure

No data available

Aspiration hazard: No data available

Additional information

To the best of our knowledge, the chemical, physical and toxicological properties have not been thoroughly investigated.

12. ECOLOGICAL INFORMATION

Toxicity

Toxicity to fish: Semi-static test LC50 – Danio rerio (Zebra fish) - > 100 mg/l – 96 h (OECD Test Guideline 203)

Toxicity to daphnia and other invertebrates: Static test EC50 - Daphnia magne (Water flea) - > 100 mg/l – 48 h (OECD Test Guideline 202)

Toxicity to algae: Static test EC50 – Pseudokirchneriella subcapitata - > 100 mg/l – 72 h (OECD Test Guideline 201)

BOD5 and COD: Not available.

Persistence and degradability: Not available

Mobility in soil: No data available

Other adverse effects

No data available

13. DISPOSAL CONSIDERATIONS

Waste treatment methods

Product

Offer surplus and non-recyclable solutions to a licensed disposal company

Contaminated packaging

Dispose of as unused product

14. TRANSPORT INFORMATION

UN number

ADR/RID: - IMDG: - IATA-DGR: -

UN proper shipping name

ADR/RID:	Not dangerous goods
IMDG:	Not dangerous goods
IATA-DGR:	Not dangerous goods

Transport hazard class

ADR/RID: - IMDG: - IATA-DGR: -

Packaging group

ADR/RID: - IMDG: - IATA-DGR: -

Environmental hazards

ADR/RID: no IMDG Marine pollutant: no IATA-DGR: no

Special precautions for user

No data available

15. REGULATORY INFORMATION

Safety, Health and environmental regulations/legislation specific for the substance or mixture

Standard for the Uniform Scheduling of medicines and poisons

No data available

Carcinogen classification under the WHS REguation 2011, Schedule 10

Not listed

16. OTHER INFORMATION

Safety Data Sheet – Graphene Manufacturing Australia Pty Ltd (GMA); 25/10/2017

This material safety data sheet has been prepared by GMA.

This SDS summarises to our best knowledge at the date of issue, the chemical health and safety hazards of the material and general guidance on how to safely handle the material in the workplace. Since GMA cannot anticipate or control the conditions under which the product may be used, each user must, prior to usage, assess and control the risks arising from its use of the material.

If clarification or further information is needed, the user should contact their GMA representative at the contact details on page 1.

GMA responsibility for the material as sold is subject to the terms and conditions of sale, a copy of which is available upon request.

SAFETY DATA SHEET

JOTUN
Jotun Protects Property

Jotacote 605 Comp A

Section 1. Identification

Product name	:	Jotacote 605 Comp A
Code	:	15962
Product description	:	Paint.
Product type	:	Liquid.
Other means of identification	:	Not available.

Relevant identified uses of the substance or mixture and uses advised against

Not applicable.

Identified uses
Use in coatings - Professional use

Manufacturer : Jotun Australia
9 Cawley Road
Brooklyn 3012
Australia

Telephone + 61 39314 0722
Fax + 61 39314 0423

SDSJotun@jotun.com

Emergency telephone number : Medical Emergencies 24 hours: Poisons Information Centre (Australia) 131 126

Section 2. Hazard(s) identification

Classification of the substance or mixture : FLAMMABLE LIQUIDS - Category 3
SKIN CORROSION/IRRITATION - Category 2
SERIOUS EYE DAMAGE/EYE IRRITATION - Category 2A
SKIN SENSITISATION - Category 1
SPECIFIC TARGET ORGAN TOXICITY - REPEATED EXPOSURE (central nervous system (CNS)) - Category 2
LONG-TERM (CHRONIC) AQUATIC HAZARD - Category 2

GHS label elements

Hazard pictograms :

Signal word : **WARNING**

Section 2. Hazard(s) identification

Hazard statements	: **H226 - Flammable liquid and vapour.** **H319 - Causes serious eye irritation.** **H315 - Causes skin irritation.** **H317 - May cause an allergic skin reaction.** **H373 - May cause damage to organs through prolonged or repeated exposure. (central nervous system (CNS))** **H411 - Toxic to aquatic life with long lasting effects.**

Precautionary statements

Prevention	: P280 - Wear protective gloves. Wear eye or face protection. P210 - Keep away from heat, hot surfaces, sparks, open flames and other ignition sources. No smoking. P233 - Keep container tightly closed. P273 - Avoid release to the environment. P260 - Do not breathe vapour. P264 - Wash hands thoroughly after handling.
Response	: P391 - Collect spillage. P314 - Get medical attention if you feel unwell. P302 + P352 + P362 + P363 - IF ON SKIN: Wash with plenty of soap and water. Take off contaminated clothing. Wash contaminated clothing before reuse. P333 + P313 - If skin irritation or rash occurs: Get medical attention. P305 + P351 + P338 - IF IN EYES: Rinse cautiously with water for several minutes. Remove contact lenses, if present and easy to do. Continue rinsing. P337 + P313 - If eye irritation persists: Get medical attention.
Storage	: P403 - Store in a well-ventilated place. P235 - Keep cool.
Disposal	: P501 - Dispose of contents and container in accordance with all local, regional, national and international regulations.
Supplemental label elements	: Not applicable.
Other hazards which do not result in classification	: None known.

Section 3. Composition and ingredient information

Substance/mixture	: Mixture
Other means of identification	: Not available.

CAS number/other identifiers

CAS number	: Not applicable.
EC number	: Mixture.
Product code	: 15962

Ingredient name	% (w/w)	CAS number
epoxy resin (MW ≤ 700)	≥30 - ≤60	1675-54-3
hydrocarbons, C9-C12, n-alkanes, isoalkanes, cyclics, aromatics (2-25%), (<0.1% Benzene)	<10	64742-82-1
xylene	≤3	1330-20-7

There are no additional ingredients present which, within the current knowledge of the supplier and in the concentrations applicable, are classified as hazardous to health or the environment and hence require reporting in this section.

Occupational exposure limits, if available, are listed in Section 8.

Section 4. First aid measures

Description of necessary first aid measures

Eye contact	: Immediately flush eyes with plenty of water, occasionally lifting the upper and lower eyelids. Check for and remove any contact lenses. Continue to rinse for at least 10 minutes. Get medical attention.
Inhalation	: Remove victim to fresh air and keep at rest in a position comfortable for breathing. If not breathing, if breathing is irregular or if respiratory arrest occurs, provide artificial respiration or oxygen by trained personnel. It may be dangerous to the person providing aid to give mouth-to-mouth resuscitation. Get medical attention following exposure or if feeling unwell. If unconscious, place in recovery position and get medical attention immediately. Maintain an open airway. Loosen tight clothing such as a collar, tie, belt or waistband.
Skin contact	: Wash with plenty of soap and water. Remove contaminated clothing and shoes. Wash contaminated clothing thoroughly with water before removing it, or wear gloves. Continue to rinse for at least 10 minutes. Get medical attention. In the event of any complaints or symptoms, avoid further exposure. Wash clothing before reuse. Clean shoes thoroughly before reuse.
Ingestion	: Wash out mouth with water. Remove dentures if any. Remove victim to fresh air and keep at rest in a position comfortable for breathing. If material has been swallowed and the exposed person is conscious, give small quantities of water to drink. Stop if the exposed person feels sick as vomiting may be dangerous. Do not induce vomiting unless directed to do so by medical personnel. If vomiting occurs, the head should be kept low so that vomit does not enter the lungs. Get medical attention following exposure or if feeling unwell. Never give anything by mouth to an unconscious person. If unconscious, place in recovery position and get medical attention immediately. Maintain an open airway. Loosen tight clothing such as a collar, tie, belt or waistband.

Most important symptoms/effects, acute and delayed

Potential acute health effects

Eye contact	: Causes serious eye irritation.
Inhalation	: No known significant effects or critical hazards.
Skin contact	: Causes skin irritation. May cause an allergic skin reaction.
Ingestion	: No known significant effects or critical hazards.

Over-exposure signs/symptoms

Eye contact	: Adverse symptoms may include the following: pain or irritation watering redness
Inhalation	: No specific data.
Skin contact	: Adverse symptoms may include the following: irritation redness
Ingestion	: No specific data.

Indication of immediate medical attention and special treatment needed, if necessary

Notes to physician	: Treat symptomatically. Contact poison treatment specialist immediately if large quantities have been ingested or inhaled.
Specific treatments	: No specific treatment.
Protection of first-aiders	: No action shall be taken involving any personal risk or without suitable training. It may be dangerous to the person providing aid to give mouth-to-mouth resuscitation. Wash contaminated clothing thoroughly with water before removing it, or wear gloves.

See toxicological information (Section 11)

Section 5. Firefighting measures

Extinguishing media

Suitable extinguishing media	: Use dry chemical, CO_2, water spray (fog) or foam.
Unsuitable extinguishing media	: Do not use water jet.
Specific hazards arising from the chemical	: Flammable liquid and vapour. Runoff to sewer may create fire or explosion hazard. In a fire or if heated, a pressure increase will occur and the container may burst, with the risk of a subsequent explosion. This material is toxic to aquatic life with long lasting effects. Fire water contaminated with this material must be contained and prevented from being discharged to any waterway, sewer or drain.
Hazardous thermal decomposition products	: Decomposition products may include the following materials: carbon dioxide carbon monoxide sulfur oxides metal oxide/oxides
Special protective actions for fire-fighters	: Promptly isolate the scene by removing all persons from the vicinity of the incident if there is a fire. No action shall be taken involving any personal risk or without suitable training. Move containers from fire area if this can be done without risk. Use water spray to keep fire-exposed containers cool.
Special protective equipment for fire-fighters	: Fire-fighters should wear appropriate protective equipment and self-contained breathing apparatus (SCBA) with a full face-piece operated in positive pressure mode.
Hazchem code	: •3Y

Section 6. Accidental release measures

Personal precautions, protective equipment and emergency procedures

For non-emergency personnel	: No action shall be taken involving any personal risk or without suitable training. Evacuate surrounding areas. Keep unnecessary and unprotected personnel from entering. Do not touch or walk through spilt material. Shut off all ignition sources. No flares, smoking or flames in hazard area. Avoid breathing vapour or mist. Provide adequate ventilation. Wear appropriate respirator when ventilation is inadequate. Put on appropriate personal protective equipment.
For emergency responders	: If specialised clothing is required to deal with the spillage, take note of any information in Section 8 on suitable and unsuitable materials. See also the information in "For non-emergency personnel".
Environmental precautions	: Avoid dispersal of spilt material and runoff and contact with soil, waterways, drains and sewers. Inform the relevant authorities if the product has caused environmental pollution (sewers, waterways, soil or air). Water polluting material. May be harmful to the environment if released in large quantities. Collect spillage.

Methods and material for containment and cleaning up

Small spill	: Stop leak if without risk. Move containers from spill area. Use spark-proof tools and explosion-proof equipment. Dilute with water and mop up if water-soluble. Alternatively, or if water-insoluble, absorb with an inert dry material and place in an appropriate waste disposal container. Dispose of via a licensed waste disposal contractor.
Large spill	: Stop leak if without risk. Move containers from spill area. Use spark-proof tools and explosion-proof equipment. Approach the release from upwind. Prevent entry into sewers, water courses, basements or confined areas. Wash spillages into an effluent treatment plant or proceed as follows. Contain and collect spillage with non-combustible, absorbent material e.g. sand, earth, vermiculite or diatomaceous earth and place in container for disposal according to local regulations (see Section 13). Dispose of via a licensed waste disposal contractor. Contaminated absorbent

Section 6. Accidental release measures

material may pose the same hazard as the spilt product. Note: see Section 1 for emergency contact information and Section 13 for waste disposal.

Section 7. Handling and storage

The information in this section contains generic advice and guidance. The list of Identified Uses in Section 1 should be consulted for any available use-specific information provided in the Exposure Scenario(s).

Precautions for safe handling

Protective measures : Put on appropriate personal protective equipment (see Section 8). Persons with a history of skin sensitization problems should not be employed in any process in which this product is used. Do not get in eyes or on skin or clothing. Do not breathe vapour or mist. Do not ingest. Avoid release to the environment. Use only with adequate ventilation. Wear appropriate respirator when ventilation is inadequate. Do not enter storage areas and confined spaces unless adequately ventilated. Keep in the original container or an approved alternative made from a compatible material, kept tightly closed when not in use. Store and use away from heat, sparks, open flame or any other ignition source. Use explosion-proof electrical (ventilating, lighting and material handling) equipment. Use only non-sparking tools. Take precautionary measures against electrostatic discharges. Empty containers retain product residue and can be hazardous. Do not reuse container.

Advice on general occupational hygiene : Eating, drinking and smoking should be prohibited in areas where this material is handled, stored and processed. Workers should wash hands and face before eating, drinking and smoking. Remove contaminated clothing and protective equipment before entering eating areas. See also Section 8 for additional information on hygiene measures.

Conditions for safe storage, including any incompatibilities : Store in accordance with local regulations. Store in a segregated and approved area. Store in original container protected from direct sunlight in a dry, cool and well-ventilated area, away from incompatible materials (see Section 10) and food and drink. Eliminate all ignition sources. Separate from oxidizing materials. Keep container tightly closed and sealed until ready for use. Containers that have been opened must be carefully resealed and kept upright to prevent leakage. Do not store in unlabelled containers. Use appropriate containment to avoid environmental contamination. See Section 10 for incompatible materials before handling or use.

See Technical Data Sheet / packaging for further information.

Section 8. Exposure controls and personal protection

The information in this section contains generic advice and guidance. The list of Identified Uses in Section 1 should be consulted for any available use-specific information provided in the Exposure Scenario(s).

Control parameters

Occupational exposure limits

epoxy resin (MW ≤ 700)	**DFG MAC-values list (Germany, 7/2018). Absorbed through skin. Skin sensitiser.**
xylene	**Safe Work Australia (Australia, 4/2018).** STEL: 655 mg/m³ 15 minutes. STEL: 150 ppm 15 minutes. TWA: 350 mg/m³ 8 hours. TWA: 80 ppm 8 hours.

Appropriate engineering controls : Use only with adequate ventilation. Use process enclosures, local exhaust ventilation or other engineering controls to keep worker exposure to airborne contaminants below any recommended or statutory limits. The engineering controls also need to keep gas, vapour or dust concentrations below any lower explosive limits. Use explosion-proof ventilation equipment.

Section 8. Exposure controls and personal protection

Environmental exposure controls	: Emissions from ventilation or work process equipment should be checked to ensure they comply with the requirements of environmental protection legislation. In some cases, fume scrubbers, filters or engineering modifications to the process equipment will be necessary to reduce emissions to acceptable levels.

Individual protection measures

Hygiene measures	: Wash hands, forearms and face thoroughly after handling chemical products, before eating, smoking and using the lavatory and at the end of the working period. Appropriate techniques should be used to remove potentially contaminated clothing. Contaminated work clothing should not be allowed out of the workplace. Wash contaminated clothing before reusing. Ensure that eyewash stations and safety showers are close to the workstation location.
Eye/face protection	: Safety eyewear complying to EN 166 should be used when a risk assessment indicates this is necessary to avoid exposure to liquid splashes, mists, gases or dusts. If contact is possible, the following protection should be worn, unless the assessment indicates a higher degree of protection: chemical splash goggles.

Skin protection

Hand protection	: Chemical-resistant, impervious gloves complying with an approved standard should be worn at all times when handling chemical products if a risk assessment indicates this is necessary. Considering the parameters specified by the glove manufacturer, check during use that the gloves are still retaining their protective properties. It should be noted that the time to breakthrough for any glove material may be different for different glove manufacturers. In the case of mixtures, consisting of several substances, the protection time of the gloves cannot be accurately estimated. There is no one glove material or combination of materials that will give unlimited resistance to any individual or combination of chemicals. The breakthrough time must be greater than the end use time of the product. The instructions and information provided by the glove manufacturer on use, storage, maintenance and replacement must be followed. Gloves should be replaced regularly and if there is any sign of damage to the glove material. Always ensure that gloves are free from defects and that they are stored and used correctly. The performance or effectiveness of the glove may be reduced by physical/chemical damage and poor maintenance. Barrier creams may help to protect the exposed areas of the skin but should not be applied once exposure has occurred. Wear suitable gloves tested to EN374. Recommended, gloves(breakthrough time) > 8 hours: nitrile rubber, 4H, Teflon May be used, gloves(breakthrough time) 4 - 8 hours: butyl rubber Not recommended, gloves(breakthrough time) < 1 hour: neoprene, PVC
Body protection	: Personal protective equipment for the body should be selected based on the task being performed and the risks involved and should be approved by a specialist before handling this product. When there is a risk of ignition from static electricity, wear anti-static protective clothing. For the greatest protection from static discharges, clothing should include anti-static overalls, boots and gloves.
Other skin protection	: Appropriate footwear and any additional skin protection measures should be selected based on the task being performed and the risks involved and should be approved by a specialist before handling this product.
Respiratory protection	: Based on the hazard and potential for exposure, select a respirator that meets the appropriate standard or certification. Respirators must be used according to a respiratory protection program to ensure proper fitting, training, and other important aspects of use.

Section 9. Physical and chemical properties

Appearance	
Physical state	: Liquid.
Colour	: Various
Odour	: Characteristic.
Odour threshold	: Not applicable.
pH	: Not applicable.
Melting point	: Not applicable.
Boiling point	: Lowest known value: 136.16°C (277.1°F) (xylene). Weighted average: 278.91°C (534°F)
Flash point	: Closed cup: 55°C (131°F)
Evaporation rate	: Highest known value: 0.77 (xylene) Weighted average: 0.23compared with butyl acetate
Flammability (solid, gas)	: Not available.
Lower and upper explosive (flammable) limits	: 0.3 - 7.6%
Vapour pressure	: Highest known value: 2.7 kPa (20.3 mm Hg) (at 20°C) (hydrocarbons, C9-C12, n-alkanes, isoalkanes, cyclics, aromatics (2-25%), (<0.1% Benzene)). Weighted average: 0.33 kPa (2.48 mm Hg) (at 20°C)
Vapour density	: Highest known value: 11.7 (Air = 1) (epoxy resin (MW ≤ 700)). Weighted average: 11.46 (Air = 1)
Relative density	: 1.28 to 1.615 g/ cm^3
Solubility	: Insoluble in the following materials: cold water and hot water.
Partition coefficient: n-octanol/water	: Not available.
Auto-ignition temperature	: Lowest known value: 280 to 470°C (536 to 878°F) (hydrocarbons, C9-C12, n-alkanes, isoalkanes, cyclics, aromatics (2-25%), (<0.1% Benzene)).
Decomposition temperature	: Not available.
Viscosity	: Kinematic (40°C (104°F)): >0.205 cm^2/s (>20.5 mm^2/s)

Section 10. Stability and reactivity

Reactivity	: No specific test data related to reactivity available for this product or its ingredients.
Chemical stability	: The product is stable.
Possibility of hazardous reactions	: Under normal conditions of storage and use, hazardous reactions will not occur.
Conditions to avoid	: Avoid all possible sources of ignition (spark or flame). Do not pressurise, cut, weld, braze, solder, drill, grind or expose containers to heat or sources of ignition.
Incompatible materials	: Keep away from the following materials to prevent strong exothermic reactions: oxidising agents, strong alkalis, strong acids.
Hazardous decomposition products	: Under normal conditions of storage and use, hazardous decomposition products should not be produced.

Section 11. Toxicological information

There are no data available on the mixture itself. The mixture has been assessed following the conventional method of the CLP Regulation (EC) No 1272/2008 and is classified for toxicological properties accordingly. See Sections 2 and 3 for details.

Exposure to component solvent vapour concentrations in excess of the stated occupational exposure limit may result in adverse health effects such as mucous membrane and respiratory system irritation and adverse effects on the kidneys, liver and central nervous system. Symptoms and signs include headache, dizziness, fatigue, muscular weakness, drowsiness and, in extreme cases, loss of consciousness.

Section 11. Toxicological information

Solvents may cause some of the above effects by absorption through the skin. Repeated or prolonged contact with the mixture may cause removal of natural fat from the skin, resulting in non-allergic contact dermatitis and absorption through the skin.
If splashed in the eyes, the liquid may cause irritation and reversible damage.
Ingestion may cause nausea, diarrhea and vomiting.
This takes into account, where known, delayed and immediate effects and also chronic effects of components from short-term and long-term exposure by oral, inhalation and dermal routes of exposure and eye contact.

Based on the properties of the epoxy constituent(s) and considering toxicological data on similar mixtures, this mixture may be a skin sensitiser and an irritant. It contains low molecular weight epoxy constituents which are irritating to eyes, mucous membrane and skin. Repeated skin contact may lead to irritation and to sensitisation, possibly with cross-sensitisation to other epoxies. Skin contact with the mixture and exposure to spray mist and vapour should be avoided.

Contains 2,2'-[(1-methylethylidene)bis(4,1-phenyleneoxymethylene)]bisoxirane. May produce an allergic reaction.

Information on toxicological effects

Acute toxicity

Product/ingredient name	Result	Species	Dose	Exposure
epoxy resin (MW ≤ 700)	LD50 Dermal	Rabbit	20 g/kg	-
xylene	LC50 Inhalation Vapour	Rat	20 mg/l	4 hours
	LD50 Oral	Rat	4300 mg/kg	-
	TDLo Dermal	Rabbit	4300 mg/kg	-

Irritation/Corrosion

Product/ingredient name	Result	Species	Score	Exposure	Observation
epoxy resin (MW ≤ 700)	Eyes - Severe irritant	Rabbit	-	24 hours 2 mg	-
	Skin - Mild irritant	Rabbit	-	500 mg	-

Sensitisation

Not available.

Mutagenicity

Not available.

Carcinogenicity

Not available.

Reproductive toxicity

Not available.

Teratogenicity

Not available.

Specific target organ toxicity (single exposure)

Name	Category	Route of exposure	Target organs
naphtha (petroleum), hydrodesulphurized heavy, (<0.1% Benzene)	Category 3	Not applicable.	Narcotic effects
xylene	Category 3	Not applicable.	Respiratory tract irritation

Specific target organ toxicity (repeated exposure)

Name	Category	Route of exposure	Target organs
naphtha (petroleum), hydrodesulphurized heavy, (<0.1% Benzene)	Category 1	Not determined	central nervous system (CNS)

Aspiration hazard

Section 11. Toxicological information

Name	Result
naphtha (petroleum), hydrodesulphurized heavy, (<0.1% Benzene)	ASPIRATION HAZARD - Category 1
xylene	ASPIRATION HAZARD - Category 1

Information on likely routes of exposure : Not available.

Potential acute health effects

Eye contact : Causes serious eye irritation.
Inhalation : No known significant effects or critical hazards.
Skin contact : Causes skin irritation. May cause an allergic skin reaction.
Ingestion : No known significant effects or critical hazards.

Symptoms related to the physical, chemical and toxicological characteristics

Eye contact : Adverse symptoms may include the following:
pain or irritation
watering
redness
Inhalation : No specific data.
Skin contact : Adverse symptoms may include the following:
irritation
redness
Ingestion : No specific data.

Delayed and immediate effects as well as chronic effects from short and long-term exposure

Short term exposure

Potential immediate effects : Not available.
Potential delayed effects : Not available.

Long term exposure

Potential immediate effects : Not available.
Potential delayed effects : Not available.

Potential chronic health effects

Not available.

General : May cause damage to organs through prolonged or repeated exposure. Once sensitized, a severe allergic reaction may occur when subsequently exposed to very low levels.
Carcinogenicity : No known significant effects or critical hazards.
Mutagenicity : No known significant effects or critical hazards.
Teratogenicity : No known significant effects or critical hazards.
Developmental effects : No known significant effects or critical hazards.
Fertility effects : No known significant effects or critical hazards.

Numerical measures of toxicity

Acute toxicity estimates

Route	ATE value
Dermal	63923.7 mg/kg
Inhalation (vapours)	639.2 mg/l

Section 11. Toxicological information

Section 12. Ecological information

Toxicity

Product/ingredient name	Result	Species	Exposure
epoxy resin (MW ≤ 700)	Acute EC50 1.4 mg/l	Daphnia	48 hours
	Acute LC50 3.1 mg/l	Fish - pimephales promelas	96 hours
	Chronic NOEC 0.3 mg/l	Fish	21 days
naphtha (petroleum), hydrodesulphurized heavy, (<0.1% Benzene)	Acute EC50 <10 mg/l	Daphnia	48 hours
	Acute IC50 <10 mg/l	Algae	72 hours
	Acute LC50 <10 mg/l	Fish	96 hours

Persistence and degradability

Product/ingredient name	Aquatic half-life	Photolysis	Biodegradability
epoxy resin (MW ≤ 700)	-	-	Not readily
naphtha (petroleum), hydrodesulphurized heavy, (<0.1% Benzene)	-	-	Not readily
xylene	-	-	Readily

Bioaccumulative potential

Product/ingredient name	$LogP_{ow}$	BCF	Potential
epoxy resin (MW ≤ 700)	2.64 to 3.78	31	low
naphtha (petroleum), hydrodesulphurized heavy, (<0.1% Benzene)	-	10 to 2500	high
xylene	3.12	8.1 to 25.9	low

Mobility in soil

Soil/water partition coefficient (K_{OC}) : Not available.

Other adverse effects : No known significant effects or critical hazards.

Section 13. Disposal considerations

Disposal methods : The generation of waste should be avoided or minimised wherever possible. Disposal of this product, solutions and any by-products should at all times comply with the requirements of environmental protection and waste disposal legislation and any regional local authority requirements. Dispose of surplus and non-recyclable products via a licensed waste disposal contractor. Waste should not be disposed of untreated to the sewer unless fully compliant with the requirements of all authorities with jurisdiction. Waste packaging should be recycled. Incineration or landfill should only be considered when recycling is not feasible. This material and its container must be disposed of in a safe way. Care should be taken when handling emptied containers that have not been cleaned or rinsed out. Empty containers or liners may retain some product residues. Vapour from product residues may create a highly flammable or explosive atmosphere inside the container. Do not cut, weld or grind used containers unless they have been cleaned thoroughly internally. Avoid dispersal of spilt material and runoff and contact with soil, waterways, drains and sewers.

Do not allow to enter drains or watercourses. Material and/or container must be disposed of as hazardous waste.

Section 13. Disposal considerations

Section 14. Transport information

	ADG	ADR/RID	IMDG	IATA
UN number	UN1263	UN1263	UN1263	UN1263
UN proper shipping name	Paint	Paint	Paint	Paint
Transport hazard class(es)	3 	3 	3 	3 
Packing group	III	III	III	III
Environmental hazards	Yes. The environmentally hazardous substance mark is not required.	Yes.	Yes.	Yes. The environmentally hazardous substance mark is not required.
Additional information	**Hazchem code** •3Y	The environmentally hazardous substance mark is not required when transported in sizes of ≤5 L or ≤5 kg. **Hazard identification number** 30 **Tunnel code** (D/E)	The marine pollutant mark is not required when transported in sizes of ≤5 L or ≤5 kg. **Emergency schedules** F-E, S-E	The environmentally hazardous substance mark may appear if required by other transportation regulations.

Special precautions for user : **Transport within user's premises:** always transport in closed containers that are upright and secure. Ensure that persons transporting the product know what to do in the event of an accident or spillage.

Transport in bulk according to Annex II of Marpol and the IBC Code : Not available.

Marine pollutant substances : epoxy resin (MW ≤ 700)

Transport within user's premises: always transport in closed containers that are upright and secure. Ensure that persons transporting the product know what to do in the event of an accident or spillage.

Transport in accordance with ADR/RID, IMDG/IMO and ICAO/IATA and national regulation.

Marking : The environmental hazardous / marine pollutant mark is only applicable for packages containing more than 5 litres for liquids and 5 kg for solids.

Section 15. Regulatory information

Standard Uniform Schedule of Medicine and Poisons

5

Model Work Health and Safety Regulations - Scheduled Substances

No listed substance

Australia inventory (AICS) : All ingredients are listed on AICS or are exempt.

International regulations

Chemical Weapon Convention List Schedules I, II & III Chemicals

Section 15. Regulatory information

Not listed.

Montreal Protocol (Annexes A, B, C, E)

Not listed.

Stockholm Convention on Persistent Organic Pollutants

Not listed.

Rotterdam Convention on Prior Informed Consent (PIC)

Not listed.

UNECE Aarhus Protocol on POPs and Heavy Metals

Not listed.

International lists

National inventory

Canada	: Not determined.
China	: Not determined.
Europe	: Not determined.
Japan	: **Japan inventory (ENCS)**: Not determined. **Japan inventory (ISHL)**: Not determined.
Malaysia	: Not determined.
New Zealand	: Not determined.
Philippines	: Not determined.
Republic of Korea	: Not determined.
Taiwan	: Not determined.
United States	: Not determined.

Section 16. Any other relevant information

History

Date of printing	: 31.05.2019
Date of issue/Date of revision	: 31.05.2019
Date of previous issue	: 18.08.2016
Version	: 1.03
Key to abbreviations	: ADG = Australian Dangerous Goods ATE = Acute Toxicity Estimate BCF = Bioconcentration Factor GHS = Globally Harmonized System of Classification and Labelling of Chemicals IATA = International Air Transport Association IBC = Intermediate Bulk Container IMDG = International Maritime Dangerous Goods LogPow = logarithm of the octanol/water partition coefficient MARPOL = International Convention for the Prevention of Pollution From Ships, 1973 as modified by the Protocol of 1978. ("Marpol" = marine pollution) NOHSC = National Occupational Health and Safety Commission SUSMP = Standard for the Uniform Scheduling of Medicines and Poisons UN = United Nations

Procedure used to derive the classification

Section 16. Any other relevant information

Classification	Justification
Flam. Liq. 3, H226	On basis of test data
Skin Irrit. 2, H315	Calculation method
Eye Irrit. 2A, H319	Calculation method
Skin Sens. 1, H317	Calculation method
STOT RE 2, H373 (central nervous system (CNS))	Calculation method
Aquatic Chronic 2, H411	Calculation method

References : Not available.

Indicates information that has changed from previously issued version.

Disclaimer

The information in this document is given to the best of Jotun's knowledge, based on laboratory testing and practical experience. Jotun's products are considered as semi-finished goods and as such, products are often used under conditions beyond Jotun's control. Jotun cannot guarantee anything but the quality of the product itself. Minor product variations may be implemented in order to comply with local requirements. Jotun reserves the right to change the given data without further notice.

Users should always consult Jotun for specific guidance on the general suitability of this product for their needs and specific application practices.

If there is any inconsistency between different language issues of this document, the English (United Kingdom) version will prevail.

Appendix B

Three-Point Bending Test for the MGP10 and Radiata Pine Members

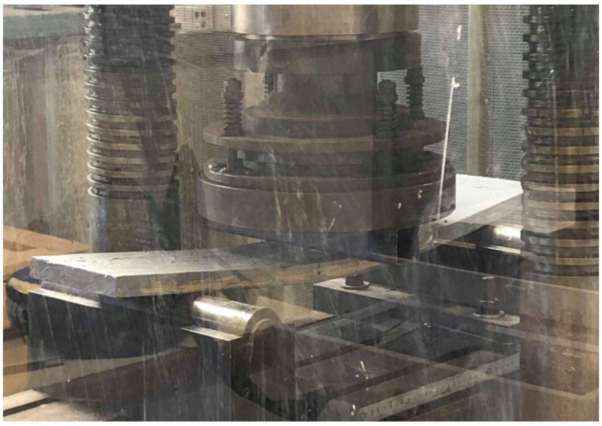

184 mm by 19 mm radiata member reinforced with 0.25% graphene

45 mm by 70 mm MGP10 structural pine member reinforced with 0.25% graphene

70 mm by 45 mm MGP10 structural pine member reinforced with 0.25% graphene

184 mm by 19 mm radiata member reinforced with 0.5% graphene

70 mm by 35 mm MGP10 pine member

45 mm by 70 mm MGP10 structural pine member reinforced with 0.5% graphene

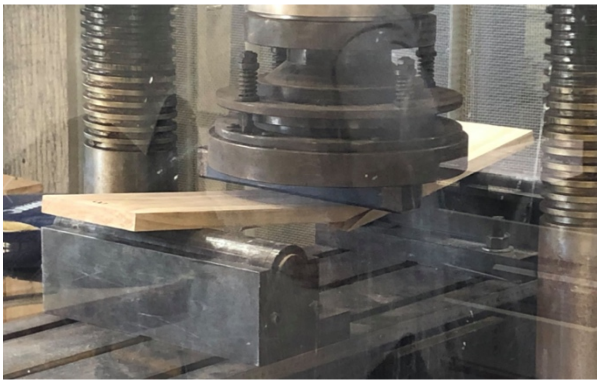

184 mm by 19 mm radiata member

70 mm by 45 mm MGP10 structural pine member

Appendix C

Effective Material Properties of Graphene/Epoxy Nanocomposites

GPL/polymer nanocomposites layer based dimension are;

$$l_{GPL} = 2.5\ \mu m, w_{GPL} = 1.5\mu m\ and\ h_{GPL} = 1.5nm$$

Vm	*Vf*	*EL*	*ET*	*w.t.%GPL*	*w.t.*	**Ec (MPa)**	**Vc**	**pc**
1.0000	0.0000	3000.0000	3000.0000	0.000	0.0	3000.0000	0.34000	1200.0000
0.9989	0.0011	4035.8402	3976.3956	0.001	0.1	3998.6873	0.33983	1199.8415
0.9977	0.0023	5071.3477	4952.5929	0.002	0.2	4997.1260	0.33965	1199.6831
0.9966	0.0034	6106.9330	5928.9788	0.003	0.3	5995.7116	0.33948	1199.5247
0.9955	0.0045	7142.4591	6905.4245	0.004	0.4	6994.3124	0.33930	1199.3664
0.9943	0.0057	8177.9261	7881.9297	0.005	0.5	7992.9284	0.33913	1199.2081
0.9932	0.0068	9213.3341	8858.4947	0.006	0.6	8991.5595	0.33895	1199.0498
0.9921	0.0079	10248.6830	9835.1193	0.007	0.7	9990.2057	0.33878	1198.8916
0.9910	0.0090	11283.9728	10811.8036	0.008	0.8	10988.8671	0.33861	1198.7334
0.9898	0.0102	12319.2036	11788.5476	0.009	0.9	11987.5436	0.33843	1198.5753
0.9887	0.0113	13354.3753	12765.3513	0.010	1.0	12986.2353	0.33826	1198.4172
0.9876	0.0124	14389.4879	13742.2147	0.011	1.1	13984.9421	0.33809	1198.2591
0.9864	0.0136	15424.5415	14719.1378	0.012	1.2	14983.6642	0.33791	1198.1011
0.9853	0.0147	16459.5360	15696.1206	0.013	1.3	15982.4014	0.33774	1197.9432
0.9842	0.0158	17494.4715	16673.1632	0.014	1.4	16981.1538	0.33756	1197.7852
0.9831	0.0169	18529.3480	17650.2654	0.015	1.5	17979.9214	0.33739	1197.6273
0.9819	0.0181	19564.1655	18627.4274	0.016	1.6	18978.7042	0.33722	1197.4695
0.9808	0.0192	20598.9239	19604.6491	0.017	1.7	19977.5021	0.33704	1197.3117
0.9797	0.0203	21633.6233	20581.9306	0.018	1.8	20976.3153	0.33687	1197.1539
0.9785	0.0215	22668.2636	21559.2718	0.019	1.9	21975.1437	0.33670	1196.9962
0.9774	0.0226	23702.8450	22536.6727	0.020	2.0	22973.9873	0.33652	1196.8385
0.9763	0.0237	24737.3674	23514.1335	0.021	2.1	23972.8462	0.33635	1196.6809
0.9752	0.0248	25771.8308	24491.6539	0.022	2.2	24971.7202	0.33618	1196.5233
0.9740	0.0260	26806.2351	25469.2342	0.023	2.3	25970.6095	0.33600	1196.3658
0.9729	0.0271	27840.5805	26446.8742	0.024	2.4	26969.5141	0.33583	1196.2082
0.9718	0.0282	28874.8669	27424.5740	0.025	2.5	27968.4338	0.33566	1196.0508
0.9707	0.0293	29909.0943	28402.3336	0.026	2.6	28967.3688	0.33548	1195.8933
0.9695	0.0305	30943.2628	29380.1529	0.027	2.7	29966.3191	0.33531	1195.7360
0.9684	0.0316	31977.3723	30358.0321	0.028	2.8	30965.2847	0.33514	1195.5786
0.9673	0.0327	33011.4228	31335.9711	0.029	2.9	31964.2654	0.33496	1195.4213
0.9662	0.0338	34045.4143	32313.9698	0.030	3.0	32963.2615	0.33479	1195.2640
0.9650	0.0350	35079.3469	33292.0284	0.031	3.1	33962.2728	0.33462	1195.1068

0.9639	0.0361	36113.2206	34270.1468	0.032	3.2	34961.2995	0.33444	1194.9496
0.9628	0.0372	37147.0353	35248.3250	0.033	3.3	35960.3414	0.33427	1194.7925
0.9617	0.0383	38180.7910	36226.5631	0.034	3.4	36959.3985	0.33410	1194.6354
0.9606	0.0394	39214.4879	37204.8609	0.035	3.5	37958.4710	0.33393	1194.4784
0.9594	0.0406	40248.1258	38183.2186	0.036	3.6	38957.5588	0.33375	1194.3213
0.9583	0.0417	41281.7048	39161.6362	0.037	3.7	39956.6619	0.33358	1194.1644
0.9572	0.0428	42315.2248	40140.1136	0.038	3.8	40955.7803	0.33341	1194.0074
0.9561	0.0439	43348.6860	41118.6509	0.039	3.9	41954.9140	0.33324	1193.8505
0.9550	0.0450	44382.0882	42097.2480	0.040	4.0	42954.0631	0.33306	1193.6937
0.9538	0.0462	45415.4315	43075.9050	0.041	4.1	43953.2274	0.33289	1193.5369
0.9527	0.0473	46448.7160	44054.6219	0.042	4.2	44952.4072	0.33272	1193.3801
0.9516	0.0484	47481.9415	45033.3986	0.043	4.3	45951.6022	0.33255	1193.2234
0.9505	0.0495	48515.1082	46012.2352	0.044	4.4	46950.8126	0.33237	1193.0667
0.9494	0.0506	49548.2159	46991.1317	0.045	4.5	47950.0383	0.33220	1192.9101
0.9482	0.0518	50581.2648	47970.0881	0.046	4.6	48949.2794	0.33203	1192.7535
0.9471	0.0529	51614.2549	48949.1044	0.047	4.7	49948.5358	0.33186	1192.5969
0.9460	0.0540	52647.1860	49928.1806	0.048	4.8	50947.8077	0.33168	1192.4404
0.9449	0.0551	53680.0583	50907.3168	0.049	4.9	51947.0948	0.33151	1192.2839
0.9438	0.0562	54712.8717	51886.5128	0.050	5.0	52946.3974	0.33134	1192.1275

Appendix D

Member Deflection Testing Data's

Member with cross section 45 mm by 70 mm

0.25% Graphene-45x70			Control Sample-45x70			0.5% Graphene-45x70		
PlayTime	LoadValue (kN)	PositionValue (mm)	PlayTime	LoadValue	PositionValue	PlayTime	LoadValue	PositionValue
0	166.5968	0	0	225.5999	4.6896E-13	0	205.9322	0.00649484
0.035	172.3814	0	0.034	219.8153	6.9633E-13	0.034	198.9907	0.00964385
0.067	166.5968	0	0.067	212.8737	8.1002E-13	0.068	186.2645	0.01121835
0.102	166.5968	0	0.101	205.9322	8.6686E-13	0.102	198.9907	0.0120056
0.134	172.3814	0	0.133	212.8737	8.9528E-13	0.134	186.2645	0.01239923
0.168	172.3814	0	0.168	219.8153	9.0949E-13	0.166	179.323	0.01259604
0.201	179.323	0	0.202	232.5414	9.0949E-13	0.201	186.2645	0.01259604
0.234	179.323	0	0.233	232.5414	9.0949E-13	0.234	193.2061	0.01259604
0.269	172.3814	0	0.267	225.5999	9.0949E-13	0.267	198.9907	0.01259604
0.302	172.3814	0	0.299	212.8737	9.0949E-13	0.3	186.2645	0.01259604
0.334	166.5968	0	0.333	205.9322	9.0949E-13	0.334	186.2645	0.01259604
0.367	166.5968	0	0.366	205.9322	9.0949E-13	0.367	186.2645	0.01259604
0.401	166.5968	0	0.4	219.8153	9.0949E-13	0.4	186.2645	0.01259604
0.436	172.3814	0	0.433	219.8153	9.0949E-13	0.434	193.2061	0.01259604
0.469	159.6553	0	0.467	225.5999	9.0949E-13	0.468	198.9907	0.01259604
0.501	159.6553	0	0.5	212.8737	9.0949E-13	0.502	186.2645	0.01259604
0.534	172.3814	0	0.534	212.8737	9.0949E-13	0.535	172.3814	0.01259604
0.567	166.5968	0	0.568	212.8737	9.0949E-13	0.567	186.2645	0.01259604
0.601	172.3814	0	0.6	219.8153	9.0949E-13	0.6	198.9907	0.01259604
0.634	172.3814	0	0.635	219.8153	9.0949E-13	0.634	179.323	0.01259604
0.668	166.5968	0	0.667	225.5999	9.0949E-13	0.668	186.2645	0.01259604
0.702	172.3814	0	0.7	219.8153	9.0949E-13	0.701	179.323	0.01259604
0.734	172.3814	0	0.733	225.5999	9.0949E-13	0.735	186.2645	0.01259604
0.768	166.5968	0	0.767	219.8153	9.0949E-13	0.768	186.2645	0.01259604
0.801	159.6553	0	0.8	219.8153	9.0949E-13	0.8	186.2645	0.01259604
0.834	159.6553	0	0.833	212.8737	9.0949E-13	0.834	186.2645	0.01259604
0.868	152.7138	0	0.867	225.5999	9.0949E-13	0.867	193.2061	0.01259604
0.901	159.6553	0	0.901	225.5999	0.00649484	0.901	193.2061	0.01259604
0.934	172.3814	0	0.933	225.5999	0.00964385	0.935	186.2645	0.01259604
0.967	172.3814	0	0.966	225.5999	0.01121835	0.966	186.2645	0.01259604
1.001	172.3814	0	1	219.8153	0.0120056	1.001	186.2645	0.01259604
1.034	166.5968	0	1.033	225.5999	0.01239923	1.033	186.2645	0.01259604
1.068	159.6553	0	1.068	232.5414	0.01259604	1.067	186.2645	0.01259604
1.103	159.6553	0	1.1	219.8153	0.01259604	1.102	186.2645	0.01259604
1.134	152.7138	0	1.133	212.8737	0.01259604	1.134	186.2645	0.01259604
1.168	152.7138	0	1.167	219.8153	0.01259604	1.167	193.2061	0.01259604
1.201	159.6553	0	1.2	219.8153	0.01259604	1.202	186.2645	0.01259604
1.235	159.6553	0	1.234	225.5999	0.01259604	1.234	186.2645	0.01259604
1.269	152.7138	0	1.266	219.8153	0.01259604	1.267	186.2645	0.01259604
1.301	159.6553	0	1.3	212.8737	0.01259604	1.301	179.323	0.01259604
1.336	152.7138	0	1.333	219.8153	0.01259604	1.333	179.323	0.01259604
1.368	159.6553	0	1.367	212.8737	0.01259604	1.367	186.2645	0.01259604
1.401	159.6553	0	1.4	212.8737	0.01259604	1.401	193.2061	0.01259604
1.435	159.6553	0	1.434	212.8737	0.01259604	1.434	205.9322	0.01259604
1.468	166.5968	0	1.467	225.5999	0.01259604	1.468	186.2645	0.01259604
1.501	159.6553	0	1.5	225.5999	0.01259604	1.501	186.2645	0.01259604
1.535	152.7138	0	1.533	225.5999	0.01259604	1.535	193.2061	0.01259604
1.567	152.7138	0	1.568	219.8153	0.01259604	1.567	193.2061	0.01259604
1.601	159.6553	0	1.6	219.8153	0.01259604	1.601	193.2061	0.01259604
1.634	172.3814	0	1.633	225.5999	0.01259604	1.634	198.9907	0.01259604
1.668	159.6553	0	1.667	219.8153	0.01259604	1.667	205.9322	0.01259604
1.702	159.6553	0	1.7	219.8153	0.01259604	1.7	193.2061	0.01259604
1.735	166.5968	0	1.735	225.5999	0.01259604	1.734	186.2645	0.01259604
1.767	166.5968	0	1.767	225.5999	0.01259604	1.767	186.2645	0.01259604
1.801	159.6553	0	1.802	212.8737	0.01259604	1.8	198.9907	0.01259604
1.835	159.6553	0	1.833	219.8153	0.01259604	1.833	186.2645	0.01259604
1.867	152.7138	0	1.868	225.5999	0.01259604	1.867	179.323	0.01259604
1.901	166.5968	0	1.9	225.5999	0.01259604	1.901	186.2645	0.01259604
1.935	166.5968	0	1.933	225.5999	0.01259604	1.933	198.9907	0.01259604
1.967	159.6553	0	1.966	225.5999	0.01259604	1.967	198.9907	0.01259604
2.001	159.6553	0	2.001	219.8153	0.01259604	2.001	193.2061	0.01259604
2.035	152.7138	0	2.033	225.5999	0.01259604	2.035	198.9907	0.01259604
2.068	152.7138	0	2.066	225.5999	0.01259604	2.067	198.9907	0.01259604
2.102	152.7138	0	2.1	232.5414	0.01259604	2.101	198.9907	0.01259604
2.134	159.6553	0	2.134	239.4829	0.01259604	2.134	198.9907	0.01259604
2.168	159.6553	0	2.168	219.8153	0.01259604	2.169	198.9907	0.01259604
2.202	152.7138	0	2.2	225.5999	0.01259604	2.201	198.9907	0.01259604
2.234	159.6553	0	2.234	225.5999	0.01259604	2.234	212.8737	0.01259604

Member with cross section 70 mm by 45 mm

0.25% Graphene			Control Sample			0.5% Graphene		
PlayTime	LoadValue (kN)	PositionValue (mm)	PlayTime	LoadValue	PositionValue	PlayTime	LoadValue	PositionValue
0	193.2061	0	0	198.9907	4.6896E-13	0	212.8737	0
0.032	193.2061	0	0.033	205.9322	6.9633E-13	0.031	212.8737	0
0.067	186.2645	0	0.067	212.8737	8.1002E-13	0.066	212.8737	0
0.099	186.2645	0	0.1	205.9322	8.6686E-13	0.1	212.8737	0
0.133	179.323	0	0.134	198.9907	8.9528E-13	0.132	212.8737	0
0.166	186.2645	0	0.166	193.2061	9.0949E-13	0.166	205.9322	0
0.2	166.5968	0	0.202	205.9322	9.0949E-13	0.198	205.9322	0
0.233	172.3814	0	0.233	198.9907	0.00649484	0.232	212.8737	0
0.266	179.323	0	0.267	198.9907	0.00964385	0.265	212.8737	0
0.299	186.2645	0	0.3	198.9907	0.01121835	0.299	212.8737	0
0.332	193.2061	0	0.334	198.9907	0.0120056	0.332	205.9322	0
0.366	193.2061	0	0.367	212.8737	0.01239923	0.367	212.8737	0
0.401	186.2645	0	0.401	198.9907	0.01259604	0.399	205.9322	0
0.433	172.3814	0	0.434	193.2061	0.01259604	0.433	212.8737	0
0.466	179.323	0	0.466	198.9907	0.01259604	0.465	212.8737	0
0.501	179.323	0	0.501	198.9907	0.01259604	0.498	212.8737	0
0.534	166.5968	0	0.534	198.9907	0.01259604	0.532	219.8153	0
0.566	179.323	0	0.566	193.2061	0.01259604	0.565	212.8737	0
0.6	179.323	0	0.6	198.9907	0.01259604	0.599	219.8153	0
0.632	186.2645	0	0.634	193.2061	0.01259604	0.633	212.8737	0
0.666	179.323	0	0.667	205.9322	0.01259604	0.666	205.9322	0
0.699	179.323	0	0.702	198.9907	0.01259604	0.699	205.9322	0
0.733	186.2645	0	0.734	198.9907	0.01259604	0.732	219.8153	0
0.766	179.323	0	0.766	205.9322	0.01259604	0.766	225.5999	0
0.8	172.3814	0	0.801	198.9907	0.01259604	0.798	225.5999	0
0.833	172.3814	0	0.833	205.9322	0.01259604	0.832	219.8153	0
0.866	179.323	0	0.867	205.9322	0.01259604	0.865	212.8737	0
0.899	172.3814	0	0.9	205.9322	0.01259604	0.899	198.9907	0
0.932	172.3814	0	0.935	198.9907	0.01259604	0.933	205.9322	0
0.966	186.2645	0	0.968	205.9322	0.01259604	0.965	212.8737	0
0.999	179.323	0	1.002	205.9322	0.01259604	0.999	212.8737	0
1.033	179.323	0	1.035	198.9907	0.01259604	1.032	225.5999	0
1.066	186.2645	0	1.067	198.9907	0.01259604	1.066	212.8737	0
1.1	172.3814	0	1.1	193.2061	0.01259604	1.099	205.9322	0.00649484
1.132	172.3814	0	1.133	193.2061	0.01259604	1.134	212.8737	0.00964385
1.166	172.3814	0	1.167	198.9907	0.01259604	1.167	212.8737	0.01121835
1.199	179.323	0	1.201	198.9907	0.01259604	1.199	212.8737	0.0120056
1.232	179.323	0	1.233	205.9322	0.01259604	1.232	212.8737	0.01239923
1.266	172.3814	0	1.267	205.9322	0.01259604	1.265	219.8153	0.01259604
1.299	172.3814	0	1.299	193.2061	0.01259604	1.299	212.8737	0.01259604
1.332	179.323	0	1.333	205.9322	0.01259604	1.332	225.5999	0.01259604
1.366	179.323	0	1.367	205.9322	0.01259604	1.366	219.8153	0.01259604
1.399	179.323	0	1.401	205.9322	0.01259604	1.399	212.8737	0.01259604
1.432	179.323	0	1.435	205.9322	0.01259604	1.432	212.8737	0.01259604
1.466	179.323	0	1.467	198.9907	0.01259604	1.466	219.8153	0.01259604
1.499	166.5968	0	1.5	205.9322	0.01259604	1.498	212.8737	0.01259604
1.532	179.323	0	1.533	198.9907	0.01259604	1.532	212.8737	0.01259604
1.567	179.323	0	1.567	198.9907	0.01259604	1.565	212.8737	0.01259604
1.6	172.3814	0	1.602	198.9907	0.01259604	1.599	212.8737	0.01259604
1.632	172.3814	0	1.633	193.2061	0.01259604	1.632	205.9322	0.01259604
1.666	172.3814	0	1.667	193.2061	0.01259604	1.666	219.8153	0.01259604
1.699	179.323	0	1.7	198.9907	0.01259604	1.699	212.8737	0.01259604
1.733	172.3814	0	1.733	193.2061	0.01259604	1.732	212.8737	0.01259604
1.766	172.3814	0	1.766	205.9322	0.01259604	1.766	219.8153	0.01259604
1.8	172.3814	0	1.8	205.9322	0.01259604	1.8	219.8153	0.01259604
1.832	179.323	0	1.834	198.9907	0.01259604	1.831	212.8737	0.01259604
1.866	166.5968	0	1.867	193.2061	0.01259604	1.865	219.8153	0.01259604
1.9	166.5968	0	1.9	205.9322	0.01259604	1.899	219.8153	0.01259604
1.932	166.5968	0	1.933	205.9322	0.01259604	1.933	212.8737	0.01259604
1.966	166.5968	0	1.967	198.9907	0.01259604	1.965	219.8153	0.01259604
1.999	172.3814	0	2	198.9907	0.01259604	1.998	225.5999	0.01259604
2.033	166.5968	0	2.035	212.8737	0.01259604	2.034	232.5414	0.01259604
2.067	166.5968	0	2.066	205.9322	0.01259604	2.067	212.8737	0.01259604
2.099	172.3814	0	2.1	198.9907	0.01259604	2.099	212.8737	0.01259604
2.133	172.3814	0	2.133	198.9907	0.01259604	2.133	205.9322	0.01259604
2.166	172.3814	0	2.167	198.9907	0.01259604	2.165	212.8737	0.01259604
2.199	166.5968	0	2.2	198.9907	0.01259604	2.199	219.8153	0.01259604
2.233	166.5968	0	2.233	198.9907	0.01259604	2.233	212.8737	0.01259604
2.267	172.3814	0	2.267	198.9907	0.01259604	2.265	219.8153	0.01259604

Member with cross section 70 mm by 35 mm

PlayTime	LoadValue	PositionValue	PlayTime	LoadValue	PositionValue	PlayTime	LoadValue	PositionValue
0	205.9322	4.6896E-13	0	205.9322	0	0	205.9322	0
0.034	212.8737	6.9633E-13	0.034	198.9907	0	0.034	198.9907	0
0.067	205.9322	8.1002E-13	0.067	205.9322	0	0.067	205.9322	0
0.1	205.9322	8.6686E-13	0.101	198.9907	0	0.1	198.9907	0
0.133	198.9907	8.9528E-13	0.135	198.9907	0	0.135	198.9907	0
0.167	198.9907	9.0949E-13	0.168	205.9322	0	0.167	193.2061	0
0.2	193.2061	9.0949E-13	0.2	205.9322	0	0.2	193.2061	0
0.234	198.9907	9.0949E-13	0.233	193.2061	0	0.235	198.9907	0
0.266	198.9907	9.0949E-13	0.268	198.9907	0	0.266	205.9322	0
0.3	186.2645	9.0949E-13	0.3	198.9907	0	0.301	205.9322	0
0.335	198.9907	9.0949E-13	0.334	205.9322	0	0.333	205.9322	0
0.367	198.9907	9.0949E-13	0.367	198.9907	0	0.367	205.9322	0
0.401	198.9907	9.0949E-13	0.401	198.9907	0	0.4	198.9907	0.00649484
0.433	198.9907	9.0949E-13	0.433	198.9907	0	0.433	198.9907	0.00964385
0.466	193.2061	9.0949E-13	0.467	198.9907	0	0.468	198.9907	0.01121835
0.501	193.2061	9.0949E-13	0.501	198.9907	0	0.501	205.9322	0.0120056
0.533	198.9907	9.0949E-13	0.533	198.9907	0	0.534	198.9907	0.01239923
0.566	198.9907	9.0949E-13	0.567	193.2061	0	0.569	205.9322	0.01259604
0.6	193.2061	9.0949E-13	0.602	198.9907	0	0.6	205.9322	0.01259604
0.633	198.9907	9.0949E-13	0.634	205.9322	0	0.633	205.9322	0.01259604
0.667	198.9907	9.0949E-13	0.666	198.9907	0	0.666	212.8737	0.01259604
0.699	205.9322	9.0949E-13	0.702	193.2061	0	0.7	205.9322	0.01259604
0.734	198.9907	9.0949E-13	0.735	193.2061	0	0.734	205.9322	0.01259604
0.768	193.2061	9.0949E-13	0.767	198.9907	0	0.768	205.9322	0.01259604
0.802	186.2645	9.0949E-13	0.8	212.8737	0	0.8	198.9907	0.01259604
0.834	193.2061	9.0949E-13	0.834	205.9322	0	0.833	193.2061	0.01259604
0.866	198.9907	9.0949E-13	0.866	198.9907	0	0.867	205.9322	0.01259604
0.9	205.9322	9.0949E-13	0.9	193.2061	0	0.9	205.9322	0.01259604
0.934	186.2645	9.0949E-13	0.933	193.2061	0	0.933	205.9322	0.01259604
0.966	186.2645	9.0949E-13	0.968	193.2061	0	0.967	205.9322	0.01259604
1	193.2061	9.0949E-13	1.001	193.2061	0	1.001	205.9322	0.01259604
1.033	198.9907	9.0949E-13	1.034	212.8737	0	1.033	198.9907	0.01259604
1.068	198.9907	9.0949E-13	1.067	198.9907	0	1.067	198.9907	0.01259604
1.1	198.9907	9.0949E-13	1.1	205.9322	0	1.1	186.2645	0.01259604
1.134	186.2645	9.0949E-13	1.135	205.9322	0	1.133	198.9907	0.01259604
1.167	193.2061	9.0949E-13	1.167	198.9907	0	1.167	205.9322	0.01259604
1.2	198.9907	9.0949E-13	1.202	193.2061	0	1.2	205.9322	0.01259604
1.233	198.9907	9.0949E-13	1.234	193.2061	0	1.234	198.9907	0.01259604
1.267	193.2061	9.0949E-13	1.267	198.9907	0	1.266	205.9322	0.01259604
1.301	186.2645	9.0949E-13	1.3	205.9322	0	1.3	205.9322	0.01259604
1.335	193.2061	9.0949E-13	1.334	205.9322	0	1.334	198.9907	0.01259604
1.368	193.2061	9.0949E-13	1.367	198.9907	0	1.367	198.9907	0.01259604
1.4	193.2061	9.0949E-13	1.401	205.9322	0	1.401	198.9907	0.01259604
1.433	186.2645	9.0949E-13	1.434	205.9322	0	1.434	198.9907	0.01259604
1.467	186.2645	9.0949E-13	1.466	198.9907	0	1.467	205.9322	0.01259604
1.5	186.2645	9.0949E-13	1.5	198.9907	0	1.501	205.9322	0.01259604
1.534	193.2061	9.0949E-13	1.534	198.9907	0	1.533	205.9322	0.01259604
1.566	186.2645	9.0949E-13	1.566	198.9907	0	1.567	205.9322	0.01259604
1.6	186.2645	9.0949E-13	1.6	198.9907	0	1.601	212.8737	0.01259604
1.633	186.2645	9.0949E-13	1.634	205.9322	0	1.633	212.8737	0.01259604
1.667	186.2645	9.0949E-13	1.666	205.9322	0	1.668	205.9322	0.01259604
1.7	186.2645	9.0949E-13	1.7	198.9907	0	1.7	205.9322	0.01259604
1.733	186.2645	9.0949E-13	1.734	205.9322	0	1.733	205.9322	0.01259604
1.767	179.323	9.0949E-13	1.768	198.9907	0	1.767	205.9322	0.01259604
1.801	198.9907	9.0949E-13	1.802	193.2061	0	1.8	205.9322	0.01259604
1.833	205.9322	9.0949E-13	1.833	205.9322	0	1.834	198.9907	0.01259604
1.867	193.2061	9.0949E-13	1.868	205.9322	0	1.866	186.2645	0.01259604
1.9	193.2061	9.0949E-13	1.9	205.9322	0	1.9	193.2061	0.01259604
1.934	193.2061	9.0949E-13	1.934	205.9322	0	1.934	198.9907	0.01259604
1.966	193.2061	9.0949E-13	1.968	205.9322	0	1.967	205.9322	0.01259604
2	198.9907	9.0949E-13	2.002	198.9907	0	2	186.2645	0.01259604
2.033	193.2061	9.0949E-13	2.034	205.9322	0	2.034	198.9907	0.01259604
2.067	193.2061	9.0949E-13	2.067	198.9907	0	2.067	198.9907	0.01259604
2.101	193.2061	9.0949E-13	2.102	198.9907	0	2.1	198.9907	0.01259604
2.133	193.2061	9.0949E-13	2.134	198.9907	0	2.133	205.9322	0.01259604
2.167	186.2645	9.0949E-13	2.167	193.2061	0	2.167	198.9907	0.01259604
2.2	198.9907	9.0949E-13	2.2	198.9907	0	2.2	205.9322	0.01259604
2.233	193.2061	9.0949E-13	2.233	205.9322	0	2.234	205.9322	0.01259604
2.267	193.2061	9.0949E-13	2.267	193.2061	0	2.266	198.9907	0.01259604

Member with cross section 184 mm by 19 mm

0.25% Graphene			Control Sample			0.5% Graphene		
PlayTime	LoadValue	PositionValue	PlayTime	LoadValue	PositionValue	PlayTime	LoadValue	PositionValue
0	193.2061	0	0	198.9907	0	0	179.323	-4.69E-13
0.032	193.2061	0	0.033	193.2061	0	0.032	193.2061	-6.963E-13
0.066	205.9322	0	0.067	193.2061	0	0.065	186.2645	-8.1E-13
0.099	193.2061	0	0.102	198.9907	0	0.098	198.9907	-8.669E-13
0.133	198.9907	0	0.134	193.2061	0	0.133	198.9907	-8.953E-13
0.167	198.9907	0	0.167	186.2645	0	0.165	186.2645	-9.095E-13
0.2	198.9907	0	0.201	186.2645	0	0.198	186.2645	-9.095E-13
0.232	198.9907	0	0.233	186.2645	0	0.233	193.2061	-9.095E-13
0.266	198.9907	0	0.268	193.2061	0	0.266	186.2645	-9.095E-13
0.299	198.9907	0	0.3	193.2061	0	0.299	186.2645	-9.095E-13
0.333	198.9907	0	0.333	186.2645	0	0.331	179.323	-9.095E-13
0.366	198.9907	0	0.367	198.9907	0	0.365	186.2645	-9.095E-13
0.4	205.9322	0	0.4	198.9907	0	0.399	186.2645	-9.095E-13
0.433	193.2061	0	0.433	186.2645	0	0.432	179.323	-9.095E-13
0.466	198.9907	0	0.467	193.2061	0	0.467	186.2645	-9.095E-13
0.499	193.2061	0	0.501	186.2645	0	0.5	193.2061	-9.095E-13
0.533	198.9907	0	0.533	179.323	0	0.532	186.2645	-9.095E-13
0.566	198.9907	0	0.567	186.2645	0	0.566	186.2645	-9.095E-13
0.6	198.9907	0	0.6	198.9907	0	0.598	186.2645	-9.095E-13
0.633	198.9907	0	0.634	198.9907	0	0.632	186.2645	-9.095E-13
0.666	198.9907	0	0.666	198.9907	0	0.665	179.323	-9.095E-13
0.699	198.9907	0	0.701	186.2645	0	0.7	193.2061	-9.095E-13
0.733	198.9907	0	0.734	186.2645	0	0.733	198.9907	-9.095E-13
0.766	205.9322	0	0.769	186.2645	0	0.767	193.2061	-9.095E-13
0.799	205.9322	0	0.802	186.2645	0	0.799	198.9907	-9.095E-13
0.833	198.9907	0	0.833	186.2645	0	0.832	193.2061	-9.095E-13
0.866	198.9907	0	0.867	193.2061	0	0.865	198.9907	-9.095E-13
0.9	198.9907	0	0.901	193.2061	0	0.9	193.2061	-9.095E-13
0.932	198.9907	0	0.934	193.2061	0.00649484	0.933	186.2645	-9.095E-13
0.966	193.2061	0	0.966	186.2645	0.00964385	0.965	198.9907	-9.095E-13
1	193.2061	0	1	186.2645	0.01121835	0.999	186.2645	-9.095E-13
1.032	186.2645	0	1.034	186.2645	0.0120056	1.032	186.2645	-9.095E-13
1.066	198.9907	0	1.067	198.9907	0.01239923	1.065	193.2061	-9.095E-13
1.1	198.9907	0	1.1	198.9907	0.01259604	1.099	198.9907	-9.095E-13
1.133	205.9322	0	1.133	186.2645	0.01259604	1.132	186.2645	-9.095E-13
1.166	198.9907	0	1.167	193.2061	0.01259604	1.166	186.2645	-9.095E-13
1.201	198.9907	0	1.2	193.2061	0.01259604	1.198	198.9907	-9.095E-13
1.234	193.2061	0	1.234	193.2061	0.01259604	1.232	193.2061	-9.095E-13
1.266	186.2645	0	1.267	193.2061	0.01259604	1.266	186.2645	-9.095E-13
1.299	198.9907	0	1.301	193.2061	0.01259604	1.298	186.2645	-9.095E-13
1.332	198.9907	0	1.335	193.2061	0.01259604	1.333	186.2645	-9.095E-13
1.366	193.2061	0	1.367	186.2645	0.01259604	1.365	186.2645	-9.095E-13
1.4	193.2061	0	1.401	205.9322	0.01259604	1.399	193.2061	-9.095E-13
1.432	193.2061	0	1.433	193.2061	0.01259604	1.433	193.2061	-9.095E-13
1.467	193.2061	0	1.467	193.2061	0.01259604	1.465	186.2645	-9.095E-13
1.499	186.2645	0	1.501	193.2061	0.01259604	1.499	186.2645	-9.095E-13
1.533	186.2645	0	1.533	193.2061	0.01259604	1.532	198.9907	-9.095E-13
1.566	193.2061	0	1.567	198.9907	0.01259604	1.566	186.2645	-9.095E-13
1.6	198.9907	0.00649484	1.6	193.2061	0.01259604	1.599	193.2061	-9.095E-13
1.633	198.9907	0.00964385	1.633	186.2645	0.01259604	1.632	198.9907	-9.095E-13
1.667	193.2061	0.01121835	1.668	198.9907	0.01259604	1.667	193.2061	-9.095E-13
1.701	193.2061	0.0120056	1.7	198.9907	0.01259604	1.698	198.9907	-9.095E-13
1.733	198.9907	0.01239923	1.734	193.2061	0.01259604	1.732	198.9907	-9.095E-13
1.766	198.9907	0.01259604	1.767	193.2061	0.01259604	1.766	198.9907	0.00649484
1.799	193.2061	0.01259604	1.801	198.9907	0.01259604	1.8	186.2645	0.00964385
1.833	193.2061	0.01259604	1.833	186.2645	0.01259604	1.833	179.323	0.01121835
1.866	198.9907	0.01259604	1.867	186.2645	0.01259604	1.866	186.2645	0.0120056
1.9	193.2061	0.01259604	1.9	193.2061	0.01259604	1.899	186.2645	0.01239923
1.933	193.2061	0.01259604	1.934	186.2645	0.01259604	1.931	186.2645	0.01259604
1.968	186.2645	0.01259604	1.967	193.2061	0.01259604	1.965	198.9907	0.01259604
2.001	198.9907	0.01259604	2.002	198.9907	0.01259604	1.999	198.9907	0.01259604
2.034	198.9907	0.01259604	2.034	198.9907	0.01259604	2.031	198.9907	0.01259604
2.067	198.9907	0.01259604	2.067	193.2061	0.01259604	2.065	198.9907	0.01259604
2.1	193.2061	0.01259604	2.1	193.2061	0.01259604	2.099	193.2061	0.01259604
2.134	186.2645	0.01259604	2.135	198.9907	0.01259604	2.132	205.9322	0.01259604
2.166	193.2061	0.01259604	2.166	193.2061	0.01259604	2.167	198.9907	0.01259604
2.201	198.9907	0.01259604	2.2	193.2061	0.01259604	2.199	193.2061	0.01259604
2.232	193.2061	0.01259604	2.234	198.9907	0.01259604	2.231	193.2061	0.01259604